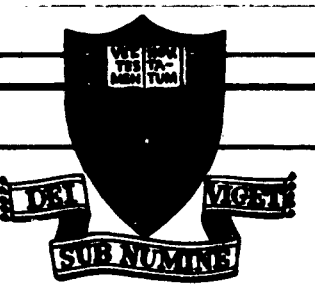

PRINCETON UNIVERSITY

DEPARTMENT OF AERONAUTICAL ENGINEERING

DEPARTMENT OF THE NAVY
OFFICE OF NAVAL RESEARCH

Contract Nonr 1858(31)
(ARPA Order No. 206-61)

A FINAL REPORT ON

HEAT TRANSFER FROM A PARTIALLY IONIZED GAS TO A GASEOUS COOLANT

Aeronautical Engineering Laboratory

Report No. 651

Prepared by: Peter M. Williams
Peter M. Williams
Research Staff Member

Martin P. Sherman
Martin P. Sherman
Research Assistant

and: Paul F. Jacobs
Paul F. Jacobs
Assistant in Research

Approved by: Jerry Grey
Jerry Grey
Project Leader
Associate Professor

June 1963

Guggenheim Laboratories for the Aerospace Propulsion Sciences
PRINCETON UNIVERSITY
Princeton, New Jersey

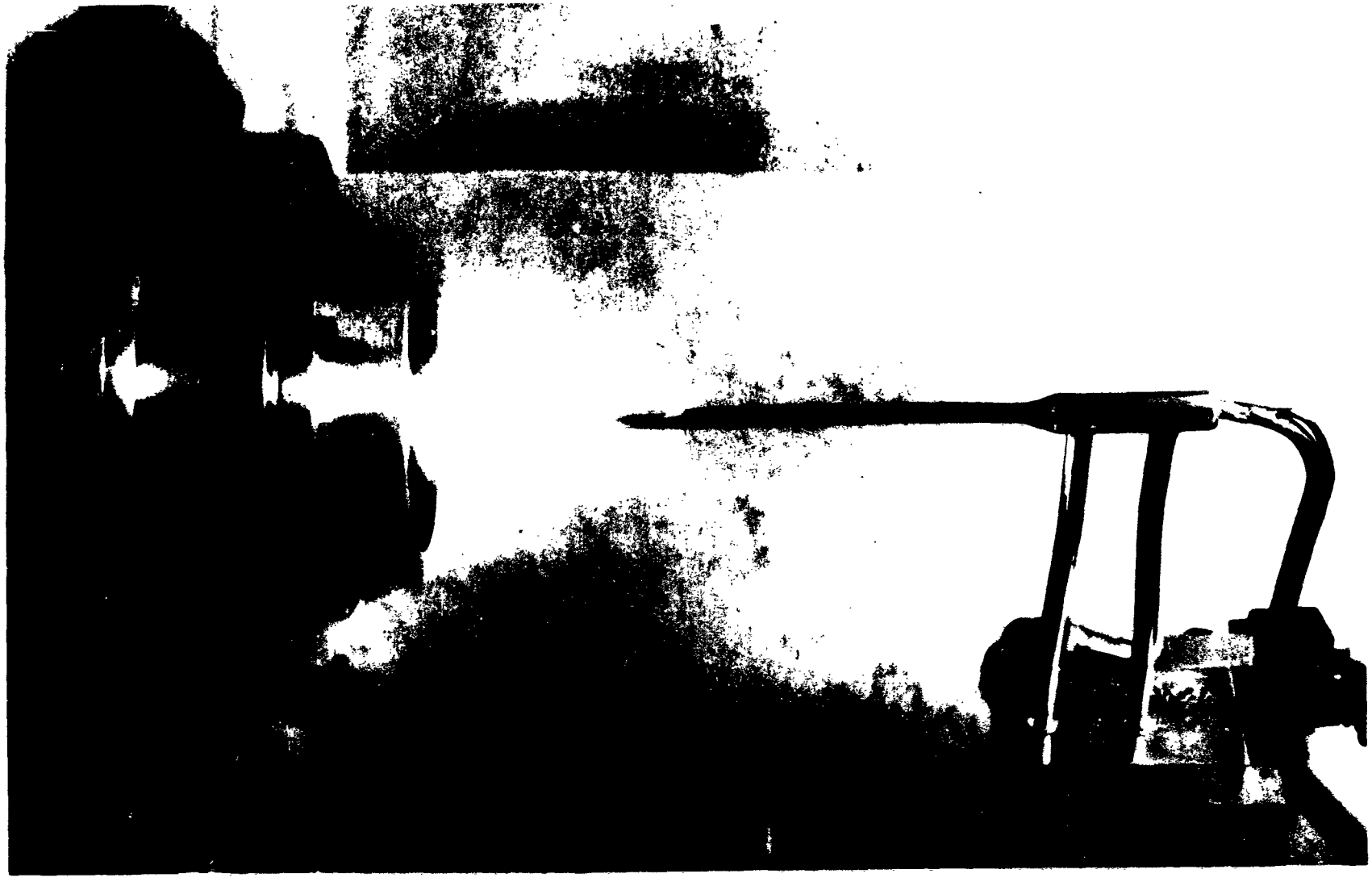

CALORIMETRIC PROBE IN ARGON PLASMA

PREFACE

This is a final report for a project entitled "Heat Transfer from an Ionized Gas to a Gaseous Coolant". Work was sponsored by the Advanced Research Projects Agency and performed under contract with the Office of Naval Research, (Contract No. Nonr 1858(31)) during the period February 1959 to 30 September 1962. During this period two semi-annual reports(1), (2)*, nine quarterly letter reports, and four technical reports (3), (4), (5), (6), were issued. This report summarizes the material presented in these earlier reports and generally presents the status of the project as of 30 September 1962.

The project has continued under the sponsorship of the Aeronautical Research Laboratories, Wright-Patterson Air Force Base, Contract No. AF33(657)9962. Some of the research performed in the continuation study, included in this report, were pertinent to the clarification of the earlier work.

---

* Numbers in parenthesis indicate references at the end of the report.

TABLE OF CONTENTS

LIST OF TABLES

LIST OF FIGURES

I. SUMMARY

Theoretical and experimental studies were made of subsonic mixing between a partially-ionized gas jet and a cool, coaxial gas flow. The gases studied were argon and helium. Both turbulent and laminar mixing regimes were investigated. In the turbulent mixing study, analytical expressions were closely verified by experiment. In laminar mixing, theoretical transport properties were computed and used to analyze the laminar mixing case.

In the turbulent mixing experiments argon was heated to temperatures up to 14,000°K by a commercial arcjet and exhausted as a 3/4-inch diameter jet into a coaxial flow of helium at room temperature. A water-cooled calorimetric probe 1/8-inch in diameter was developed and used to survey the jet core and mixing regions for enthalpy, gas composition and stagnation pressure. Temperature, velocity and composition profiles of the jet and mixing region were obtained with good accuracy, as indicated by detailed surveys providing mass and energy balances of the jet. Good agreement between measured data and analytical studies was obtained, with the analysis correctly predicting the spreading boundaries of the jet and the axial decay of energy, momentum, and argon concentration.

In support of both the laminar and turbulent studies a detailed analysis of the approach to equilibrium of the

jet was performed, and the radiation from the jet was studied. It was concluded that electrons were close to thermal equilibrium with other components of the jet in the zone studied. An experimental determination of the radiation loss confirmed theoretical estimates that between 5 and 10 per cent of the jet energy was lost by radiation in the temperature range of interest.

II. INTRODUCTION

The general purpose of this work was to establish methods of dealing with the very high temperature gas-gas interactions required by certain advanced space propulsion concepts. Specifically, the effects on conventional gas mixing and heat transfer theories of (a) high ionized fraction, (b) high temperature gradients, (c) electron equilibrium and (d) radiation from the jet were investigated.

The work was performed to yield an understanding of the basic transport phenomena and not with orientation to any immediate application. Nevertheless, it is expected that work accomplished in this study and in similar studies will have eventual application in several advanced propulsion systems.

One of the possible applications is the gaseous-core nuclear rocket (e.g., see References (7), (8), (9)), in which it is necessary to transfer energy from a heavily-ionized, fissionable fuel plasma to a propellant gas such as hydrogen or helium. Economic considerations require that only very small leakage of fuel ions be allowed (7). Hence it is essential that all the nuclear energy developed be delivered to the light propellant gas, the ionized fuel being retained by magnetic fields, centrifugal separation, or some combination of these effects. Performance of these powerplants is therefore dictated by the energy-exchange

processes between the ionized fuel atoms and the propellant gas.

A second application occurs in case it becomes necessary to obtain short-term high thrust levels from a low-thrust, high-specific impulse propulsion system (e.g., thermal arcjet). This can most easily be done by diluting the high-energy jet with additional cold propellant, thus reducing the effective exhaust velocity but increasing the thrust. Here the attainable performance is a critical function of the mixing process between cold and hot gases.

A third application, which may turn out to be the most important, is the film cooling of chambers for extreme-energy propulsion systems. These would be either of the gaseous-core nuclear type discussed earlier, or, possibly, magnetohydrodynamic accelerators using high-temperature ionized gases.

In general, it is often necessary to know the characteristics of extreme-temperature gas flows. Rocket exhaust nozzles at the low pressures required for space operations, arcjet engine exhausts, low-pressure flows through heat-transfer-type nuclear reactor cores slated for space propulsion systems, etc. are examples of non-equilibrium flows whose analysis is not yet possible because of a lack of high-temperature gas data.

III. THEORY AND ANALYSIS

A. Turbulent Mixing

1. Introduction

History

After the initial work of O. Reynolds in 1883 on the laws of instability of streamline motion and the basic ideas of turbulent flow, the first major study of turbulence was due to G. I. Taylor (10) in his 1920 paper "Diffusion by Continuous Movement". However, this theory treats only the case of isotropic turbulence and cannot be used on even relatively simple flow problems with any great degree of success.

In contrast to Taylor's statistical approach, certain phenomenological theories were later developed, the best known of these being the mixing length theory due to L. Prandtl (11). Tollmeim (12), in 1926, applied the Prandtl mixing length theory to the following incompressible cases: (a) The mixing of a parallel stream with an adjacent fluid at rest, (b) The mixing of a two-dimensional jet, issuing from a very narrow opening, with a medium at rest.

In 1941 Reichardt (13) introduced the "constant exchange-coefficient" theory as an improvement upon the Prandtl "mixing length" theory. This essentially corresponds to the assumption of a constant exchange coefficient over the entire mixing region of a free jet. All the above work

considered the case of incompressible turbulent mixing of a single medium, and was therefore concerned only with momentum transfer.

Experimental work by Forstall and Shapiro (14) on the mixing of a free jet with an external gas of a different type then showed that the transport of specie concentration occurs more rapidly than does the transport of momentum. W. Warren (15) in 1957 further extended the study of free turbulent mixing, using an integral analysis of a compressible, heated jet issuing into a medium at rest. As a result of comments by Prandtl (16) on the Reichardt "constan exchange coefficient" theory, a "modified exchange-coefficient" concept was employed. This concept requires the exchange coefficient to be constant across a given axial station but to vary with axial position. Agreement with the data of Corrsin and Uberoi (17) for axial temperature decay, jet temperature spreading, axial velocity decay, and jet velocity spreading was excellent. However, the temperature range was quite small, extending only about 500°R from the room temperature reference. This study was done for subsonic and supersonic jets with both primary and secondary gases of the same species. Velocity and temperature profiles were also measured at various axial positions.

Existing Phenomenological Theories

The study of turbulent flow problems generally

requires the application of one of the following semi-empirical theories:

1. Momentum transfer theory due to Prandtl.
2. Modified vorticity transfer theory due to Taylor.
3. One of the various exchange coefficient theories due primarily to Reichardt.

The basic purpose of each of these theories is to relate the turbulent shear mechanism to mean flow properties so that the differential or integral equations describing the problem may be solved. In a sense each of these theories is somewhat unrealistic (i.e., it has been experimentally verified (14), (15), (17), (13), (19), (20) that both the mixing length and the exchange coefficient vary over the flow field), although certain modifications of these ideas can produce reasonably good results.

Prandtl's momentum transfer theory is based on the hypothesis that a quantity of fluid moves through a stream region as an entity, retaining its original momentum until it traverses one "mixing length". At this point, the fluid then mixes with the surrounding fluid, causing a local velocity fluctuation proportional to the difference between the initial and final mean flow velocities. This theory suffers from the major drawback that it predicts similar rates of transfer of momentum and energy, whereas experimental investigations (14), (15), (17), (18) show that energy transfer is more rapid than that of momentum.

The general vorticity transfer theory simply assumes vorticity to be conserved through the mixing process. Since no practical calculations can be made on this basis, Taylor proposed a modified vorticity transfer theory which is essentially the same as the Prandtl theory except that we are now concerned with vorticity instead of momentum components. This theory does predict different spreading characteristics for velocity and temperature, but does not give prediction of profiles which are in as good agreement with experiment as does the momentum transfer theory.

The constant-exchange-coefficient theory and its modifications suffer from lack of physical interpretation, but seem to give by far the best agreement with experiment (15).

In all three theories the turbulent shear stress is written $\tau = \varepsilon\rho\frac{\partial\bar{u}}{\partial r}$ (by analogy to $\tau = \mu\frac{du}{dr}$ in the laminar case) where ρ = gas density, $\frac{\partial\bar{u}}{\partial r}$ = mean velocity gradient, and τ = turbulent shear stress. The fundamental question concerns the nature of ε, which, unlike the viscosity μ in laminar flow, is not a simple property of the fluid. Notice the dimensional equivalence of ε to a kinematic viscosity. This quantity is described by the theories in question as follows:

1. <u>Momentum transfer theory</u>: $\varepsilon = l^2\frac{\partial\bar{u}}{\partial r}$
   which makes $\tau \sim \left(\frac{\partial u}{\partial r}\right)^2$

2. Modified vorticity transfer theory: $\mathcal{E} = -\ell^2 \frac{\partial}{\partial r}\left(r \frac{\partial \bar{U}}{\partial r}\right)$ Thus $\tau = \ell^2 \rho \frac{\partial \bar{U}}{\partial r} \frac{\partial}{\partial r}\left(r \frac{\partial \bar{U}}{\partial r}\right)$. However, τ is still proportional essentially to $\left(\frac{\partial \bar{U}}{\partial r}\right)^2$, with an additional second derivative term which is usually quite small.

3. Modified Exchange Coefficient Theory: $\mathcal{E} = K R_c^M U_c$ where U_c is the centerline value of the velocity at a given axial location and $R_c^M = R_c^M(\xi)$ = the outer momentum jet boundary. The basic point here is that τ is linearly proportional to $\frac{\partial \bar{U}}{\partial r}$. This expression, simple as it is, seems to provide best agreement with experimental results.

2. Analysis

There are three well-known analytical methods for the study of mixing in a turbulent free jet. The first method is a point-source diffusion of momentum, mass, and temperature. This method is only valid for large downstream distances (18) and hence is not applicable in the regions of greatest interest near and around the nozzle exit.

The second method involves a solution of the boundary layer form of the Navier-Stokes equations, using one of the various transport theories to relate the turbulent shear stress to the other flow properties. These transport theories are:

(a) Momentum transport, using the mixing length concept.

(b) Vorticity transport, using a similar mixing length concept.

(c) Exchange coefficient theory, using a form analogous to thermal conduction and diffusion for turbulent momentum transfer.

(d) Von Karman similarity theory (21).

(e) Statistical theory (10), (21).

The third method involves the solution of a set of integral equations of the von Karman type (22).

Of the three methods, the last is by far the simplest and most applicable to the present study. The integral analysis leads to a series of simultaneous integro-differential equations which present relatively minor mathematical difficulties (23), (24) compared to the basically non-linear Navier-Stokes equations. The integral analysis, of course, suffers from the disadvantage that while differential equations require only certain boundary values, the integral equations require both boundary values and specification of a set of initial profiles for the field variables. However, since the various profiles were measured with excellent accuracy (see data to follow) and since integral analyses are generally quite insensitive to the shape of the initial profiles (19), the choice of the integral method appeared justified.

Equations of Turbulent Mixing

We now consider the rather general problem of the subsonic turbulent mixing of a partially-ionized gas with a cool gas stream under conditions of axial symmetry as shown in Figure 1. The equations presented here in final, non-dimensional form are derived in Reference 5. Quantities

are defined in the List of Symbols, Section V-F

1. Argon - Argon Ion - Electron Continuity:

$$\int_0^{R_o^c} \frac{\partial}{\partial \xi}\left[f(c,\theta)\frac{U}{\theta}\right] R\,dR = \frac{1}{i_o}\int_0^{R_o^c} \frac{\partial}{\partial \xi}\left[\frac{cU}{\theta}\right] R\,dR$$

2. Helium Diffusion:

$$\frac{\partial}{\partial \xi}\int_0^{R_o^c} \frac{cU}{\theta} R\,dR = \left[\frac{c R_o^c}{\theta N_{Re} N_{Sc}} \frac{\partial c}{\partial R}\right]_{R=R_o^c}$$

3. Momentum:

$$\frac{\partial}{\partial \xi}\int_c^{R_c^M} \frac{fU^2}{\theta} R\,dR = \lambda \frac{\partial}{\partial \xi}\int_0^{R_c^c} \frac{fU}{\theta} R\,dR + \frac{\Gamma}{N_{Rer}}\left[\frac{fR^2}{\theta}\frac{\partial U}{\partial R}\right]_{R=R_o^M}$$

4. Energy:

$$\frac{\partial}{\partial \xi}\int_0^{R_o^E} \frac{fUh(c,\theta)}{\theta} R\,dR = \frac{R_c^E}{N_{Re} N_{PR}}\left\{\left(\frac{d\theta}{dR}\right)_{R_o^E} + \frac{R_o^E}{2}\left(\frac{d^2\theta}{d\xi^2}\right)_{R=0} + \left(\frac{d\theta}{d\xi}\right)\left(\frac{dR_o^E}{d\xi}\right)\right\}$$

5. Spreading Relations:

$$\frac{R_o^E}{R_o^M} = 1 + A_1\xi \qquad \frac{R_o^c}{R_o^M} = 1 + A_2\xi$$

Assumptions

The following assumptions were used in the analysis. Each assumption is followed by a statement of its justification.

1. No Pressure Gradients: The pressure in a free jet of low subsonic flow is essentially constant.

2. Equilibrium: This assumption is necessary in order to (a) calculate a temperature and (b) allow the use of an equation of state for the multicomponent gas.

Justification for use of the equilibrium condition is given in Section III-C.

3. No External Body Forces: There were no electric or magnetic fields applied to the flow, and the effects of gravity were certainly negligible.

4. Steady: Although not applicable on a small time scale, time-averaged quantities were considered steady. This was experimentally verified by comparing integrated instantaneous data records with time-averaged values.

5. Argon Singly-Ionized Only: The temperatures were much too low for the appearance of appreciable doubly-ionized argon (25), (26).

6. Helium Does Not Ionize: The temperatures were also too low for ionization of helium.

7. Neutral Plasma: Since the argon was singly-ionized only, and there were no fields present to cause charge separation, the number of positively-charged ions was equal to the number of negatively-charged electrons in every region of the flow. The Debye length was much smaller than the characteristic dimension for temperatures of interest.

8. Perfect Gas: At the low particle density prevailing, the accuracy of this assumption was at least as good as that of the measurements.

9. "Incompressible" Fluid: Mach number < 0.1. Thus the test medium was a variable-density (due to temperature and concentration changes) "incompressible" fluid.

10. Stagnation Temperature Equal to Static Temperature; Again, Mach number < 0.1.

11. Prandtl and Schmidt Numbers Less Then Unity: This was required by the form of the spreading relations. Experimental data have justified this assumption. Also see (14), (15) and Table 3.

12. Frozen Flow Between Boundaries: This condition did not actually exist, but because the different boundaries were so very close to each other, as verified by experiment, the effects of changes between the boundaries may be neglected.

13. Axially Symmetric Flow: This was verified experimentally.

14. Profiles in the Mixing Region were Similar: See (27) and (19). It should, however, be pointed out here that the profiles were definitely dissimilar in the so called "potential core" near the jet exit, and the similarity assumption was therefore not used in the potential core. Experimental profiles in the main mixing region were observed to be strikingly similar.

15. Inertial Frame of Reference: The boundaries which determine the frame of reference were fixed (i.e., did not accelerate).

16. Profiles May be Represented by Cosine Functions: See (27) and (19). Further, the experimentally-observed profiles (see data) were in reasonable agreement with this assumption.

17. Shear Work Term Negligible in Energy Equation: An order-of-magnitude analysis demonstrated that this term was 10^{-3} of the conduction terms.

18. No Chemical Effects Other than Ionization: Both argon and helium are inert, monatomic gases and the impurity level was too low to require consideration.

19. Radiation was neglected as a Mode of Energy Transfer: This is discussed in Section III-D.

20. Reichardt Theory was Used: As discussed earlier, this model appeared to provide the best agreement with experiment (15).

As a result of these conditions, the problem essentially represents an extension of the previous work in the field of turbulent mixing in several ways:

(a) Variations in composition, temperature, and velocity were considered simultaneously.

(b) Effects of ionization, very high temperature, and extreme temperature gradient were examined.

(c) Plasma-to-gas heat transfer was significant.

Nature of The Solution:

A detailed description of the numerical solution on the IBM 1620 and Control Data Corporation 1604 computers is given in Reference (5). The basic concepts of this solution are considered here.

Due to the immense mathematical difficulties associated with even the simplest description of multi-component turbulent mixing, a closed-form analytical description is practically impossible without recourse to rather unrealistic assumptions (23), (28). Thus, a method requiring a numerical solution on high-speed digital electronic computers was employed. While numerical solutions do suffer from the difficulty that no direct functional dependence can be obtained, it must be realized that at present the knowledge of turbulent transfer processes at very high temperature is quite meager and realistic functional solutions do not appear to be possible.

The fundamental method of solution of the integral equations was by successive Weddle-rule numerical integrations (29) of variables with respect to the radial coordinate at a fixed axial coordinate (see Reference (5)). Initial profiles (i.e., at the nozzle exit, $x = 0$) must be specified*. From this start, the equations result in a matrix of derivatives of the field variables with respect to the axial coordinate. The coefficients of the matrix are themselves integrals in the radial coordinate whose upper limit is one of three outer jet boundaries. These boundaries are unknown functions

---

* These initial profiles were obtained from the experimental measurements. Other experimental inputs necessary to obtain the solutions appear in Table I.

of axial position but do obey the boundary condition that they all shall be unity (i.e., the non-dimensional equivalent of the physical nozzle radius) at the nozzle exit $\xi = 0$. With these initial constraints, the first set of derivatives may be calculated, and upon application of the Runge-Kutta technique, new properties at $\xi = \Delta\xi$ are determined. There are six equations in the six dimensionless unknowns:

(a) Helium concentration, C_{He}

(b) Velocity/(Velocity on the centerline at x = 0), U

(c) Temperature/(Temperature on the centerline and at x = 0), Θ

(d) (Outer concentration boundary)/(Primary nozzle radius), R_o^c

(e) (Outer momentum boundary)/(Primary nozzle radius), R_o^m

(f) (Outer energy boundary)/(Primary nozzle radius), R_o^e

Thus the solution is uniquely determined provided the equations are independent. This solution at $\xi = \Delta\xi$ then yields new values for the upper limits of the integral coefficients and the solution continues to propagate along the axial coordinate, continuously calculating new values for the field variables c, u, and Θ. The region of interest for such solutions was within $R = \pm 2$ and for ξ (x/nozzle radius) from zero to eight. Beyond $\xi = 8$ the jet was essentially decayed.

The Matrix

Upon differentiating the integral equations within the integrals themselves (using Leibniz's Rule) a

resulting set of integro-differential equations was obtained of the form (see Equation B-47, Reference (5)).

$$a_{1,1}\left(\frac{dU_2}{d\xi}\right)+a_{1,2}\left(\frac{dC_2}{d\xi}\right)+a_{1,3}\left(\frac{d\theta_2}{d\xi}\right)+a_{1,4}\left(\frac{dR_e^M}{d\xi}\right)+0=a_{1,5}$$

$$a_{2,1}\left(\frac{dU_2}{d\xi}\right)+a_{2,2}\left(\frac{dC_2}{d\xi}\right)+a_{2,3}\left(\frac{d\theta}{d\xi}\right)+a_{2,4}\left(\frac{dR_0^M}{d\xi}\right)+0=a_{2,5}$$

$$a_{3,1}\left(\frac{dU_2}{d\xi}\right)+a_{3,2}\left(\frac{dC_2}{d\xi}\right)+a_{3,3}\left(\frac{d\theta}{d\xi}\right)+a_{3,4}\left(\frac{dR_0^M}{d\xi}\right)+0=a_{3,5}$$

$$a_{4,1}\left(\frac{dU_2}{d\xi}\right)+a_{4,2}\left(\frac{dC_2}{d\xi}\right)+a_{4,3}\left(\frac{d\theta}{d\xi}\right)+a_{4,4}\left(\frac{dR_e^M}{d\xi}\right)+a_{4,5}\left(\frac{d\theta}{d\xi}\right)\left(\frac{dR_0^M}{d\xi}\right)=a_{4,6}$$

where $U=U_1(R,R_0^M)U_2(\xi)$ $C_e=C_1(R,R_0^C)C_2(\xi)$ $\theta=\theta_1(R,R_0^E)\theta_2(\xi)$

Inspection of this matrix immediately indicates a non-linearity due to the presence of the term in $\left(\frac{d\theta_2}{d\xi}\right)\left(\frac{dR_e^M}{d\xi}\right)$ However, this set is in fact "quasi-linear", that is, if we apply Cramer's Rule to the first three equations (i.e., striking out the fourth row and fifth column) there exists a set of three equations in four unknowns. While this is indeterminate, by using the methods given in Reference (5) one may solve for $\left(\frac{dU_2}{d\xi}\right)$, $\left(\frac{d\theta_2}{d\xi}\right)$ and $\left(\frac{dC_2}{d\xi}\right)$ in terms of linear combinations of $\left(\frac{dR_e^M}{d\xi}\right)$ Then, upon substitution of these relations into the fourth equation, all terms are linear in $\left(\frac{dR_e^M}{d\xi}\right)$ except for the fourth, which is quadratic in $\left(\frac{dR_e^M}{d\xi}\right)$. Hence $\left(\frac{dR_e^M}{d\xi}\right)$ is now the unknown

in a simple quadratic equation and may readily be computed in terms of the various integral coefficients (see Equation B-56, Reference (5)).

Nevertheless, as $\left(\frac{dR_o^n}{d\xi}\right)$ is now the solution to an algebraic quadratic equation, there are in general two distinct roots. However, as there is dissipative shear between the high-velocity primary jet and the low-velocity secondary jet, the primary jet must accelerate the secondary flow at the expense of its own momentum. Acceleration of the secondary flow to a velocity greater than U_∞, which was its initial value, insures an outward spread of velocity. Since the velocity boundary is defined as the locus of points nearest to the centerline at which $U = U_\infty$, it is clear that in all physical situations R_o^n must increase with axial position. Thus the only physically significant solution is that which has a positive value for $\left(\frac{dR_o^n}{d\xi}\right)$.

However, there are still two problems to be considered. The first of these is the possibility that both roots are positive numbers. Fortunately, this did not occur in any of the numerical solutions despite the use of a wide range of input parameters. This does not, however, preclude such a possibility. The physical interpretation of a doubly-positive set of roots is not clear, and may be worthy of further investigation.

A second difficulty which did appear in a few of the numerical solutions concerns the discriminant $\frac{1}{4}[\alpha(a_{i,j})]^2 - \beta(a_{i,j})$ of the quadratic (Equation B-56, Reference (5)). If $4\beta > \alpha^2$ the root is imaginary, and $\left(\frac{dR^n_e}{d\xi}\right)$, and therefore all the other axial derivatives of the field variables, become complex numbers with an imaginary part. Since such results (i.e., complex values of velocity, temperature and concentration) appear to have no direct physical significance, such solutions were considered meaningless. The physical interpretation of these solutions may also bear further study.

The stability, or presence of "meaningful" solutions in the sense of the above discussion, is related to the integral coefficients which are correspondingly related to various input parameters. Since the purpose of the analytical study was primarily to furnish information on the nature of the turbulent mixing process, a complete investigation of "meaningless" or "unstable" solutions has not been performed. However, certain broad and rather significant conclusions may be drawn:

1. The boundaries must be reasonably close to each other. Whenever large values of A_1 or A_2 were used (corresponding to boundaries greatly separated at reasonable axial positions) solutions were of the "unstable" type. This might well be the result of severe violation of the assumption of frozen flow between the boundaries.

2. Large values of the forcing functions; i.e., small values of the equivalent turbulent Reynolds numbers, resulted in "unstable" solutions.

3. Excessive dominance of any one transfer process (i.e., material diffusion, momentum transport, or turbulent heat transfer) expressed via the driving parameter, resulted in "unstable" solutions. Specifically, "unstable" solutions were found to occur whenever

(a) $A_1 > 0.0080$
$A_2 > 0.0100$

(b) $N_{Re_D} = N_{Re} N_{PR} = N_{JA} < 200$
$N_{Re_T} < 200$
$N_{Re} N_{PR} = N_{Pe} < 200$

(c) Cases in which any one of the parameters N_{JA}, N_{Re_T}, N_{Pe} differed by more than a factor of 10 from any other.

The accuracy of a numerical solution, particularly those involving repeated numerical integration schemes and the Runge-Kutta method,is always subject to question. The best method of checking the extent or at least the nature of the error is by using finer and finer increments. It was found that variation of increment or "mesh" size over an order of magnitude had no effect on the solution beyond the fifth digit after the decimal point. This excellent accuracy was probably due to the smooth, monotonic, single-valued nature of all the various functions employed.

Finally, the assumption of "similar solutions" (i.e., functionally similar, affinely related profiles) for the field variables must be considered. The work of Squire and Trouncer (27) indicates that the solutions are similar in the mixing region, but are not similar in the potential core. This was observed experimentally. Thus, in order to obtain a more physically reasonable solution it was necessary to include a potential core. However, as the number of available equations had been exhausted, it was necessary to do this empirically. Reduced experimental data provided the necessary information. This somewhat arbitrary constraint was then included in the program for the numerical solution. Comparison of results with and without a potential core indicated that there was little or no effect on spreading, although there was observed the anticipated effect upon both initial radial profiles and initial axial decay. To provide a bit more generality, the length of the cone-shaped core was allowed to vary. This variation had little effect on the nature of the radial spreading of velocity, concentration, and temperature.

The numerical results of this analysis and their comparison with experimental data are given later in Section IV.

B. Laminar Transport Properties

Considerable theoretical study and analysis of the transport properties for helium and ionized argon

mixtures was performed during the contract period. This work is shortly to be completed, and a technical report presenting the analysis and results will be issued at that time. An introductory statement of the problem and the methods of attack are presented here. Figures 2 and 3 show the results of viscosity calculations (typical of the general class of transport property results to appear in the forthcoming technical report.)

1. The Problem

The problem considered here is the determination of the viscosity, thermal conductivity, diffusion, and thermal diffusion coefficients of argon-helium mixtures at temperatures up to 15,000°K and pressures around one atmosphere. At the high temperature end of this region, a considerable fraction of the argon is singly ionized. The helium, having a much higher ionization potential, can be considered as inert. The fraction of doubly ionized argon is negligible.

2. Composition

Since the mole fraction of argon atoms or ions with excited electronic states is always small compared to the mole fraction in their ground states, the composition of the mixture could be considered as a four component system consisting of the following:

(a) Argon atoms (ground state)

(b) Argon ions (singly ionized in their ground state)

(c) Electrons

(d) Helium atoms (ground state)

The system was also considered to be in thermal equilibrium, as will be discussed in III-C. The mole fractions of argon neutrals, argon ions and electrons was obtained from the statistical mechanics computation of (30) and (31) using the expressions

$$\frac{X_e}{X_a} = 2.309 \times 10^{-6}\left(\frac{1}{P}\right)T^{2.551}\exp\left[-\left(\frac{1.828 \times 10^5}{T}\right)\right]$$

where P = pressure in atmospheres

T = temperature in ^{o}K

X_e = mole fraction of electrons or argon ions

X_a = mole fraction of argon neutrals

This is essentially the Saha equation with empirical corrections for the effect of the electronic partition functions. It should be pointed out that an uncertainty in the results exists because of the arbitrary position of the cutoff in the argon electronic partition function. This uncertainty is not large, however, and is not felt to appreciably affect the subsequent calculation of the transport properties.

3. Transport Property Theories

The difficulties encountered in the calculation of transport properties can be grouped into three types:

(a) The obtaining of a suitable theory.

(b) The obtaining of the physical information needed by the theory; e.g., collision cross sections.

(c) Carrying out the complex calculations.

The theories for the computation of transport properties can be divided into two groups, the formal or "exact" theories and the admittedly approximate ones. For any exact theory, and probably for the approximate ones, the labor of computing the transport properties of multicomponent mixtures is so enormous that the use of electronic computers is essential. All the computations were performed on an IBM 1620 digital computer.

Obtaining the physical information used by the theory is usually the most difficult part of the entire procedure. Since the information is usually fragmentary or unavailable, considerable personal judgment enters into this phase. As an illustration of the possible difficulties in the interaction of an argon atom with an argon ion at energies corresponding to the temperatures of interest (1 to 2 electron volts), the long-range polarization force is not important, but it is nevertheless considered so in certain references.

In the computation of the transport properties of an ionized or partially ionized gas the difficulty of obtaining a suitable theory arises. For neutral rare gases at temperatures and pressures where they are nearly perfect gases, the transport properties can be rather accurately computed by the use of the Chapman-Enskog theory (32, 33). The mechanics of using this theory have been so developed (33) that its use by engineers in accurate computation of transport properties is nearly universal. Unfortunately in applying this technique to ionized and partially ionized gases, problems arise which at the very least make the computations more difficult, and perhaps throw the reliability of the entire method in doubt.

The Chapman-Enskog method is derived from the Boltzmann equation in which the collision term considers only binary collisions. It is assumed that during most of the time a particle exists it is far enough from the other particles that the effect of their intermolecular force fields on the trajectory of the particle is negligible. Then events occur in which two particles pass so close together that we can say an encounter or collision has occurred. It is assumed that the likelihood that three or more particles will be close enough to significantly influence each other's paths is negligible compared to the two-body collisions. The derivation of the Chapman-Enskog

theory leads to the "collision cross sections" and "collision integrals" by which the specific intermolecular forces enter into the computations. When the coulombic potential is introduced, the collision cross sections and collision integrals become divergent as the integration is extended to large "impact parameters" (the minimum distance the two particles would approach one another if their paths had not been deflected). This is overcome in (32) by cutting off the integration at the mean interparticle distance. It is probably more accurate to use the Debye length as the cutoff.

This difficulty is, however, symptomatic of the unusual properties of the Coulomb potential. This potential falls off so slowly compared to the usual intermolecular potential that the cumulative effects of long-range weak interactions on the trajectory of a charged particle are greater than the effect of "collisions" (34, 35). The differences in the behavior of plasmas, even without externally applied electric and magnetic fields, from that of ordinary gases is so great that a new kinetic theory is really needed to deal with them. Since this has not been developed to the point that it can be used to compute transport properties, ordinary kinetic theory with suitable alterations was used.

A second difficulty with the Chapman-Enskog method is that almost all computations use only the lowest approximation in the variational scheme of (33). This is usually sufficient to give excellent results, but for plasmas, at least a second approximation should be made for the diffusion coefficients (36, 37).

In an ordinary gas the only important characteristic distance is the mean interparticle distance. In a plasma the important characteristic distances are

(a) The mean impact parameter for a 90^{o}deflection,P

(b) The mean interparticle distance d.

(c) The Debye length λ .

For most plasmas of interest,

$$p_o << d << \lambda$$

Out to p_o the collisions are of the strong-encounter, two-body type considered in ordinary gases. Beyond the Debye length the effect of a particle is assumed to be shielded, and particles beyond are assumed not to have an effect in the computation of transport properties (34). The important regions are between the Debye length and the mean interparticle distance and between this distance and p_o. To handle this weak interaction successfully, a model has been developed which uses instead of the ordinary Boltzmann equation with a binary-encounter collision term, a Boltzmann equation with a special collision term supposedly more suitable, called the Fokker-

Planck equation (34, 35). This has been used thus far to compute the transport properties of fully ionized gases. When the results are compared to those of the Chapman-Enskog theory, suitably carried out to enough approximations (37), similar results are found.

There are numerous approximate schemes for computing transport properties based on mean free path concepts, etc., which may or may not use refinements like persistance-of-motion corrections. It is generally known that these methods can be fairly successful for viscosity and thermal conductivity calculations, but are poor for diffusion. A "Relaxation Time" method was used in the present analysis for the computation of viscosity. The results agree fairly well with results of the complex Chapman-Enskog method, as can be seen from Figures 2 and 3.

C. Arcjet Equilibrium

1. Introduction

The state of a fluid in a region can not be in equilibrium if there are finite gradients of temperature, composition, or velocity. The equilibrium state for a fluid in a small region, nonetheless containing many molecules, is that state the fluid would eventually approach were it suddenly isolated. For a great number of problems the actual values of quantities such as density, mole fractions, translational energy, internal energy, etc. are negligibly different from equilibrium values so that these flows are called "equilibrium" flows. One could relax the criteria to all flows in which the differences from equilibrium were at most only a few percent from equilibrium values. The latter criterion is the one used in this work.

2. Problem

The problem considered here is whether the argon plasma generated in a plasmajet under certain conditions is in equilibrium as it leaves the nozzle of the plasmajet, and if it remains in equilibrium as it is rapidly cooled in the mixing region downstream. The flow is at low subsonic Mach numbers, and thus is at ambient (in this case atmospheric) pressure. The peak temperature of the jet leaving the nozzle is about $14{,}000^{\circ}K$.

Two modes of operation are considered, turbulent and laminar. In the former case peak flow velocities are about 500 ft/sec, mass flows around 4×10^{-3} lb/sec, current about 2000 amp, and voltages about 30 volts. The nozzles used had a length of eight inches from

the arc to the nozzle exit. In the laminar case the velocities are much lower, the flow rates about 5×10^{-4} lb/sec, the current about 500 amp, and the voltages about 25 volts. The nozzles used are about 1 1/2 inches long. Thus the times spent in traveling between the arc and the nozzle exit are about the same in both cases. The gradients in the mixing region will be more severe in the turbulent flow; hence "equilibrium" of the turbulent jet is the limiting case. Equilibrium of the turbulent jet was investigated in Ref. (2). This analysis is an improvement of the treatment used therein.

For this problem the criteria for equilibrium can be stated (39) as:

Are the mole fractions of argon neutrals, argon ions, and electrons near equilibrium?

Are the electron and ion temperatures close?

Are the populations of the excited electronic states near equilibrium?

The concept of different electron and heavy-particle temperatures results from the extreme ineffectiveness of energy transfer in electron-heavy particle elastic collisions compared to that in collisions between particles of equal mass. The electrons rapidly attain a near-Maxwellian distribution after a few electron-electron collisions, and the heavy particles also attain a near-Maxwellian distribution after a few heavy particle-heavy particle collisions. However, the two distributions can correspond to different temperatures, called the electron and the heavy-particle temperatures respectively. It takes the order of 40,000 electron-heavy particle

collisions to "thermalize" an electron.

3. The Physical Processes

Energy is added to the gas as it passes through a DC arc struck between a tungsten cathode and a copper anode. Both electrodes are internally water cooled. Almost the entire current consists of electrons. It is believed that the electrons are thermionically emitted from the cathode. Note that a current of 2000 amperes corresponds to about 10^{22} electrons/sec.

The energy of the arc first goes into increasing the electron translational energy. Many ions may be formed by the electrons in the arc and many are formed by thermal ionization downstream of the arc. At argon flow rates of 4×10^{-3} lb/sec the number of ions that must be created for a 15,000°K jet in equilibrium is 2.6×10^{22}/sec. It is clear that because there is always such a large number of electrons present, atom-atom ionization will be negligible compared to electron-atom ionization. It will be shown that thermal ionization by electrons is sufficient to produce the required number of ions.

The cross section for the ionization of a ground state argon atom by an electron is fairly well known. Fox (40) and Tozer and Craggs (41) show a roughly linear rise in cross-section from a threshold at the ionization potential. Petschek and Byron (39) use a cross-section with a threshold at the critical potential, 11.5 electron-volts. This they attribute to a multiple-stage ionization process. The lower number of atoms in the excited states is balanced

by the increased number of electrons capable of ionizing the excited states as compared to the ground state. The cross section for ionization of an excited state is probably higher than that for the ground state (42). For an optically thin plasma the excited atom populations could be much smaller than the equilibrium values because of the relative decrease in radiative excitations as compared with radiative decay of the excited states. In this case, collisional excitation must be sufficient so that the spontaneous radiative decay does not depopulate the excited levels. Typical lifetimes for the excited states before radiative decay are 10^{-6} to 10^{-8} sec. (43). This is short. However, there are at least two mechanisms which increase the effective lifetimes: first, argon has metastable excited states, and second, under the conditions of the problem the "mean free path" of resonance radiation is extremely small. Thus the energy must be passed from atom to atom before leaving the plasma, and it therefore appears likely that most ionization will occur via at least a two-step process.

The ionization process removes 15.75 electron-volts per ion from the translational energy of the electrons. It is reasonable to believe that the bulk of the electrons will not have energies above the critical potential of argon, 11.5 electron-volts, due to inelastic collisions, and hence it is quite conservative to consider that electrons lose their translational energy (from 11.5 electron-volts to thermal energies) only by elastic collisions. The electron-ion cross section is so much larger than the electron-atom cross section that we may ignore energy transfer by the latter-type collisions. It has been computed(44) that at only 0.1%

ionization, electron-ion energy transfer by elastic collision is equal to the electron-atom energy transfer.

In the mixing region of the case under consideration, energy is lost by the heavy particles to the atoms of a cool outer helium flow. The electrons must transfer their energy to the atoms or ions in order to keep the electron temperature close to the heavy particle temperature. As the temperature falls, the equilibrium concentration of electrons falls, requiring that the electrons recombine with the ions. Unfortunately, even today the subject of electronic recombination in rare gases is not well understood. Physicists have devoted a great deal of effort to this subject, but all too often their results confuse rather than clarify. As an illustration of the difficulties, 20 years ago the accepted rate of recombination in argon was 1/1000 the presently accepted value. The rate of recombination is usually given by

$$\frac{dN_e}{dt} = -\alpha N_e N_i = -\alpha N_e^2 \quad (N_e = N_i \text{ , quasineutrality condition}).$$

The recombination coefficient, α , is a strong function of the temperature and also a function of the electron density. Most of the measurements of α were at low temperatures and low electron densities. Drastic extrapolations are needed to obtain values for plasmajet conditions.

Even if accurate experimental values of the recombination coefficient for the conditions of interest existed, it would still be of great value to know the type of mechanisms predominating. If the energy released by the recombination does

not go back into electron kinetic energy, but is either lost to the plasma by radiant emission or goes into heavy particle kinetic energy, the electron temperature will more closely follow the heavy particle temperature.

The presently accepted recombination mechanisms for argon are: (a) radiative recombination, (b) dielectronic recombination, (c) dissociative recombination, and (d) three body recombination. Radiative recombination involves the collision of an electron and a positive ion with the radiative emission of energy. This mechanism has been studied using quantum mechanics. For the hydrogen atom, tables of recombination coefficients exist, together with a breakdown of the relative importance of the recombination to the various energy levels of the atom, (45, 46). They show that in hydrogen large fractions of the recombination are to the ground state and the other low levels. Values of the radiative recombination rate α_r appear below

RADIATIVE RECOMBINATION COEFFICIENT α_r IN HYDROGEN (8, 9)

Temperature (°K)	α_r (cm.^{3}/sec.)
8,000	4.83×10^{-13}
16,000	2.93×10^{-13}
32,000	1.72×10^{-13}

From the results given in (45) and (46), it appears the recombination coefficients for the rare gases are close to that for hydrogen. If

this is the case, then radiative recombination will be a small but not negligible part of the total recombination.

Dielectronic recombination involves the collision of an electron and a positive ion in which the two are bound in a level above the ionization potential. This may occur, for example, by excitation of two electrons. In order for the recombination to proceed, this level must be deexcited by either radiative emission or by superelastic collisions before it reionizes. Quantitative models for dielectronic recombination are very crude, but it appears that the rates are at most as large as those of radiative recombination. At high temperatures and high electron densities dielectronic recombination is probably negligible.

In the past fifteen years experiments in which cold argon at low pressures was ionized by microwave pulses seemed to indicate that the dominating mechanism was dissociative recombination (52). The existence of rare gas molecular ions has been verified. According to this model, the recombining electron dissociates the molecule, transferring its energy into breaking the molecular bond, translation of the atoms, and electronic excitation. Most of the energy probably appears as electronic excitation.

In order that this mechanism be the dominant mechanism for recombination in a near-equilibrium plasma, the inverse process, associative ionization,

$$A + A \longrightarrow A_2^+ + e$$

must be the dominant mechanism of ionization, in accordance with the principle of detailed balancing. This mechanism has not been

reported to be important in rare gases. If we consider that the formation of A_2^+, such as by three body collisions of the type

$$A + A^+ + M \rightleftharpoons A_2^+ + M$$

where M is some third body,

are very rapid we can write an equilibrium relation for $N_{A_2^+}$:

$$K_{(T)} = \frac{N_{A_2^+}}{N_A N_{A^+}}$$

To compute the value of the equilibrium constant, $K_{(T)}$ we need the value of the binding energy and other molecular constants. The binding energy for He_2^+ is about 2.1 e.v. (11), so if we assume that the formation of A_2^+ is comparable, we take its binding energy at about 2 e.v.. It can be shown that although $K_{(T)}$ is very small at high temperatures, it can be quite large at low temperatures. Hence in the microwave experiments, since $K_{(T)}$ and N_{A^+} (compared to N_A) are large, $N_{A_2^+}$ can be large, and dissociative recombination will dominate. At plasmajet conditions, however, the mole fraction of A_2^+ is estimated at 10^{-5} to 10^{-6}. Although small, this mole fraction is not so small that dissociative recombination can definitely be neglected. If the cross section for dissociative recombination of A_2^+ is large, this mechanism can still be important. The uncertainties are thus so great that it can not be determined if dissociative recombination in argon at plasmajet conditions is negligible, significant, or dominant.

In the past few years there has been a great deal of work on the study of three body recombination

$$e + e + A^+ \rightleftharpoons A + e$$

For the hydrogen atom (46) gives the recombination coefficients listed in below.

THREE BODY RECOMBINATION COEFFICIENT FOR HYDROGEN

($cm.^3/sec.$)

ELECTRON DENSITY ($cm.^{-3}$)	TEMPERATURE (^oK)		
	8000	16,000	32,000
10^{16}	8.4×10^{-11}	5.0×10^{-12}	7.3×10^{-13}
10^{17}	3.4×10^{-10}	1.4×10^{-11}	1.8×10^{-12}
10^{18}	2.5×10^{-9}	9.6×10^{-11}	1.2×10^{-11}

Extrapolations of values for helium (47) give $\alpha \approx 10^{-11}$ $cm.^3/sec$ for $N_e = 10^{17}$, T = 15,000 K, which is about the same as that for hydrogen. The three-body recombination coefficient for argon is also probably close to the values quoted in Table II for hydrogen. Existing models indicate that recombination directly to the ground or low-lying states is rare, but that most of the recombinations take place to intermediate levels. The inverse of this process, electron-atom collisional ionization, is generally accepted to be the dominant ionization process. It is most likely that in the present region of interest, this recombination mechanism is the dominant one.

By standards used in recombination studies, the jet exhaust must be considered as full of impurities. Although the rare gases have the lowest recombination coefficients, impurities

will accelerate the recombination. At low temperatures (5000°K) the impurities act as "seeding" materials for the production of electrons, and thus the electron concentration could be orders of magnitude higher than the equilibrium value for argon. However, the mole fraction of the electrons appears to be sufficiently small that their effect on the thermodynamic properties will not be significant.

4. Elastic Collisions

The problem of the rate of energy transfer by elastic collisions would be straightforward were it not for the unusual properties of the Coulomb potential. Because of the slow falloff of this potential, the effects of small deflection, long range encounters are more important than those of close encounters. Energy transfer by electron-atom collisions is negligible compared to electron-ion interactions if there is even 1% ionization. Since the important collisions are no longer of the two-body type, the Fokker-Planck equation can be used to treat this case. The results are essentially the same as those of Petschek and Byron (39).

Petschek and Byron's method consists of taking an expression for the energy transfer occurring in an elastic electron-ion collision of a given deflection, and suitably integrating over all collisions (39). The electrons are assumed to be in a Maxwellian distribution, and the electron mass is considered small compared to the ion mass. The result (37) is

$$\Delta E = \frac{N_e N_i}{M_i} e^4 \left(\frac{8\pi M_e}{kT_e}\right)^{\frac{1}{2}} \left(\frac{T_e - T_i}{T_e}\right) \ln\left[\frac{9(kT_e)^3}{8\pi N_e e^6}\right]$$

where ΔE = energy transfer per unit volume

N_e = electron particle density

N_i = ion particle density

M_e = electron mass

M_i = ion mass

k = Boltzmann constant

T_e = electron temperature

T_i = ion temperature

e = electron charge

(C. G. S. electrostatic units are used throughout this report). The above formula can be expressed by

$$\Delta E = C N e^2 \left(\frac{T_e - T_i}{T_e} \right)$$

where C is almost constant at 5×10^{-22} erg. cm.^{3}/sec.

Turning now to the method using the Fokker-Planck equation, assuming spacial homogeneity and no body forces, the Boltzmann equation for the electrons is

$$\frac{\partial f_e}{\partial t} = \text{electron-electron collision term} + \text{electron-ion collision term} + \text{electron-atom collision term}$$

Assuming a Maxwellian distribution of electrons, the electron-electron collision term is zero. We neglect the electron-atom collision term for even moderate degrees of ionization as discussed earlier. Using a Fokker-Planck form for the electron-ion collision term

$$\frac{\partial f_e}{\partial t} = -N_i \frac{\partial}{\partial \underline{v}_e} \cdot \int d^3 \underline{v}_i \left(M_i f_i \frac{\partial f_e}{\partial \underline{v}_e} - M_e f_e \frac{\partial f_i}{\partial \underline{v}_i} \right) \cdot \left(V_r V_r \underline{\underline{I}} - \underline{V}_r \underline{V}_r \right) \frac{V_r \sigma M_i}{2(M_i + M_e)}$$

where: $\underline{\underline{I}}$ = unit tensor

$\sigma = \dfrac{4\pi e^4}{V_e^4} \dfrac{(M_i + M_e)^2}{M_i^2 M_e^2} \ln \Lambda$ = cross section

$$\Lambda = \frac{3(kT_e)^{3/2}}{e^3\sqrt{4\pi N_e}}$$

V_r = relative velocity

Multiplying by $1/2\ M_e v_e^2$ and integrating over all electron velocities we obtain after considerable mathematical effort

$$-\frac{\partial}{\partial t}\int \frac{1}{2} M_e v_e^2 f_e d^3 v_e = \Delta E = \frac{N_e N_i}{M_i} e^4 \left(\frac{2\pi M_e}{kT_e}\right)^{\frac{1}{2}} \left(\frac{T_e - T_i}{T_e}\right) 2 \ln \Lambda$$

This result is essentially the same as that of (39). The slight difference in the logarithm is due to a difference in definition of the Debye length.

The enthalpy per unit volume of the electrons can be expressed by: $H_e = \frac{5}{2} N_e k T_e + E_i N_e$

where E_i = ionization energy per electron = 25.2×10^{-12} erg

Hence $\frac{dH_e}{dt} = \frac{5}{2} N_e k \frac{dT_e}{dt} + \frac{5}{2} k T_e \frac{dN_e}{dt} + E_i \frac{dN_e}{dt}$

Using $\frac{dN_e}{dt} = \frac{dN_e}{dT_e}\frac{dT_e}{dt} = 4 \times 10^{13} \frac{dT_e}{dt}$

We obtain $\frac{dH_e}{dt} = \left[\frac{5}{2} N_e k + \frac{5}{2} \times 4 \times 10^{13} k T_e + 4 \times 10^{13} E_i\right] \frac{dT_e}{dt}$

The first term represents the loss in thermal energy caused by the cooling, the second term represents the loss in thermal energy caused by the removal of some of the free electrons by recombination and the third term represents the loss of ionization energy of these

electrons. The relative magnitude of these terms is roughly in the ratio 1:4:16. From the experimental data of (5), estimates of $\frac{dT}{dt}$ can be made; e.g.,

$\frac{dT}{dt}$ = velocity x gradient of temperature along a streamline

Taking maximum values from (15), we select a speed of 15,000 cm./sec. (500 ft./sec.) and a temperature gradient of 15,000°K/cm. This results in a value for dT/dt of 2.3×10^8 °K/sec. which, for lack of more precise information, will be used as an extreme upper bound. The rate of electron enthalpy decay is given in below as a function of the rate of temperature decay and local electron temperature (the numbers in parentheses are the individual contribution of the three terms). Note that 1 kw/cm^3 = 10^{10} erg/cm^3 - sec.

RATE OF ELECTRON ENTHALPY DECAY

	Enthalpy Decay (kw/cm^3)		
dT/dt (°K/sec.)	T = 12,000°K	T = 13,000°K	T = 14,000°K
1×10^7	1.21 (.02 + .17 + 1.02)	1.24 (.04 + .18 + 1.02)	1.26 (.05 + .19 + 1.02)
5×10^7	6.05	6.20	6.30
1×10^8	12.10	12.40	12.60
2.3×10^8	27.80	28.50	29.00

The problem is now to relate the electron enthalpy decay rate $\frac{d\mathcal{H}_e}{dt}$ to ΔE. For example, if there were no net energy transfer by inelastic collisions, the two would be equal, whereas

if the recombination process resulted in the energy of the electron going entirely into heavy particle translational energy, then ΔE would be roughly equal to the first term in the expression for $\frac{d\,He}{dt}$

5. Energy Exchange Processes in a Plasma

To find the fraction of the enthalpy decay of the electrons which must be transferred by elastic collisions, a qualitative understanding of the processes that take place in the plasma as it cools is necessary, as well as some quantitative estimates of the relative importance of the various processes.

Although our knowledge of these processes is very incomplete, and it is therefore not certain that any model we may postulate will be realistic, it is nevertheless of interest to at least speculate on the order of magnitude of the energy exchange. We can proceed on this basis by grouping the various states into four energy levels: the ground state, the 4S levels or critical potential levels (some of which are metastable), the upper excited states, and the free electrons. The processes can then be pictured as shown in Figure 4.

Radiative recombinations to all but the ground state cause the bulk of the translational and ionization energy of the electron to be lost, because the plasma is optically thin for these wavelengths. Radiation resulting from recombination to the ground state will be absorbed and reemitted many times before it can escape from the plasma. This in effect lengthens the mean lifetime of the lowest excited states, the 4S levels, so that collisional deexcitation is the major means

of going from these levels to the ground state.

Atom-atom or ion-atom superelastic (deexcitation) collisions in which the electronic excitation energy is converted into translational energy would be helpful in reducing the required value of ΔF. However, the process of electron-atom collisional deexcitation has an advantage over the heavy particle collisional deexcitation, because of the higher electron thermal speeds, by a factor 269. Thus, in order for the two processes to be of equal magnitude, the ratio of heavy particle density, multiplied by its superelastic cross section, to the electron density, multiplied by the electron-atom superelastic cross section, must be approximately 269.

Some information about inelastic cross sections and transition probabilities exist. Transition probabilities for 18 transitions between 5P-4S, and 4P-4S levels are given in (43), ranging from $.368 \times 10^6$ to 43.2×10^6. Considerable information exists on the cross section for production of excited states from the ground state (49, 50, 51). Using the principle of detailed balancing,

$$\omega_i \, (E + E_T) \, \overset{j}{\underset{i}{Q}}_{(E+E_T)} = \omega_j \, E \, \overset{i}{\underset{j}{Q}}_{(E)}$$

where E_T = energy difference between states j and i

ω_i = statistical weight of state i

$\overset{j}{\underset{i}{Q}}_{(K)}$ = cross section for inelastic transfer from state i to j caused by collision of an electron of energy K,

we can obtain the superelastic collision cross section. Values range from about 10^{-18} cm.^{2} to 10^{-19} and lower for transitions

from excited states to the ground state.

Inelastic cross sections from excited states to other excited states are difficult to obtain experimentally. None is known to exist for argon. Atom-atom inelastic cross section data are very scarce. It is known that the superelastic collision cross section can be quite large if the energy difference between the two states is very small, but as the difference becomes large the cross sections drop sharply(45). As an example of values for small energy differences, (46) quotes values of about 10^{-15} cm.^{2} for transitions in helium involving energy changes less than 0.1 ev.

These rather sketchy data lead to the following conclusions:

(a) Electron-atom superelastic collisions are probably the major mechanism of deexcitation from the critical potential levels, and perhaps from the upper levels to lower levels, and to the ground state.

Superelastic collisions between heavy particles may play a part in transitions between excited states, but electron-atom superelastic collisions and radiative decay are probably most important.

If these conclusions are valid, most of the enthalpy decay of the electrons is transferred by elastic collisions to the heavy particles. Therefore, we take $\Delta E = \frac{d He}{dt}$

Thus

$$Te - T_i = \frac{\frac{d He}{dt} \times Te}{5 \times 10^{-22} \cdot N_e^2}$$

Values of $Te-Ti$ are plotted versus Te for various values of dTe/dt in Figure (5), where the relation between $\frac{dTe}{dt}$ and $\frac{dNe}{dt}$ has been given in Table III.

6. Ionization and Recombination

The rate of ionization by electron-atom collisions is given by

$$\frac{dNe}{dt} = \int_0^\infty N_A Ne \sigma_i V_r f_e \, dE$$

where N_A = number density of the neutral atoms

V_r = relative velocity of electron and atom $\approx V_e = \sqrt{\frac{2E}{M_e}}$

σ_i = effective ionization cross section

we have assumed the atoms are stationary compared to the electrons.

The electron distribution can be approximated by the Maxwellian distribution

$$f_e = \left(\frac{2\pi}{2\pi kTe}\right)^{3/2} e^{-E/kTe} E^{1/2}$$

The problem is therefore that of simply finding the correct value for $\sigma_{i(ve)}$ and integrating.

The behavior of σ_i at high energies is unimportant to the calculation because of the exponential in the integral. Petschek and Byron (39) use the linear approximation

$$\sigma_i = 7 \times 10^{-18} (E' - 11.5)$$

where E' is the electron energy in electron volts. This indicates a threshold at the critical potential of argon, and hence postulates a multiple-step ionization process. Unfortunately, the data on which this expression is based are old, and thus

questionable. More recent data (40, 41) are, unfortunately, for one-step ionization, having a threshold at the ionization potential, but may be used to establish a lower limit to the ionization rate:

$$\frac{d\sigma}{dE'} = \begin{cases} 13 \times 10^{-8} \text{ cm}^2/\text{E.V.} & 15.75 < E' < 16 \text{ E.V.} \\ 18 \times 10^{-8} \text{ cm}^2/\text{EV} & E' > 16 \text{ E.V.} \end{cases}$$

Petschek and Byron's cross-section gives

$$\left(\frac{dNe}{dt}\right)_1 = 8.75 \times 10^{-6} N_A N e \left[\frac{2(kTe)^3}{\pi Me}\right]^{\frac{1}{2}} \left(\frac{T_c}{T} + 2\right) e^{-\frac{T_c}{T}}$$

where $T_c = E_c/k = 1.33 \times 10^5 \cdot K$

$E_c = 11.5 \text{ ev} = 18.4 \times 10^{-12} \text{ ERG}$

For equilibrium conditions at 15,000°K and 1 atmosphere,

$\left(\frac{dNe}{dt}\right)_1 = 2.6 \times 10^{22}$ ions/cm^3-sec (probable value)

For the higher threshold,

$$\left(\frac{dNe}{dt}\right)_2 = 2 NeN_A \left[\frac{2(kTe)^3}{\pi Me}\right]^{\frac{1}{2}} \left\{ \int_{X_1}^{\infty} e^{-X} (X^2 - X X_1) dX \times 8.1 \times 10^{-6} + 3.1 \times 10^{-6} \int_{X_2}^{\infty} e^{-X} (X^2 - X X_2) dX \right\}$$

$X = \frac{E}{kTe}$; $X_1 = \frac{1.83 \times 10^5}{Te}$; $X_2 = \frac{1.86 \times 10^5}{Te}$

which results in a value for 15,000°K and 1 atmosphere (equilibrium) of

$\left(\frac{dNe}{dt}\right)_2 = 2.8 \times 10^{21}$ ions/cm^3 - sec (lower bound)

Since the residence time of the gas in the nozzle used for the experiment is at least 10^{-4} seconds, and the equilibrium electron density at 15,000°K and 1 atmosphere would be, roughly, 2×10^{21} /cm^3,

the existence of equilibrium would require a mean ionization rate of only 2×10^{21} ions/cm^3 -sec. Thus, even if the mean rate of ionization were not much higher than that at the nozzle exhaust, and we use the lower value for ionization rate $\left(\frac{dNe}{dt}\right)_r$ it appears that ionization equilibrium is assured.

In the mixing region we must consider the reaction rate as the difference between recombination and ionization:

$$\frac{dNe}{dt} = N_e N_A I - N_e^2 \alpha$$

where I = "ionization" coefficient

α = recombination coefficient

Using equilibrium values of N_e and N_A and taking the ionization rate from (39), we obtain, at 15,000°K, $\alpha = 0.73 \times 10^{-12}$ cm^3/sec. and $I = 1.03 \times 10^{1-12}$ cm.^{3}/sec. The value of α so derived is in reasonable accord with the value expected from the assumption of three-body recombination.

Since $dNe/dT_e \sim 4 \times 10^{13}$ / cm ^{3}-°K,

$\frac{dNe}{dt} = 4 \times 10^{13} \times \frac{dT}{dt} = 9 \times 10^{21}$/cm^3-sec for the extreme case selected from (49).

For this extreme case, using (39) and the above, the relative electron densities are given in below

RELATIVE ELECTRON DENSITIES FOR EXTREME TEMPERATURE DECAY RATE

Temperature (°K)	N_e/ (N_e at equilibrium)
15,000	1.07
14,000	1.11
13,000	1.43
12,000	2.03

The computed amount of nonequilibrium electron density will decrease if higher values of the recombination coefficient are assumed. In view of the uncertainties inherent in this estimate, it can only be stated that for the "extreme" case there could be significant nonequilibrium electron density effects, but for the less severe gradients measured in (5) the electron population is near equilibrium.

The jet is optically thin in all spectral regions except those of its strongest lines, which occur in the far ultraviolet. Hence since the radiant flux is lost, the number of photoionizations will be much smaller than the number of radiative recombinations. The effect of this imbalance is to decrease the degree of ionization (52). Since the three body recombination is much larger than the radiative recombination this effect will be small.

D. Arcjet Radiation

Simple total radiation surveys of the turbulent argon arcjet were made using a collimated radiation probe. This work was first reported in Reference (4). Since this time the results have been re-examined and it was found that the total radiation loss is more in agreement with established theories than first thought. The conclusion of this new work with respect to the turbulent mixing study is the same as previously concluded, i.e., the radiation from the turbulent arcjet is sufficiently small that it does not affect the conclusions of the turbulent mixing analysis and experiments. The recent work did result, however, in the general conclusion that radiation in some case approached ten percent of the total turbulent jet power, substantially higher than first thought. Also concluded was that the radiation cannot be neglected in the mixing studies of the laminar regime.

No further discussion of arcjet radiation will be made here since a report entitled "Analytical-Experimental Correlation of Radiation Loss from an Argon Arcjet" will be issued in the very near future. The reader is referred to Reference (4) for a detailed description of the technique used to measure radiation power.

IV. CALORIMETRIC PROBE

A. Introduction

The measurement of gas properties at atmospheric pressures and temperatures above 5,000°K has long been a serious problem. Devices which depend on solid-state properties; e.g., thermocouples or thermometers of any type, would be beyond their melting points. Simple optical techniques such as pyrometry or sodium "D"-line reversal are limited by source brightness temperatures. More advanced spectroscopic methods; e.g., (54, 55) etc., are not only delicate and elaborate, but are subject to a number of difficult-to-avoid errors; e.g., depth of field in sources having high gradients, pressure broadening effects, difficulty in isolating the appropriate "temperature," etc. These errors generally result in experimental scatter on the order of 10 to 20%. Other temperature-measurement techniques which depend on gas properties such as electrical conductivity, sound velocity, etc. (56) are subject to numerous errors when applied to nonuniform regions and have been unable to provide better than 10% repeatability.

B. Description

The probe configuration developed for the required arcjet measurements is diagrammed in Figure 6. Construction of the probe itself is of copper, with stainless-steel supports. Cooling water from a high-pressure source (up to 500 psi) enters through the mounting block, passes up the

front stainless-steel support, and through the outermost coolant channel to the probe tip. It returns via the inner coolant channel. Sheathed, ungrounded thermocouple junctions are located precisely at the probe coolant channel inlet and outlet.

The central tube carries a steady flow of sample gas from the probe tip past a thermocouple junction located precisely opposite the "water out" thermocouple, and then through a gas sample tube to one or more instruments as described later.

Note that the major diameter of the sampling tube is approximately 1/8 inch. Calibration results on earlier 1/4-inch models, to be discussed below, clearly indicate the superior accuracy of the smaller probe for local measurements. A photograph of the 1/8-inch probe, also showing the exit of the arcjet used to provide the hot gas source, appears in Figure 7.

C. Methods

1. Temperature Measurement

The calorimetric method used to determine gas temperature depends heavily on a unique "tare" measurement, which effectively eliminates errors due to external cooling requirements. A valve in the gas sample line is closed, thus preventing gas from entering the probe, and observations of coolant temperature rise and flow rate are

made. The valve is then opened, allowing a gas sample to flow through the probe, and the same measurements are repeated, together with those of the steady gas sample temperature at the probe exit and steady gas sample flow rate. The rate of heat removal from the gas sample is thus given by the difference between the two coolant a rates:

$$\dot{w}_g (h_{1g} - h_{2g}) = (\dot{w}_c c_{p_c} \Delta T_c)_{flow} - (\dot{w}_c c_{p_c} \Delta T_c)_{no\ flow}$$

where $\dot{w}_g$ = gas sample mass flow rate

$\dot{w}_c$ = coolant water mass flow rate

h_{1g} = unknown gas enthalpy at probe entrance

h_{2g} = gas enthalpy at probe exit thermocouple

c_{p_c} = coolant specific heat

ΔT_c = coolant temperature rise = $(T_c)_{out} - (T_c)_{in}$

The effectiveness of the "tare" measurement (i.e., the heat removal rate with the gas sample flow shut off) is dependent on the duplication of flow conditions near the probe tip in the "flow" and "no-flow" cases. The calibration data described below appear to indicate that satisfactory duplication is achieved for the existing probe geometry.

The unknown gas enthalpy h_{1g} at the probe tip is now uniquely determined, provided the gas sample flow rate $\dot{w}_g$ and the gas enthalpy h_{2g} at the probe exit are known. Since the

sample is cooled to rather low temperatures by the time it reaches the probe exit thermocouple (e.g., $\sim 300°C$), the gas enthalpy is a direct function of the temperature, measured by the thermocouple, and the gas sample composition, determined as discussed in the next section. The flow rate of the gas sample may be measured by any convenient means; in the present study a choked orifice was used, for which knowledge of the gas composition was sufficient to provide the necessary flow rate data (see Figure 8).

2. Gas Composition

The gas sample passes from the probe through a constant-temperature oil bath, and composition can thus be determined at known equilibrium conditions by various methods. In the case of the two-component mixtures of interest in the present program (argon-helium), a simple thermal conductivity cell provided accurate composition data under steady-state gas sample flow conditions (see Figure 8). For more complex mixtures, conventional chromatography techniques may be used to measure the necessary composition data.

3. Velocity

At the time the "tare" calorimeter measurement is made, the dead-ended gas sample passage is filled with gas at the stagnation pressure of the probe-tip location in the arcjet stream. A conventional pressure transducer (see Figure 8), may be used to determine this pressure. For low subsonic gas flows, the Bernoulli equation provides a simple

velocity determination:

$$V_{lg} = \sqrt{\frac{2 \Delta P}{\rho_{lg}}}$$

where V_{lg} = free-stream velocity at the probe tip

ρ_{lg} = gas density at the probe tip

ΔP = measured pressure rise (stagnation pressure-ambient jet pressure)

Note that in supersonic flow, a knowledge of the gas composition is necessary in order to determine the free-stream Mach number, since use of the ideal-gas Rayleigh pitot formula is not valid for the partly-ionized gas jet. However, in this case the stagnation pressure determination is essentially unaffected by ion recombination in the detached shock in front of the probe, as was demonstrated experimentally for reacting flows in (57), and thus the probe could conceivably be useful in supersonic flows as well as for subsonic velocities.

D. Calibration

1. Energy Balance

The fundamental calibration technique is that of comparing the known total energy of the arcjet gas with an integrated probe energy survey across the arcjet exit plane. The net rate of energy output P_a of the arcjet is

$$P_a = E_a I_a - \dot{w}_a c_{p_a} (\Delta T)_a$$

where E_a = arcjet voltage

I_a = arcjet current

$\dot{w}_a$ = arcjet coolant mass flow rate

c_{p_a} = specific heat of arcjet coolant water

$(\Delta T)_a$ = arcjet coolant temperature rise

No account is taken of radiation, since measurements (see Section III-D) have indicated that radiation is usually small and reaches about 10 per cent of the jet energy only at the highest jet powers studied. The exit-plane energy survey is made by using the probe to measure gas velocity, composition, and enthalpy at each of approximately 15 locations across a diameter of the arcjet exit plane, and determining the value of the jet energy summation

$$P_p = \sum_{-R}^{R} \pi \rho_{lg} V_{lg} h_{lg} r \delta r$$

where R = radius of the arcjet exit (3/8")

r = radial coordinate

ρ_{lg} = gas density from probe measurements

V_{lg} = gas velocity from probe measurements

h_{lg} = gas enthalpy from probe measurements

P_p = total energy per unit time

Two assumptions are needed to evaluate this summation. First, a knowledge of the equation of state of

the partly-ionized free-stream gas is required. It was established (2) that for the low subsonic velocities of the present program, equilibrium of partly-ionized argon at low subsonic speeds and one atmosphere pressure was assured. Thus the enthalpy measurement defines a temperature which, with the measured argon-helium concentration, provides a value for gas density ρ_{lg}.

The second assumption needed is that of axial symmetry of the arcjet, since a single diametral survey is used to represent the entire exit plane. This was found not to be too stringent a requirement, and was adequately satisfied by the available arcjet source. Note that some assistance in this regard is obtained by the use of a survey which is summed over the entire diameter instead of merely a radius, as indicated by the above formulation.

The resultant ratio P_p/P_a, which represents the ratio of integrated probe-measured energy in the arcjet exit plane to actual net energy input to the gas, is plotted in Figure 9 for a number of arcjet flow rates and for two probe diameters. Agreement is consistently within 5% and the average falls within 0.5%. Standard deviation for thee 1/8" probe was calculated to be 3% and that of the 1/4" probe was 10%. Temperature in the center of the arcjet exhaust exceeded 14,000°K at the higher power levels shown in this figure, and in all cases the jet boundary (3/8" away) was pure helium at approximately 300°K.

A second important calibration reference was the mass flow rate $\dot{w}_a$ of argon gas through the arc generator, as measured by a conventional flowmeter. Again using the probe exit-plane survey data, the mass-balance ratio

$$\sum_{-R}^{R} \pi \rho_{lg} V_{lg} r \Delta r \Big/ \dot{w}_a$$

was calculated and is plotted for a number of flow rates in Figure 10. Agreement was found to be comparable with that of the energy balance, further verifying the accuracy of the probe technique.

E. Conclusions

1. Successful calibration of a water-cooled gas sampling probe capable of steady-state operation at one atmosphere and 14,000°K was accomplished by energy balance and mass balance measurements across an arcjet.

2. Statistical analysis of a series of exit-plane surveys using the probe resulted in a standard deviation of 0.03 for a 1/8" probe and 0.10 for a 1/4" probe. Note that these results give the total error of a 15-point survey, and hence it is clear that the accuracy of the individual readings making up each survey will exceed these values.

3. Superior scatter behavior of the smaller probe indicates its better suitability for local measurements; however, the fact that the average of 1/4" probe calibration ratios was quite close to unity indicates that the sampling technique itself is satisfactory; i.e., not scale-dependent.

4. The fundamental advantages of this type of probe are its high accuracy, ease and convenience of calibration and measurement, and ability to measure several flow properties simultaneously. It is able to perform these measurements under not only the extremes of pressure and temperature discussed earlier, but also in the presence of temperature gradients up to 40,000°K per inch.

5. Although operation of the copper probe would be questionable in corrosive gases, the application of gold plating, which is easily accomplished, permits such operation.

6. Some of the limitations of the probe technique are

a. Equilibrium must exist in the gas when temperature is to be measured, since the probe measures only the total gas enthalpy.

b. Transients cannot be measured; however, note that the steady-state mode of measurement has been observed to be quite effective in averaging the variations due to extreme turbulence and arc fluctuations.

c. Spatial resolution is limited by the finite sampling tube diameter (about 0.040" for the 1/8" probe).

d. Mass or energy balance calibrations require approximately axisymmetric flow. This is

not necessary once a calibration has been established, since the probe measures local gas properties directly.

e. In order to obtain temperature calibrations, simultaneous velocity and composition determinations are also necessary. Again, this does not apply once the calibration has been established.

f. The probe has to date only been applied to the measurement of subsonic gas flows; however, it is possible that equivalent property measurements in supersonic flows can be made under certain conditions.

V. TURBULENT MIXING EXPERIMENTS

A. Arcjet Apparatus

The arcjet used in these tests was manufactured by the Thermal Dynamics Corporation. The basic F-80 equipment (see Figures 11 and 12) with peak power capacity of 80 kilowatts was modified for this study by the use of a longer primary nozzle and a secondary annular helium nozzle (see Figures 13 and 14). Power was obtained from a 440-volt shunt-wound generator driven by a diesel engine. Five rectifiers were used to convert to direct current.

The cathode (see Figure 12) was constructed of ground tungsten and was water-cooled. The water-cooled copper anode also served as the primary argon nozzle. The nozzles employed in the experimental studies were of 0.750 inch diameter straight bore, with lengths of four and eight inches. This provided L/D ratios of 5.33 and 10.67 respectively (see Figure 15 and 16). The efficiencies (net gas power/electrical input power) ranged from 14% for the eight inch nozzle to about 26% for the four-inch nozzle.

One problem of special interest was that of cathode concentricity and the related gas swirl angle. In order to prevent the electrical discharge from striking the same point on the nozzle at all times, which would soon result in a thermal failure, it was necessary to obtain a rotational arc pattern. This was accomplished by introducing the gas in a vortex or swirl. Excessive swirl would make measurement of

velocity near the nozzle boundaries impossible with a pitot-type device such as the probe. Too little swirl would result in asymmetric profiles or thermal failure of the nozzle. The optimum swirl for this study was found to be 15° from axial and 15° from radial. The swirl plate used to produce the desired flow is shown in Figure 12.

B. Physical Measurements

1. Gas Enthalpy: This was measured directly by the probe, requiring the following subsidiary measurements:

(a) Inlet and exit coolant temperatures from the probe (see Figure 6). These were measured by standard copper - constantan thermocouples with electrical output observed on a recording potentiometer.

(b) Probe exit gas temperature (see Figure 6). This was measured with a chromel-alumel thermocouple with output on a recording potentiometer.

(c) Probe gas flow rate. This was measured with a calibrated critical orifice (see Figure 8). Upstream and downstream orifice pressures were measured with mercury manometers. (NOTE: Knowledge of the probe sample gas composition was necessary to determine the flow rate).

2. Gas Composition: The composition of the gas was determined in terms of the helium-argon fraction by means of a thermal conductivity cell (see Figure 8), whose output was observed on a recording potentiometer. The temperature of the gas within the cell, cooled by passage through an oil bath, was measured with a mercury thermometer. The cell was calibrated (1), (2) with known, prepared gas samples of varying argon-helium fractions, and was repeatably accurate to better than 1% (see Reference (5)).

3. Dynamic Pressure: The dynamic pressure (Mach number < .1) was measured by means of a dynamic pressure transducer (Figure 8) and observed on a recording potentiometer.

4. Probe Radial Position: The radial position of the probe was measured with a potentiometer and observed on a recording potentiometer (see Figure 17).

5. Probe Axial Position: The axial position of the probe was measured with a simple scale amplified by a hair-line magnifying glass (see Figure 17).

6. Arcjet Voltage: Measured directly with a calibrated voltmeter (see Figure 18).

7. Arcjet Current: Measured directly with a calibrated ammeter (see Figure 18).

8. Arcjet Coolant Temperature Rise: Measured by copper-constantan thermocouples, with output on a recording potentiometer (see Figure 19).

9. Probe Coolant Flow Rate: The water flow rate through the probe (necessary for the gas enthalpy measurement) was measured with a standard calibrated rotameter (see Figure 20).

10. Arcjet Coolant Flow Rate: The arcjet coolant flow rate was also measured with a calibrated rotameter (see Figure 20).

11. Argon Mass Flow Rate: The argon volumetric flow rate was measured with a calibrated rotameter (see Figure 20). Argon pressure at the rotameter was measured with a simple bourdon gauge, and argon temperature at the rotameter was measured by a mercury thermometer. These data were sufficient to calculate the mass flow rate.

12. Helium Mass Flow Rate: The measurement of the flow rate of the secondary gas was accomplished in the same manner as that of the primary argon (see Figure 20).

C. Deduced Physical Quantities

From the above physical measurements, the condition of equilibrium, and a known equation(s) of state for the multicomponent system (see Reference (5)), it was possible to calculate the following important quantities:

1. Gas Temperature
2. Gas Composition
3. Flow Velocity

It was these indirect physical quantities which were of primary importance in this study.

D. Nature of Experimental Methods

The basic purpose of the experimental program was to obtain direct local measurements over the entire flow field of interest. This was accomplished in the following manner:

After determining the various parameters of interest and assuring that the arcjet was yielding reasonably symmetric profiles (this was essential in the calibration phase, as one diametral pass was used to represent the exit plane conditions, and also of general interest due to the use of an axially-symmetric analysis), the primary jet and mixing region were investigated with the calorimetric probe. This was done by placing the probe in a fixed axial plane and then moving it radially in a series of small increments through the entire jet. At each location, steady-state readings (i.e., the time average of the turbulent fluctuations (58), whose frequency was observed to be of the order of 2000 cycles per second (see Figure (21)) of all the physical measurements listed above were taken. The probe then (typically) was moved to about 15 such locations in the given axial plane. A different axial position was then selected and the procedure repeated. The number of such axial positions was typically six or seven.

The procedure outlined above resulted in data for one fixed set of flow parameters. The need for variation of such basic flow parameters as peak temperature,

peak velocity, velocity ratio, scale and intensity of turbulence, etc. accounted for the large amount of experimental information collected. For reasons of brevity (see Table 2) only a very small portion of the data obtained has been included in this report.

From the previously stated physical measurements it was possible to determine, for various values of the flow parameters,

(a) Velocity, temperature and helium concentration profiles at various axial positions (see Figures 22, 24 and 26).

(b) The axial decay of velocity, temperature and helium concentration (see Figure 28, 29, 30).

(c) The axial and radial gradients of these properties over the flow field (see Figures 31, 32, 33).

(d) The radial spreading of these same quantities as functions of axial position (see Figure 34).

The profiles, axial centerline decay and axial centerline gradients presented no particular difficulties. However, as the determination of the radial spreading of the field variables was not quite so simple, a brief description of this matter is in order.

Essentially, the determination of the radial spreading of a field variable, say temperature, stemmed from inspection of the radial temperature profile. Since the energy or temperature outer boundary is defined as the locus of points nearest the centerline where $T = T_{\infty}$, then by determining the value of the radial position at which this condition is met, for a profile at a given axial position, the outer boundary can be related to the axial position. This was done for all the various axial positions and, of course, the other field variables.

Nonetheless, a major difficulty still remained, for the exact point at which a variable "reaches" its asymptotic limit is very hard to ascertain. Thus a value slightly removed from this limit was selected, and by repeating this procedure for different arbitrary values it was possible to extrapolate to the true boundary criteria. This procedure was employed for determination of all experimental boundary spreading.

E. Results

1. The integral mixing analysis gives good agreement with experimental results based on:

   a. Prediction of radial boundaries of concentration, temperature, and velocity (see Figure 34).

b. Axial decay of concentration, velocity and temperature (see Figures 28, 29, 30).

c. Axial gradients of concentration, velocity and temperature (see Figures 29,32, 33).

d. Radial profiles of concentration, velocity and temperature (see Figures 22, 23, 24, 25, 26 and 27).

2. The "cusped parabaloid" shapes of the spreading boundaries (Figure 34) resulting from the numerical solution of the integral equations differ from the conical boundaries calculated by Squire and Trouncer (27) and obtained by Warren (15) at low temperatures, but are in qualitative agreement with the statistical theory due to Taylor (10).

3. The Prandtl number and Schmidt number are indeed less than unity, while the Lewis number is greater than unity (see Table 3 and boundary relationship of Figure 1).

4. Both stable and "unstable" analytical solutions were obtained. "Unstable" solutions occur when:

a. The various boundaries for spreading are too widely separated.

b. The driving parameters for mass diffusion momentum transfer or heat transfer are too large.

c. Any one such driving term is larger by an

order of magnitude than the other two.

5. The axial derivatives of all the field variables are linearly proportional to the axial derivatives of their respective boundaries (see Reference (5)). This is a direct consequence of the similarity assumption regarding radial profiles.

6. The Reichardt hypothesis, used to formulate the driving term in the integral momentum equation, provides good agreement with experiment for this turbulent, highly non-isoenergetic case.

7. Analytically, the magnitude of radial spreading was found to decrease slightly with increased temperature. This effect was far more pronounced experimentally (see Result No. 12). One possible explanation for this behavior could be the analytical assumption of mean values for the diffusion coefficient and the thermal conductivity.

8. Concentration was found to spread more rapidly than both temperature and velocity, and temperature to spread more rapidly than velocity, in excellent agreement with the analytical result (see Figure 34).

9. Experimental profiles of concentration, velocity and temperature in the mixing region were observed to be strikingly similar (see Figures 22, 24, 26), supporting the similarity assumption used in the analysis.

10. A potential core for concentration, velocity, and

temperature was observed. Its length was approximately one jet diameter for all the field variables, and was relatively insensitive to temperature level. Profiles within this core were, of course, definitely dissimilar (see Figures 22 through 33).

11. Experimental spreading boundaries showed a "cusped paraboloid" shape at typical operating plasma temperatures, and a conical shape in the isoenergetic (unheated) cases (see Figure 34).

12. The magnitude of the boundary spreading of all three quantities was observed to decrease with the onset of ionization and then became constant at ionization levels greater than 10% (see Figures 35, 36, 37, 38, and 40, and Result No. 7).

13. The axial decay of concentration, velocity and temperature, while in excellent qualitative agreement with other experimental results (15), (17), (19), (59) and theoretical calculations (15), (19), and (27), is much more rapid for this high temperature case than in the earlier isoenergetic or near-isoenergetic cases reported in the literature. Typical "length to approximate full decay" in this study was eight radii (see Figures 28, 29, 30). The above papers obtained typical lengths of 40 radii.

14. The plasma was highly turbulent, with no noticeable transverse oscillations and with a longitudinal frequency of approximately 2000 cycles/second for the eight-inch nozzle. There was, however, a significant effect of nozzle L/D ratio, in that turbulence in the four-inch nozzle was not only of

much greater intensity than in the eight-inch nozzle, but also exhibited definite transverse displacements (see Figure 21).

15. The three transfer mechanisms, mass diffusion, momentum transfer, and energy transfer were found to be extremely effective in the case of hot, partially ionized argon mixing in a turbulent fashion with a cool, inert, helium stream. This is indicated by the short potential core and the very rapid axial decay rates discussed in Result No. 13.

16. The concentration and temperature boundaries were independent of variations of λ, the secondary stream to primary stream velocity ratio (see Figure 39). The momentum boundary R_o^M showed a weak linear variation with λ, in contrast to the results of Squire and Trouncer (27). However, the range of λ was limited and this trend was not conclusively established.

F. List of Symbols

a = Radius of primary nozzle

$a_{i,j}$ = Matrix integral coefficient (21 in all)

A_1 = Spreading relation parameter (Ref. 5, Equation B-4b)

A_2 = Spreading relation parameter (Ref. 5, Equation B-4b)

C = Concentration (particle fraction of a species)

a = Sonic velocity

f = Function of C_{He}, θ (see Ref. 5)

g = Function of C_{He}, θ (see Ref. 5)

h = Function of C_{He}, θ (see Ref. 5)

k = Thermal conductivity

l = Prandtl mixing length

L = Length of potential core

M = Mach number

N_{Re} = Reynolds number

N_{PR} = Prandtl number

N_{SC} = Schmidt number

N_{Le} = Lewis number

N_{Pe} = Peclet number

N_{Ja} = "Jacobs" number

P = Dimensionless number (see Ref. 5)

r = Physical radial coordinate

R = Dimensionless radial coordinate = r/a

T = Absolute temperature

$\bar{U}$ = Mean axial velocity component

U = Dimensionless axial velocity component (see Ref. 5)

x = Physical axial coordinate

Greek Letters

$\alpha(a_{i,j})$ = Function of matrix coefficients defined by Equation B-55, Ref. 5

$\beta(a_{i,j})$ = Function of matrix coefficients defined by Equation B-55, Ref. 5

β = Dimensionless parameter defined in Ref. 5

Γ = Dimensionless parameter defined in Ref. 5

Δ = Denotes finite difference

∂ = Denotes partial differentiation

ε = Turbulent momentum exchange coefficient

ξ = Dimensionless axial coordinate = x/a

θ = Dimensionless temperature (see Ref. 5)

K = Dimensionless turbulent exchange constant (see Ref. 5)

λ = Dimensionless velocity ratio (see Ref. 5)

π = 3.14159.....

ρ = Density

τ = Turbulent shear stress

μ = Laminar viscosity

ν = Kinematic viscosity

Subscripts

o = Outer boundary

He = Helium

τ = Turbulent value of

D = For diffusion

i,j = Denotes typical ith row, jth column matrix element

∞ = Values in free outer stream

Superscripts

C = Concentration

M = Momentum

E = Energy

REFERENCES

1. Grey, J., "Heat Transfer From an Ionized Gas to a Gaseous Coolant", Princeton University Aeronautical Engineering Laboratory Report No. 487-a, July, 1959.

2. Grey, J., and Sherman, M. P., "Heat Transfer from an Ionized Gas to a Gaseous Coolent", Princeton University, Aeronautical Engineering Report No. 487-b, July, 1960.

3. Grey, J., Jacobs, P. F., and Sherman, M. P., "Calorimetric Probe for the Measurement of Extremely High Temperatures", Review of Scientific Instruments, American Institute of Physics, Vol. 33, No. 7, July, 1962, p. 738. Also issued as Princeton University Aeronautical Engineering Laboratory Report No. 602, April, 1962.

4. Jacobs, P. F., and Grey, J., "Measurements of Total Energy Radiated From an Argon Arcjet", Princeton University Aeronautical Engineering Laboratory Report No. 621, August 1962.

5. Jacobs, P. F. and Grey, J., "Turbulent Mixing in a Partially Ionized Gas", Princeton University Aeronautical Engineering Laboratory Report No. 625, October, 1962.

6. Sherman, M. P., and Grey, J., "The Degree of Approach to Equilibrium in an Atmospheric-Pressure Arcjet Using Argon", Princeton University Aeronautical Engineering Laboratory Report No. 645, April, 1963.

7. Bussard, R. W., "Concepts for Future Nuclear Rocket Propulsion", Jet Propulsion 28, April, 1958, p. 223.

8. Grey, J., "A Gaseous-Core Nuclear Rocket Utilizing Hydrodynamic Containment of Fissionable Material", Paper No. 848-59, American Rocket Society, June 8, 1959.

9. Weinstein, H., and Ragsdale, R. G., "A coaxial Flow Reactor - A Gaseous Nuclear Rocket Concept," Paper No. 1518-60, American Rocket Society, presented December 6, 1960.

10. Taylor, G. I., "Diffusion by Continuous Movements", Proceedings of the London Mathematical Society, London, England, Vol. 20, 1921, p. 196.

11. Prandtl, L., Berichte uber Untersuchungen zur Ausbebildeten Turbulenz. Zeitschrift fur Angewandte Mathematik und Mechanik, 5, 1925, p. 136.

12. Tollmien, W., Berechnung der Turbulenten Ausbreitungs Vorgänge, Zeitschrift fur Angewandte Mathematik und Mechanik, 4, 1926, p. 468. NACA TM 1085, 1945.

13. Reichardt, H., Uber eine Neue Theorie der Freien Turbulenz, Zeitschrift fur Angewandte Mathematik und Mechanik, 21, 1941, p. 257. JRAS 47, 1943, p. 167.

14. Forstall, W., Jr., and Shapiro, A. H., "Momentum and Mass Transfer in Coaxial Gas Jets", Journal of Applied Mechanics, 10, 1960, p. 339.

15. Warren, W. R., "An Analytical and Experimental Study of Compressible Free Jets", Ph.D. Thesis, Princeton University, Princeton, N. J., 1957.

16. Prandtl, L., Bemurkungen zur Theorie der Freien Turbulenz, Zeitschrift fur Angewandte Mathematik und Mechanik, 22, 1942, p. 241.

17. Corrsin, S., and Uberoi, M. S., "Further Experiments on the Flow and Heat Transfer in a Heated Turbulent Air Jet", NACA TM 1965, 1949.

18. Pai, S. I., Fluid Dynamics of Jets, D. van Nostrand Company, Princeton, New Jersey, 1954.

19. Pitkin, E. T., "An Experimental Investigation of an Axially Symmetric Supersonic Jet Mixing with Free Air", Princeton University Aeronautical Engineering Laboratory Report No. 243, August, 1953.

20. John, J. E. A., "An Experimental Investigation of the Bounded Mixing of Two Compressible Axially Symmetric Jet Streams", Princeton University Aeronautical Engineering Laboratory Report No. 399, 1957.

21. Von Karman, T., "The Fundamentals of the Statistical Theory of Turbulence", Journal of the Aeronautical Sciences, 4, February 1937, p. 131.

22. Shapiro, A. H., The Dynamics and Thermodynamics of Compressibl Fluid Flow, Vols. 1 & 2, The Ronald Press Company, New York 1953.

23. Schubauer, G. B., "General Hydrodynamic Equations for the Turbulent Motion of a Compressible Fluid," and "Free Turbulent Flows," Turbulent Flows and Heat Transfer, Princeton University Press, Princeton, N.J., 1959.

24. Lin, C. C., "Mathematical Formulation of the Theory of Homogeneous Turbulence," Turbulent Flows and Heat Transfer, Princeton University Press, Princeton, N.J., 1959.

25. Cann, G. L., and Ducati, A. C., "Argon Mollier Chart," Air Force Office of Scientific Research, AF 49(638)-54, February, 1959.

26. Bosnjakovic, F., Springe, W., Knoche, K. F., and Burgholte, P., "Mollier-Enthalpie-Entropie-Diagramm fur Argon-Plasma im Gleichgewicht," Wärmetechnische Institut, Technische Hochschule, Braunschweig. (Translated by Gross, J. F.), August, 1958.

27. Squire, H. B., and Trouncer, J., "Round Jets in a General Stream," Reports and Memoranda No. 1974, British Aeronautical Research Committee, 1944.

28. Goldstein, S., Modern Developments in Fluid Dynamics, Vol. 1, Oxford University Press, Oxford, England, 1938.

29. Margenau, H., and Murphy, G. M., The Mathematics of Physics and Chemistry, D. van Nostrand Company, Princeton, N. J., Chapter 13, p. 450.

30. Cann, J. L., "Argon Mollier Chart,: Plasmadyne Report AFOSR TN 59-247.

31. Bosnjakovic, F., Springe, W., Knoche, K. F., Burgholte, "Mollier Enthalpy-Entropy Charts for High-Temperature Plasmas, ASME Symposium on Thermal Properties 1959, Thermodynamic and Transport Properties of Gases, Liquids, and Solids, p. 465.

32. Chapman, S., and Cowling, T. G., "Mathematical Theory of Non-Uniform Gases," 1939, 1952.

33. Hirschfelder, J. O., Curtiss, C. F., Bird, R. B., "Molecular Theory of Gases and Liquids," 1954.

34. Cohen, R. S., Spitzer, L., Jr., Routly, P. M., "The Electrical Conductivity of an Ionized Gas," Phy. Rev., Vol. 30, October 1950, p. 230.

35. Robinson, B. B., Bernstein, I. B., "A Variational Description of Transport Phenomena in a Plasma," Princeton University Plasma Physics Laboratory Report MATT-69, April 1961.

36. Cann, G. L., "Energy Transfer Processes in a Partially Ionized Gas," Guggenheim Aeronautical Laboratory, California Institute of Technology, Hypersonic Research Project Memorandum No. 61, June 1961.

37. Landshoff, R., "Transport Phenomena in a Completely Ionized Gas in Presence of a Magnetic Field," Physical Review, Vol. 76, October 1949, p. 904.

38. Finkelnburg, W., and Maecker, H., "Electrische Bogen und Thermisches Plasma," Encyclopedia of Physics, Vol. xxii, p. 254.

39. Petschek, H., and Byron, S., "Approach to Equilibrium Ionization Behind Strong Shock Waves in Argon," Annals of Physics, Vol. I, June 1957, p. 270.

40. Fox, R. E., "Ionization Cross Sections near Threshold by Electron Impact," Journal of Chemical Physics, Vol. 35, No. 4, October 1961, p. 1379.

41. Tozer, B. A., and Craggs, J. D., "Cross Sections for Ionization of the Inert Gases by Electron Impact," Journal of Electronics and Control, Vol. 8, 1960, p. 103.

42. Biberman, L. M., Toropkin, Y. N., and Ul'yanov, K. N., "The Theory of Multistage Ionization and Recombination," Zhurnal Tech. Fizikl, Vol. 7, January 1963, p. 605.

43. Olsen, H. N., "Measurement of Argon Transition Probabilities Using the Thermal Arc Plasma as a Radiation Source," Linde Company 1962.

44. Jahn, R., unpublished notes.

45. Massey, H. S. W., and Burhop, E. H. S., "Electronic and Ionic Impact Phenomena," 1952.

46. Bates, D. R., "Atomic and Molecular Processes," 1962.

47. Hinnov, E., and Hirschberg, J. G., "Electron-Ion Recombination in Dense Plasmas," Phy. Rev., Vol. 125, February 1962, p. 795.

48. Mason, E. A., and Vanderslice, J. T., "Determination of the Binding Energy of He_2^+ from Ion Scattering Data," Journal of Chemical Physics, Vol. 29, August 1958, p. 361.

49. Hermann, V. O., "Intersitatsmessungen in neon-und Argonspektrum Bei Anregung Durch Electronenstoss," Annal Per Physik, Vol. 5, 1936, p. 143.

50. Vockova, C. M., and Devyatov, A. M., "Effective Excitation Cross Sections of Certain Special Lines of Argon," Optikal Specrtoroski, Vol. 7, December 1959, p. 480.

51. Brown, S. C., "Basic Data in Plasma Physics," 1959.

52. Biondi, M. A., and Brown, S. C., "Measurement of Electron-Ion Recombination," Physical Review, Vol 20, December 1949, p. 1697.

53. Dewan, E. M., "Generalizations of the Saha Equation," Physics of Fluids, Vol. 4, June 1961, p. 759.

54. Dickerman, P. J., "The Determination of the Equilibrium Temperature of a Plasma," Conference on Extremely High Temperatures, John Wiley and Sons, New York, p. 77, 1958.

55. McGregor, W. K., and Dooley, M. T., "Spectroscopic Diagnostics of a Gerdien Type Plasma Stream Using Argon," Fourth Symposium on Temperature-Its Measurement and Control in Science and Industry, Paper No. B.8.3, March 27-31, 1961.

56. Suits, C. G., "High-Temperature Gas Measurements in Arcs," Symposium on Temperature-Its Measurement and Control in Science and Industry, Reinhold Publishing Corporation, New York, p. 720, 1941.

57. Grey, J., and Nagamatsu, H. T., "The Effects of Air Condensation on Properties of Flow and Their Measurement in a Hypersonic Wind Tunnel," Proceedings of the Third Midwestern Conference on Fluid Mechanics, University of Minnesota, p. 529, 1953.

58. Dryden, H. L., "Transition from Laminar to Turbulent Flow," Turbulent Flows and Heat Transfer, Princeton University Press, Princeton, N. J., 1959.

59. Willis, D. R., "The Mixing of Unbounded Axially Symmetric Turbulent Compressible Jets," Princeton University Aeronautical Engineering Laboratory Report No. 352, 1956.

60. Torda, T. P., and Stillwell, H. S., "Analytical and Experimental Investigations of Incompressible and Compressible Mixing of Streams and Jets," Wright Air Development Center, TR 55-337, March, 1956.

61. Saha, M. N., Philosophical Magazine, 40, 472, 1920.

62. Dewan, E. M., "Generalizations of the Saha Equation," Physics of Fluids, American Institute of Physics, Vol. 4, No. 6, June 1961, p. 759.

11. Prandtl, L., Berichte uber Untersuchungen zur Ausbebildeten Turbulenz. Zeitschrift fur Angewandte Mathematik und Mechanik, 5, 1925, p. 136.

12. Tollmien, W., Berechnung der Turbulenten Ausbreitungs Vorgänge, Zeitschrift fur Angewandte Mathematik und Mechanik, 4, 1926, p. 468. NACA TM 1085, 1945.

13. Reichardt, H., Uber eine Neue Theorie der Freien Turbulenz, Zeitschrift fur Angewandte Mathematik und Mechanik, 21, 1941, p. 257. JRAS 47, 1943, p. 167.

14. Forstall, W., Jr., and Shapiro, A. H., "Momentum and Mass Transfer in Coaxial Gas Jets", Journal of Applied Mechanics, 10, 1960, p. 339.

15. Warren, W. R., "An Analytical and Experimental Study of Compressible Free Jets", Ph.D. Thesis, Princeton University, Princeton, N. J., 1957.

16. Prandtl, L., Bemurkungen zur Theorie der Freien Turbulenz, Zeitschrift fur Angewandte Mathematik und Mechanik, 22, 1942, p. 241.

17. Corrsin, S., and Uberoi, M. S., "Further Experiments on the Flow and Heat Transfer in a Heated Turbulent Air Jet", NACA TM 1965, 1949.

18. Pai, S. I., Fluid Dynamics of Jets, D. van Nostrand Company, Princeton, New Jersey, 1954.

19. Pitkin, E. T., "An Experimental Investigation of an Axially Symmetric Supersonic Jet Mixing with Free Air", Princeton University Aeronautical Engineering Laboratory Report No. 243, August, 1953.

20. John, J. E. A., "An Experimental Investigation of the Bounded Mixing of Two Compressible Axially Symmetric Jet Streams", Princeton University Aeronautical Engineering Laboratory Report No. 399, 1957.

21. Von Karman, T., "The Fundamentals of the Statistical Theory of Turbulence", Journal of the Aeronautical Sciences, 4, February 1937, p. 131.

22. Shapiro, A. H., The Dynamics and Thermodynamics of Compressible Fluid Flow, Vols. 1 & 2, The Ronald Press Company, New York 1953.

23. Schubauer, G. B., "General Hydrodynamic Equations for the Turbulent Motion of a Compressible Fluid," and "Free Turbulent Flows," Turbulent Flows and Heat Transfer, Princeton University Press, Princeton, N.J., 1959.

24. Lin, C. C., "Mathematical Formulation of the Theory of Homogeneous Turbulence," Turbulent Flows and Heat Transfer, Princeton University Press, Princeton, N.J., 1959.

25. Cann, G. L., and Ducati, A. C., "Argon Mollier Chart," Air Force Office of Scientific Research, AF 49(638)-54, February, 1959.

26. Bosnjakovic, F., Springe, W., Knoche, K. F., and Burgholte, P., "Mollier-Enthalpie-Entropie-Diagramm fur Argon-Plasma im Gleichgewicht," Wåmetechnische Institut, Technische Hochschule, Braunschweig. (Translated by Gross, J. F.), August, 1958.

27. Squire, H. B., and Trouncer, J., "Round Jets in a General Stream," Reports and Memoranda No. 1974, British Aeronautical Research Committee, 1944.

28. Goldstein, S., Modern Developments in Fluid Dynamics, Vol. 1, Oxford University Press, Oxford, England, 1938.

29. Margenau, H., and Murphy, G. M., The Mathematics of Physics and Chemistry, D. van Nostrand Company, Princeton, N. J., Chapter 13, p. 450.

30. Cann, J. L., "Argon Mollier Chart,: Plasmadyne Report AFOSR TN 59-247.

31. Bosnjakovic, F., Springe, W., Knoche, K. F., Burgholte, "Mollier Enthalpy-Entropy Charts for High-Temperature Plasmas, ASME Symposium on Thermal Properties 1959, Thermodynamic and Transport Properties of Gases, Liquids, and Solids, p. 465.

32. Chapman, S., and Cowling, T. G., "Mathematical Theory of Non-Uniform Gases," 1939, 1952.

33. Hirschfelder, J. O., Curtiss, C. F., Bird, R. B., "Molecular Theory of Gases and Liquids," 1954.

34. Cohen, R. S., Spitzer, L., Jr., Routly, P. M., "The Electrical Conductivity of an Ionized Gas," Phy. Rev., Vol. 30, October 1950, p. 230.

35. Robinson, B. B., Bernstein, I. B., "A Variational Description of Transport Phenomena in a Plasma," Princeton University Plasma Physics Laboratory Report MATT-69, April 1961.

36. Cann, G. L., "Energy Transfer Processes in a Partially Ionized Gas," Guggenheim Aeronautical Laboratory, California Institute of Technology, Hypersonic Research Project Memorandum No. 61, June 1961.

37. Landshoff, R., "Transport Phenomena in a Completely Ionized Gas in Presence of a Magnetic Field," Physical Review, Vol. 76, October 1949, p. 904.

38. Finkelnburg, W., and Maecker, H., "Electrische Bogen und Thermisches Plasma," Encyclopedia of Physics, Vol. xxii, p. 254.

39. Petschek, H., and Byron, S., "Approach to Equilibrium Ionization Behind Strong Shock Waves in Argon," Annals of Physics, Vol. I, June 1957, p. 270.

40. Fox, R. E., "Ionization Cross Sections near Threshold by Electron Impact," Journal of Chemical Physics, Vol. 35, No. 4, October 1961, p. 1379.

41. Tozer, B. A., and Craggs, J. D., "Cross Sections for Ionization of the Inert Gases by Electron Impact," Journal of Electronics and Control, Vol. 8, 1960, p. 103.

42. Biberman, L. M., Toropkin, Y. N., and Ul'yanov, K. N., "The Theory of Multistage Ionization and Recombination," Zhurnal Tech. Fizikl, Vol. 7, January 1963, p. 605.

43. Olsen, H. N., "Measurement of Argon Transition Probabilities Using the Thermal Arc Plasma as a Radiation Source," Linde Company 1962.

44. Jahn, R., unpublished notes.

45. Massey, H. S. W., and Burhop, E. H. S., "Electronic and Ionic Impact Phenomena," 1952.

46. Bates, D. R., "Atomic and Molecular Processes," 1962.

47. Hinnov, E., and Hirschberg, J. G., "Electron-Ion Recombination in Dense Plasmas," Phy. Rev., Vol. 125, February 1962, p. 795.

48. Mason, E. A., and Vanderslice, J. T., "Determination of the Binding Energy of He_2^+ from Ion Scattering Data," Journal of Chemical Physics, Vol. 29, August 1958, p. 361.

49. Hermann, V. O., "Intersitatsmessungen in neon-und Argonspektrum Bei Anregung Durch Electronenstoss," Annal Per Physik, Vol. 5, 1936, p. 143.

50. Vockova, C. M., and Devyatov, A. M., "Effective Excitation Cross Sections of Certain Special Lines of Argon," Optikal Specrtoroski, Vol. 7, December 1959, p. 480.

51. Brown, S. C., "Basic Data in Plasma Physics," 1959.

52. Biondi, M. A., and Brown, S. C., "Measurement of Electron-Ion Recombination," Physical Review, Vol 20, December 1949, p. 1697.

53. Dewan, E. M., "Generalizations of the Saha Equation," Physics of Fluids, Vol. 4, June 1961, p. 759.

54. Dickerman, P. J., "The Determination of the Equilibrium Temperature of a Plasma," Conference on Extremely High Temperatures, John Wiley and Sons, New York, p. 77, 1958.

55. McGregor, W. K., and Dooley, M. T., "Spectroscopic Diagnostics of a Gerdien Type Plasma Stream Using Argon," Fourth Symposium on Temperature-Its Measurement and Control in Science and Industry, Paper No. B.8.3, March 27-31, 1961.

56. Suits, C. G., "High-Temperature Gas Measurements in Arcs," Symposium on Temperature-Its Measurement and Control in Science and Industry, Reinhold Publishing Corporation, New York, p. 720, 1941.

57. Grey, J., and Nagamatsu, H. T., "The Effects of Air Condensation on Properties of Flow and Their Measurement in a Hypersonic Wind Tunnel," Proceedings of the Third Midwestern Conference on Fluid Mechanics, University of Minnesota, p. 529, 1953.

58. Dryden, H. L., "Transition from Laminar to Turbulent Flow," Turbulent Flows and Heat Transfer, Princeton University Press, Princeton, N. J., 1959.

59. Willis, D. R., "The Mixing of Unbounded Axially Symmetric Turbulent Compressible Jets," Princeton University Aeronautical Engineering Laboratory Report No. 352, 1956.

60. Torda, T. P., and Stillwell, H. S., "Analytical and Experimental Investigations of Incompressible and Compressible Mixing of Streams and Jets," Wright Air Development Center, TR 55-337, March, 1956.

61. Saha, M. N., Philosophical Magazine, 40, 472, 1920.

62. Dewan, E. M., "Generalizations of the Saha Equation," Physics of Fluids, American Institute of Physics, Vol. 4, No. 6, June 1961, p. 759.

TABLE I

LIST OF EXPERIMENTAL DATA RUNS

CASE	TORCH CURRENT AMPERES	ARGON FLOW S.C.F.H.	HELIUM FLOW S.C.F.H.	NOZZLE LENGTH INCHES	PEAK TEMPERATURE °R	PEAK VELOCITY ft/sec	PEAK ENTHALPY btu/lb	PEAK * PERCENT IONIZATION
D-4	1500	350	5.0	8.00	22,200	440	5520	13.3
D-5	1750	350	5.0	8.00	23,000	465	6600	25.0
D-6	1250	350	5.0	8.00	22,000	400	5300	16.2
D-7	1000	350	5.0	8.00	21,900	370	5200	15.8
D-8	500	350	5.0	8.00	20,300	280	3700	7.2
D-17	0	350	5.0	8.00	530	30	0	0
D-11	1500	350	10.0	8.00	22,200	390	5530	13.3
D-12	1500	350	15.0	8.00	21,500	400	4750	10.0
D-14	1500	350	20.0	8.00	21,400	440	4650	12.5
D-10	1500	450	5.0	8.00	22,800	480	6000	22.0
D-9	1500	400	5.0	8.00	23,300	520	7000	28.0
D-15	1500	320	5.0	8.00	23,800	600	7800	34.6
D-16	0	350	5.0	4.00	530	30	0	0
D-18	500	350	5.0	4.00	21,800	360	5010	11.5
D-3	1000	350	5.0	4.00	17,000	680	2300	00.5
D-20	250	350	5.0	8.00	20,000	230	3500	5.3
D-21	2000	350	5.0	8.00				

* Note: Refers to $g_{o,o}$

TABLE 2

LIST OF ANALYTICAL CASES CONSIDERED

CASE	$T_{o\|o}$ (°R)	NRe_D	NRe_H	Ja	A_1	A_2	λ	$\frac{T_\infty}{T_{o,o}}$	L	NN (MESH SIZE)
1	18,000	500	2000	.0005	0.0120	0.0150	0.05	0.05	0	0.01
2	18,000	500	1000	.0005	0.0120	0.0150	0.05	0.05	0	0.01
3	18,000	500	1000	.0010	0.0120	0.0150	0.05	0.05	0	0.01
4	18,000	1000	2000	.0005	0.0120	0.0150	0.05	0.05	0	0.01
5	18,000	2000	4000	.0002	0.0120	0.0150	0.05	0.05	0	0.01
6	18,000	500	1000	.0001	0.0000	0.0000	0.05	0.05	0	0.01
7	18,000	500	1000	.0001	0.0040	0.0060	0.05	0.05	0	0.01
8	18,000	500	1000	.0010	0.0060	0.0080	0.05	0.05	0.00	0.01
9	18,000	500	1000	.0010	0.0070	0.0100	0.05	0.05	0.00	0.01
10	18,000	500	1000	.0010	0.0040	0.0060	0.05	0.05	0.00	0.01
11	18,000	500	1000	.0010	0.0040	0.0060	0.10	0.03	0.20	0.10
12	18,000	500	1000	.0010	0.0040	0.0060	0.15	0.03	0.50	0.10
13	18,000	500	1000	.0010	0.0040	0.0060	0.20	0.05	1.00	0.10
14	18,000	500	1000	.0010	0.0040	0.0060	0.05	0.05	2.00	0.01
15	15,000	500	500	.0025	0.0050	0.0070	0.05	0.05	2.00	0.01
16	20,000	500	500	.0025	0.0050	0.0070	0.05	0.05	2.00	0.01
17	25,000	500	500	.0025	0.0050	0.0070	0.05	0.05	2.00	0.01
18	21,600	400	400	.0030	0.0050	0.0070	0.05	0.05	2.00	0.01
19	21,600	300	300	.0040	0.0050	0.0070	0.05	0.05	2.00	0.01
20	21,600	250	250	.0040	0.0050	0.0070	0.05	0.05	2.00	0.01
21	21,600	200	200	.0050	0.0050	0.0070	0.05	0.05	2.00	0.01
22	21,600	350	300	.0060	0.0050	0.0070	0.05	0.05	2.00	0.01
23	21,600	350	300	.0050	0.0050	0.0070	0.05	0.05	2.00	0.01
24	21,600	350	300	.0040	0.0050	0.0070	0.05	0.05	2.00	0.01
25	14,300	350	300	.0040	0.0050	0.0070	0.05	0.05	2.00	0.01
26	9,000	350	300	.0040	0.0050	0.0070	0.05	0.06	2.00	0.01
27	7,200	350	300	.0040	0.0050	0.0070	0.05	0.07	2.00	0.01
28	3,600	350	300	.0040	0.0050	0.0070	0.05	0.14	2.00	0.01
29	1,800	350	300	.0040	0.0050	0.0070	0.05	0.28	2.00	0.01

TABLE 3

VALUES OF DIMENSIONLESS PARAMETERS FOR A TYPICAL ANALYTICAL CASE*

NAME	PHYSICAL MEANING	DEFINITION	SYMBOL	VALUE
Reynolds Number =	Inertial / Viscous	$\frac{2 U_{o,o} a \rho}{\mu}$	= N_{Re} =	810
Prandtl Number =	Momentum Transfer / Thermal Transfer	$\frac{\mu \bar{c}_p}{k}$	= N_{Pr} =	0.82
Schmidt Number =	Momentum Transfer / Mass Transfer	$\frac{\mu}{\rho \mathcal{D}}$	= N_{Sc} =	0.74
Lewis Number =	Mass Transfer / Thermal Transfer	$\frac{\rho \bar{c}_o \mathcal{D}}{k}$	= N_{Le} =	1.11
Pèclet Number =		$N_{Re} N_{Pr}$	= N_{Pe} =	667
"Jacobs" Number =		$N_{Re} N_{Sc}$	= N_{Ja} =	600
Turbulent Reynolds Number =	Inertial / Viscous	$\frac{2 U_o r_o^n}{\epsilon}$	= N_{Re} =	700
	Kinetic Energy / Thermal Energy	$\frac{U_{o,o}^2}{h_{o,o} g_{co}}$	= $\mathbb{P}$	= 0.0005
Mach Number =	Velocity / Sonic Velocity	$\frac{U_{o,o}}{\bar{c}_{o,o}}$	= N_M = M =	0.10

* Analytical Case 24

TABLE 4

SOME CHARACTERISTIC EXPERIMENTAL VALUES

Gas Properties:		
1)	Peak Temperature:	14,000 ^{o}K = 25,200 ^{o}R
2)	Peak Enthalphy:	5,800 cal/gram = 10,500 btu/lb
3)	Density:	40 gram/m^3 = 2 x 10^{-3} lb/ft^3
4)	% Ionization (Peak):	34%
5)	Peak Primary Velocity:	215 m/sec = 700 ft/sec
6)	Peak Mach Number:	0.10
7)	Peak Secondary Velocity:	22 m/sec = 72 ft/sec
8)	Primary Argon Flow Rate:	2 grams/sec = 4 x 10^{-3} lb/sec
Torch Properties:		
9)	Peak Current:	2000 amperes
10)	Peak Voltage:	40 volts
11)	Peak Net Power:	20 K.W. (25% efficiency)
12)	Torch Coolant Flow:	1 kg/sec = 2.2 lb/sec
13)	Torch Water Temperature Rise:	30 ^{o}C = 54 ^{o}R
Probe Properties:		
14)	Peak Probe Exit Gas Temperature:	600 ^{o}K = 1080 ^{o}R = 650 ^{o}F
15)	Probe Sample Gas Flow Rate:	3 x 10^{-2} g/sec = 7 x 10^{-5} lb/sec
16)	Coolant Temperature Rise:	30 ^{o}K = 54 ^{o}R
17)	Average Gas Velocity in Sample	100 m/sec ~ 300 ft/sec
18)	Coolant Flow Velocity:	7 m/sec ~ 20 ft/sec
19)	Probe Coolant Flow Rate:	15 gram/sec = 3 x 10^{-2} lb/sec
20)	Average Probe Wall Heat Transfer Rate:	1 btu/in^2-sec
21)	Typical Copper Wall Temperature:	360 ^{o}K = 650 ^{o}R

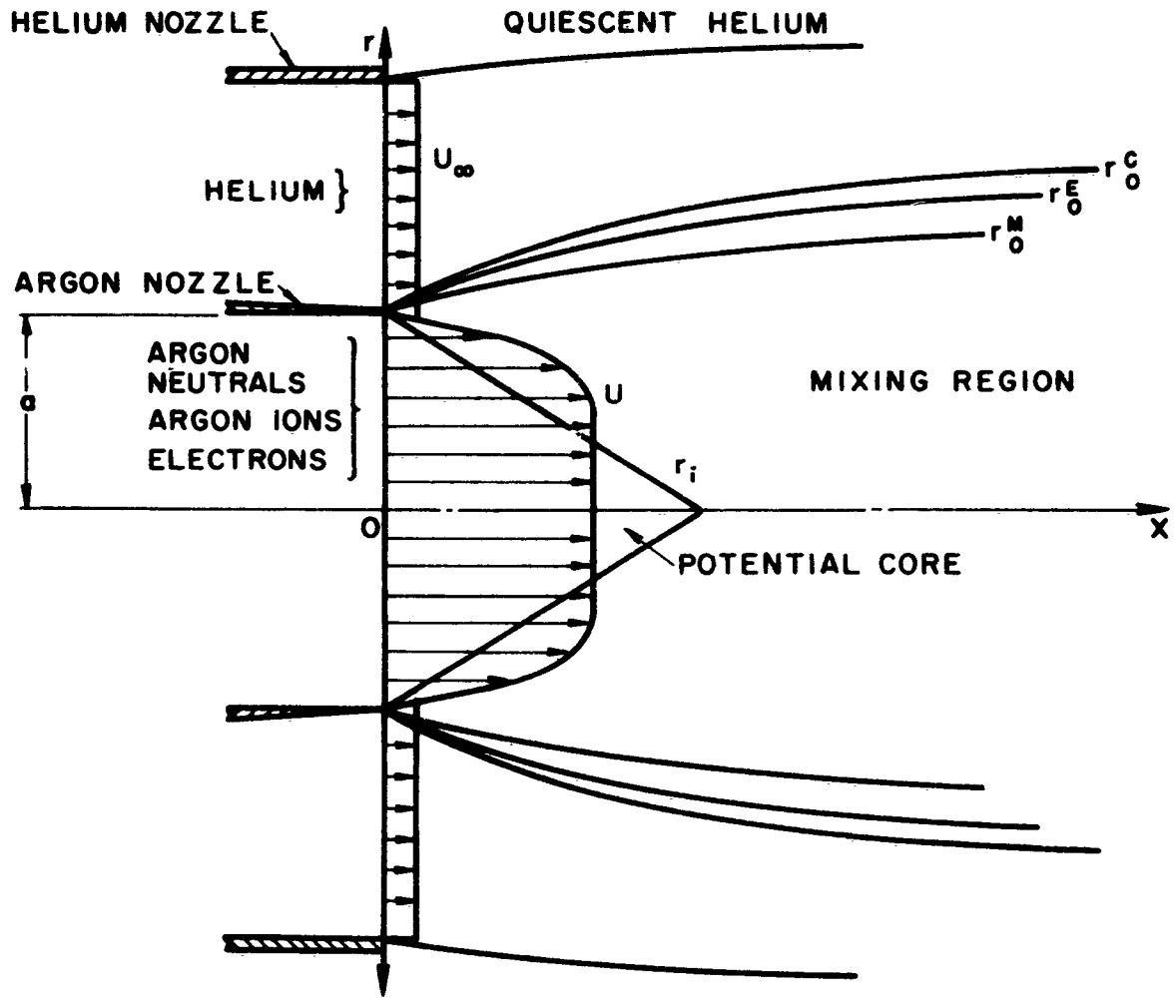

FIGURE 1

DIAGRAM OF TURBULENT MIXING REGION

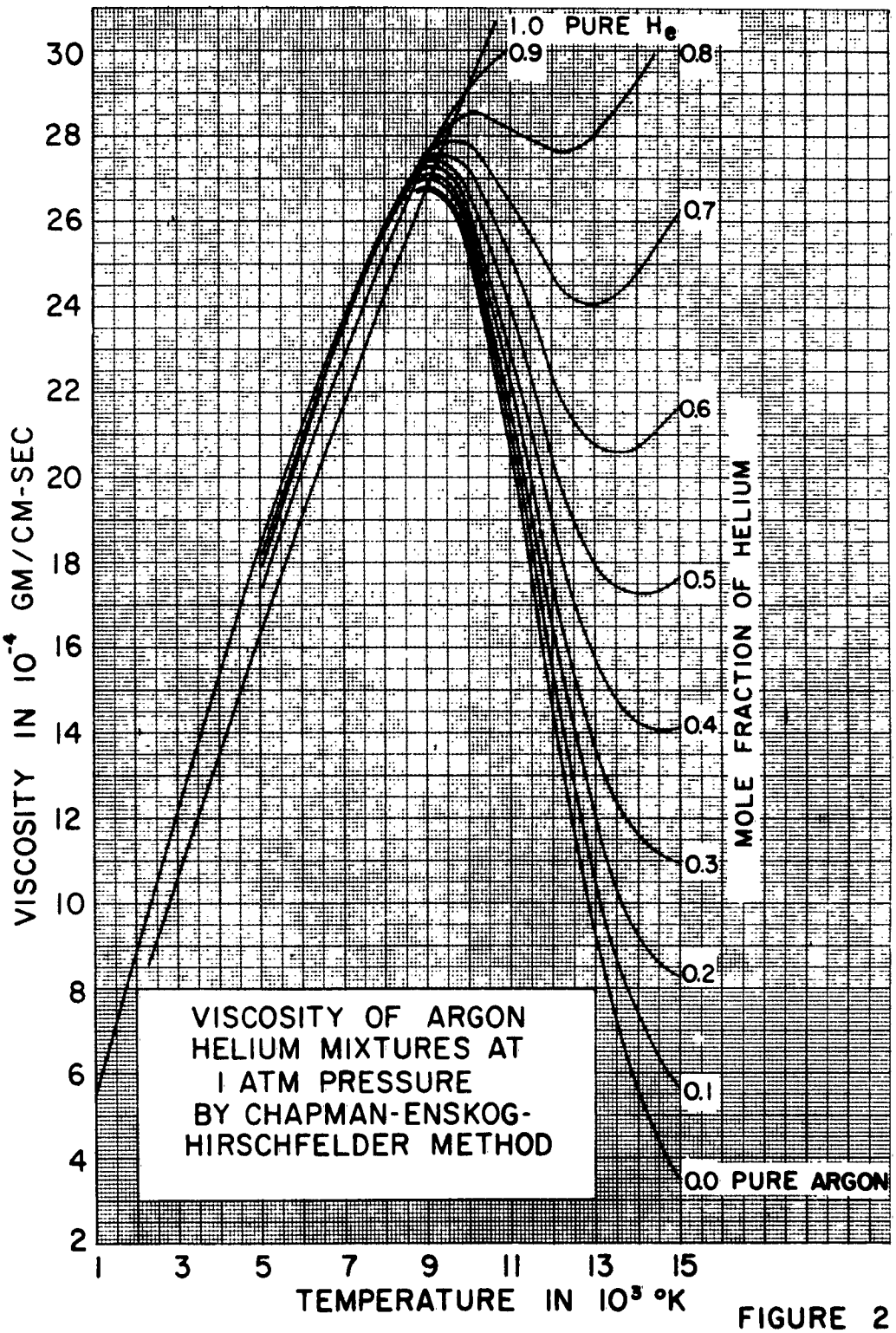
1.0 PURE He
0.9
0.8
0.7
0.6
0.5
0.4
0.3
0.2
0.1
0.0 PURE ARGON
MOLE FRACTION OF HELIUM
VISCOSITY IN 10⁻⁴ GM/CM-SEC
TEMPERATURE IN 10³ °K
VISCOSITY OF ARGON HELIUM MIXTURES AT 1 ATM PRESSURE BY CHAPMAN-ENSKOG-HIRSCHFELDER METHOD

FIGURE 2

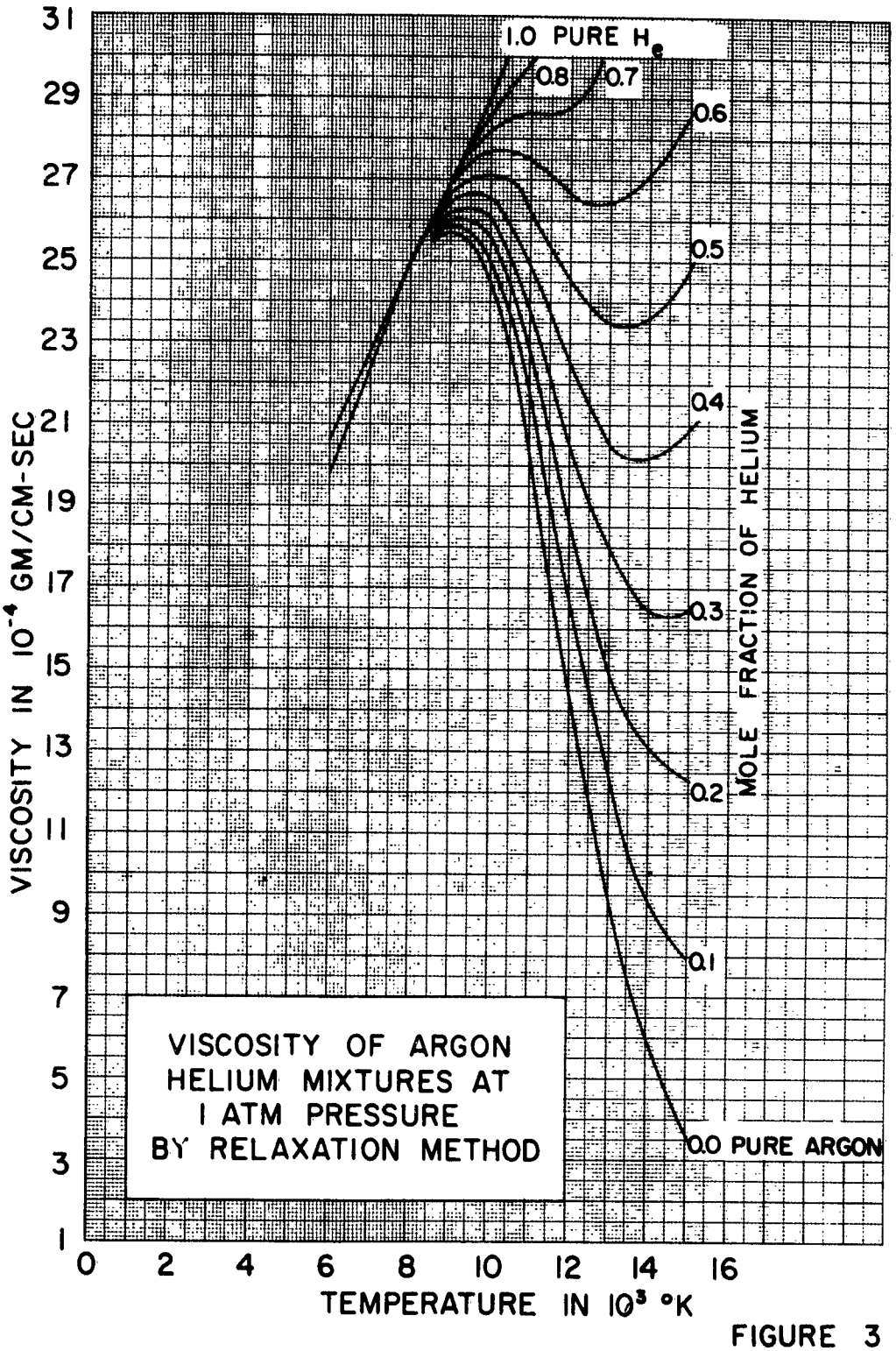
1.0 PURE He
0.8
0.7
0.6
0.5
0.4
0.3
0.2
0.1
0.0 PURE ARGON
MOLE FRACTION OF HELIUM
VISCOSITY IN 10⁻⁴ GM/CM-SEC
TEMPERATURE IN 10³ °K
VISCOSITY OF ARGON HELIUM MIXTURES AT 1 ATM PRESSURE BY RELAXATION METHOD
31
29
27
25
23
21
19
17
15
13
11
9
7
5
3
1
0
2
4
6
8
10
12
14
16

FIGURE 3

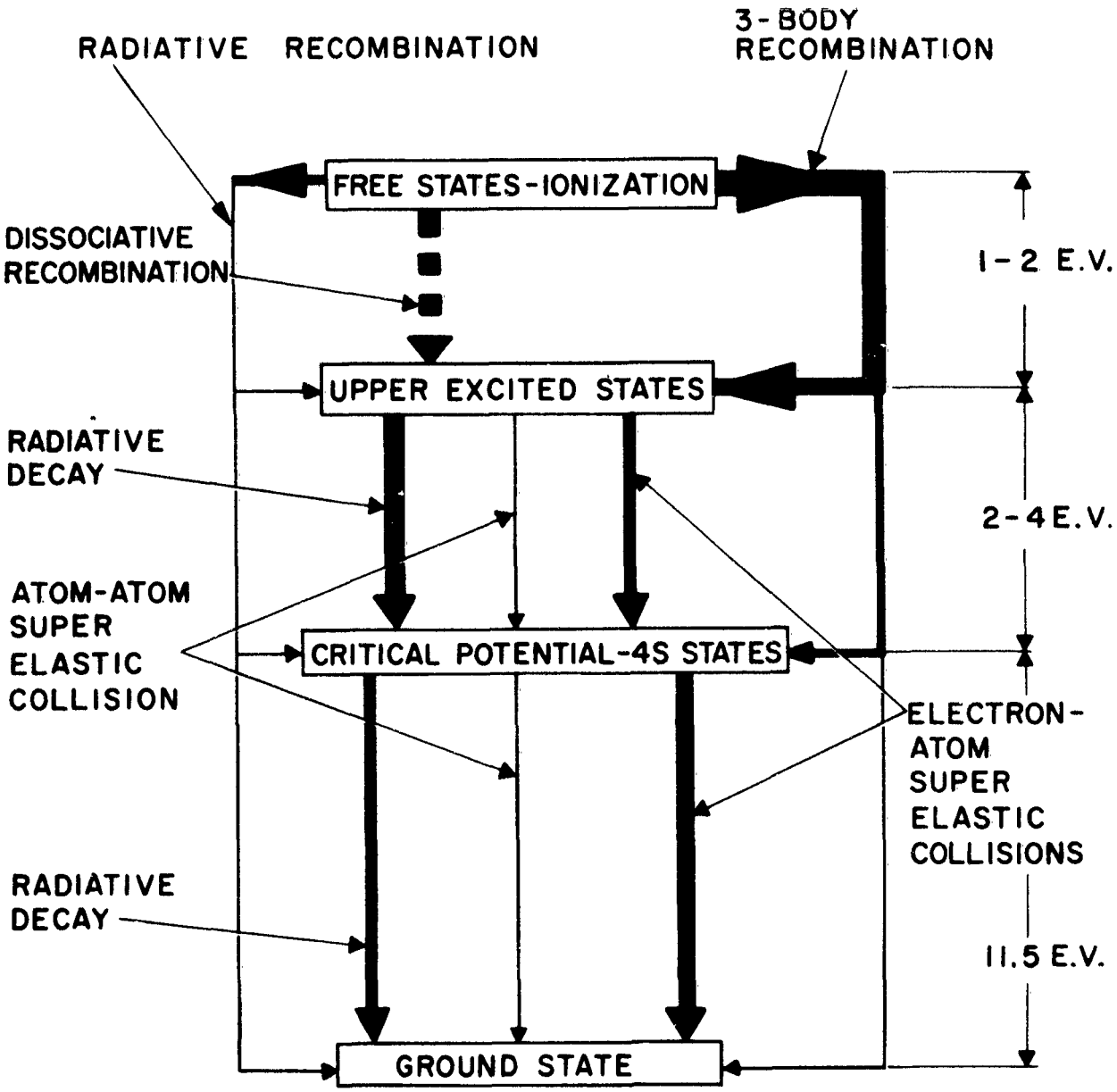

NET ENERGY EXCHANGE PROCESSES IN A COOLING ARGON PLASMA

FIGURE 4

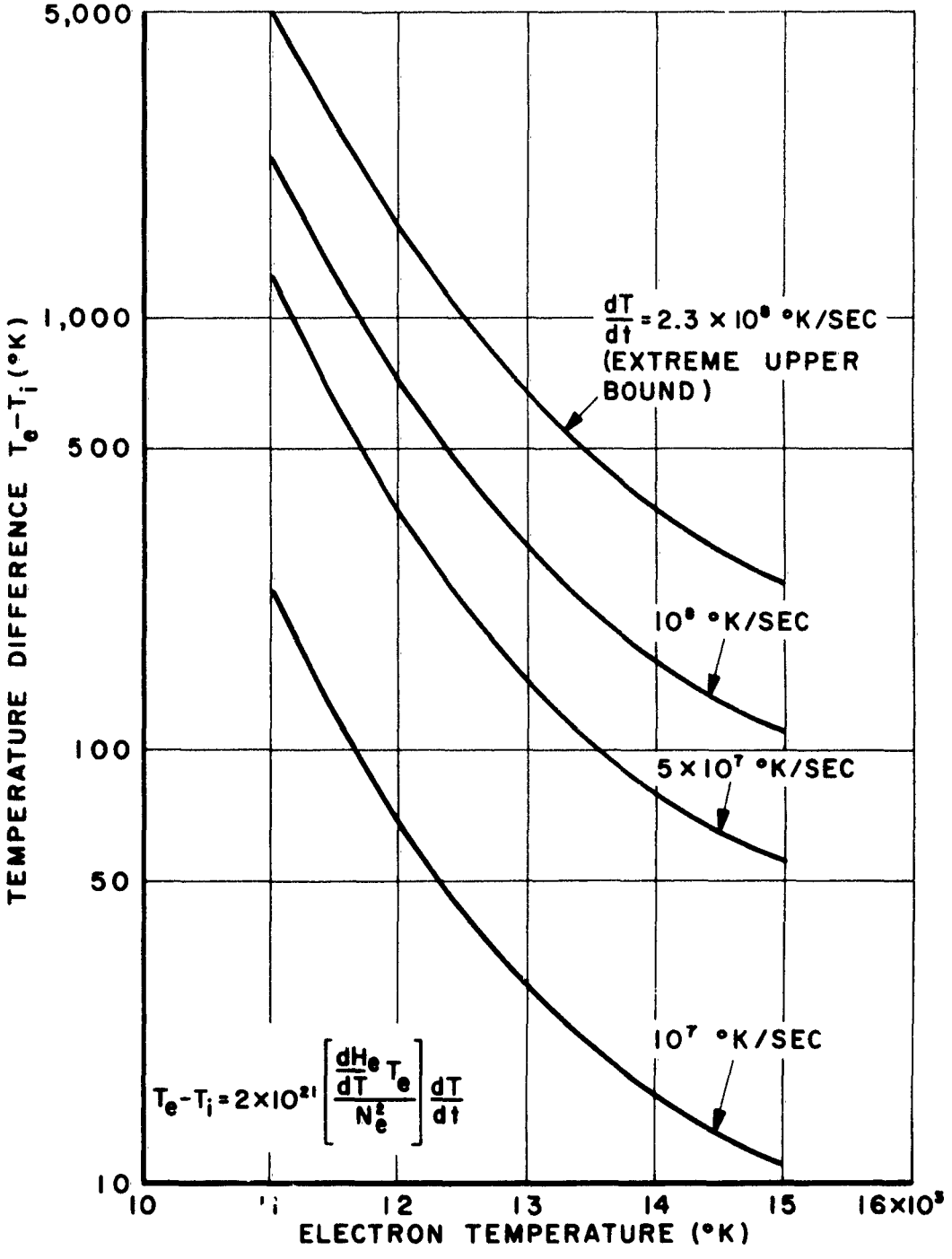

ELECTRON-ATOM TEMPERATURE DIFFERENCE FOR VARIOUS GAS COOLING RATES

FIGURE 5

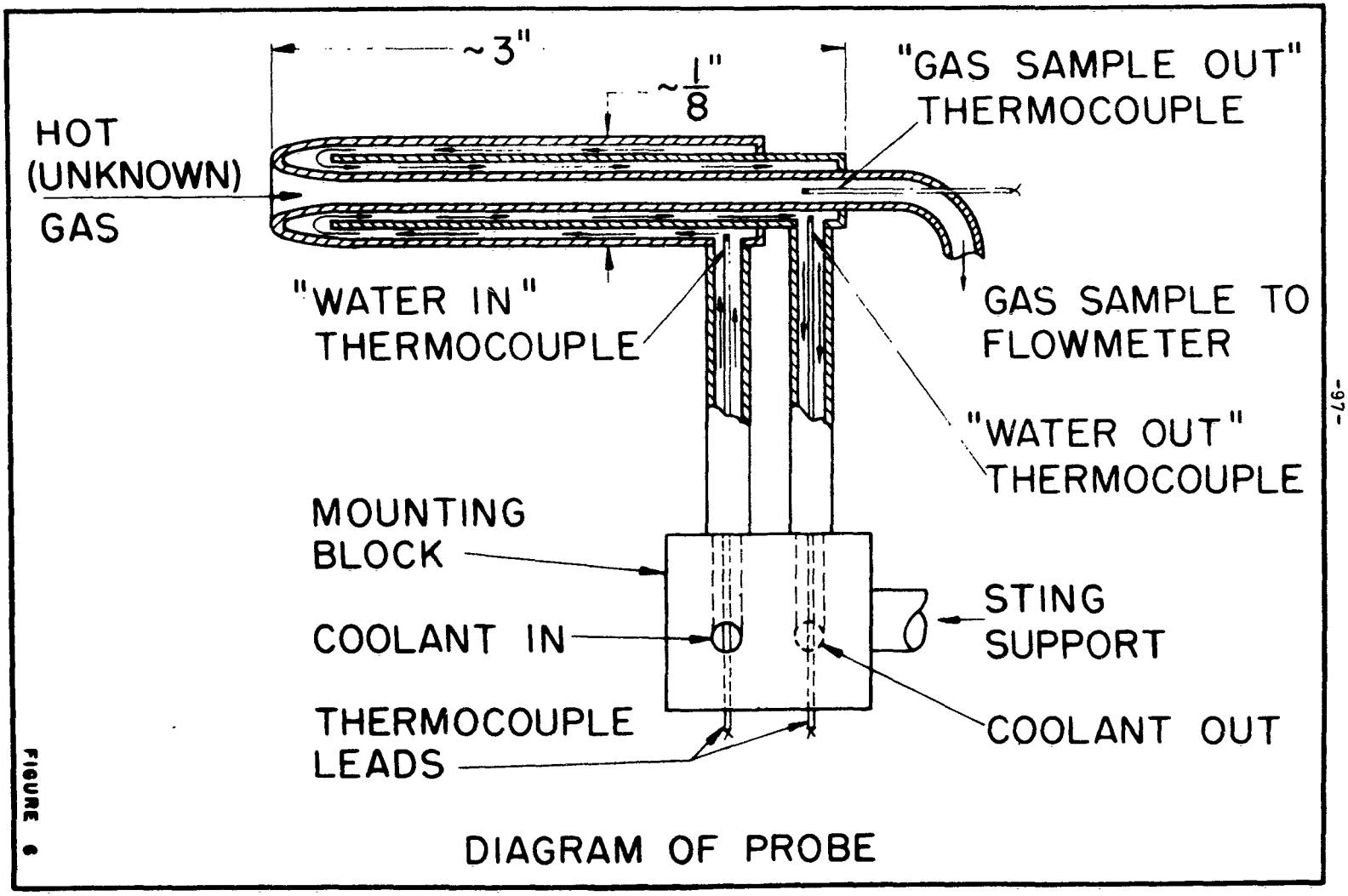

FIGURE 6

DIAGRAM OF PROBE

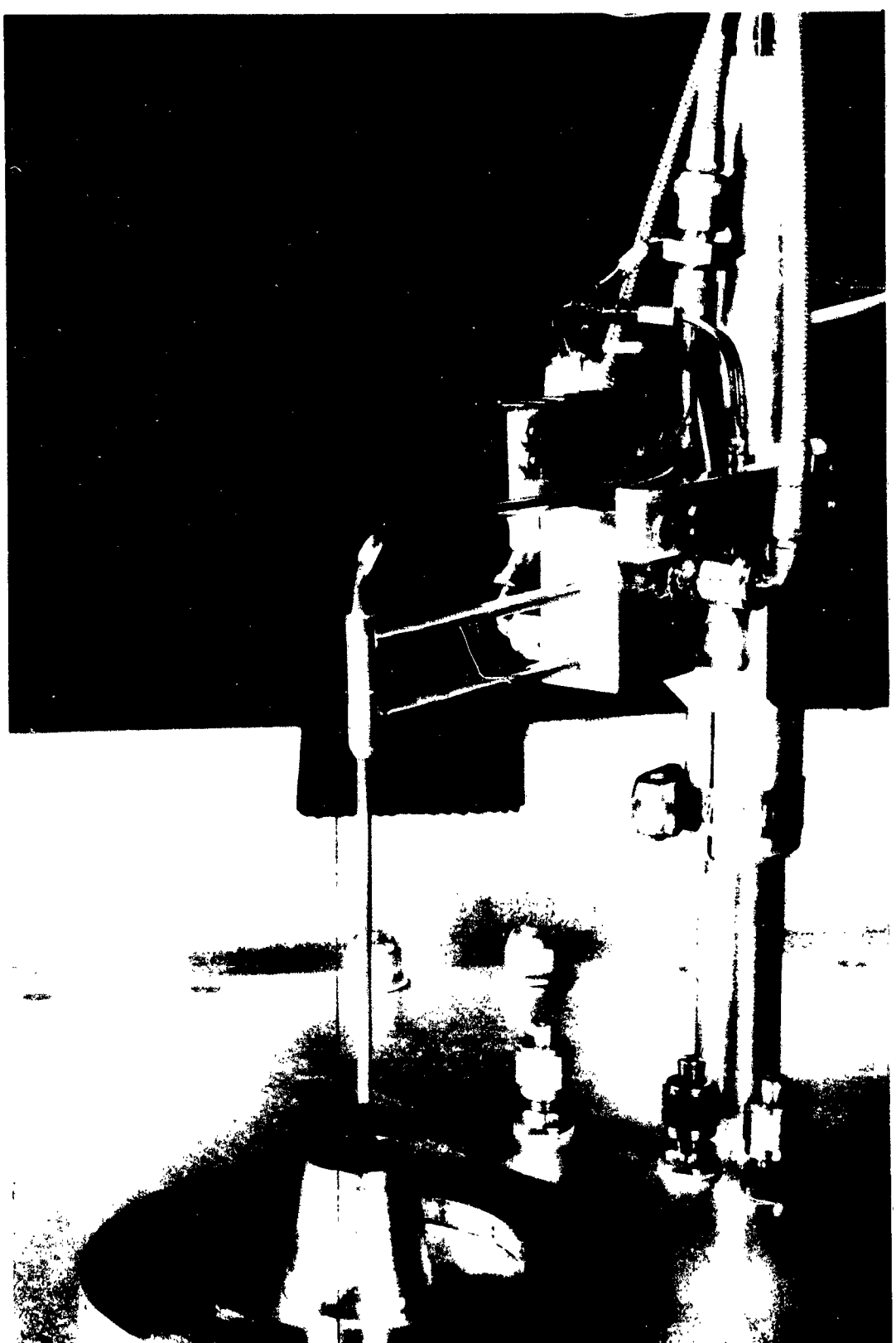

CALORIMETRIC PROBE INSTALLATION

FIGURE 7

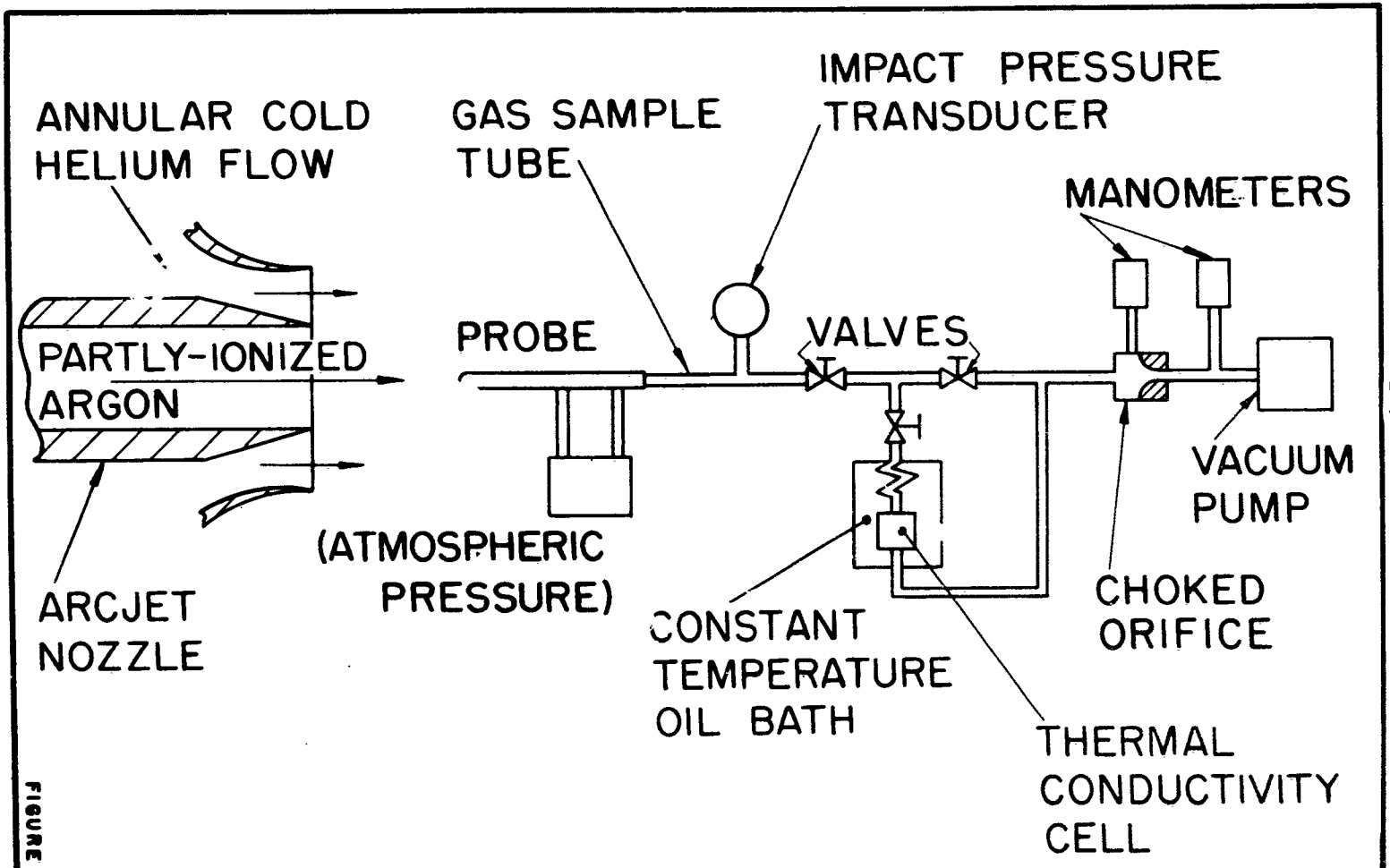

FIGURE 8

DIAGRAM OF GAS SAMPLE INSTRUMENTATION

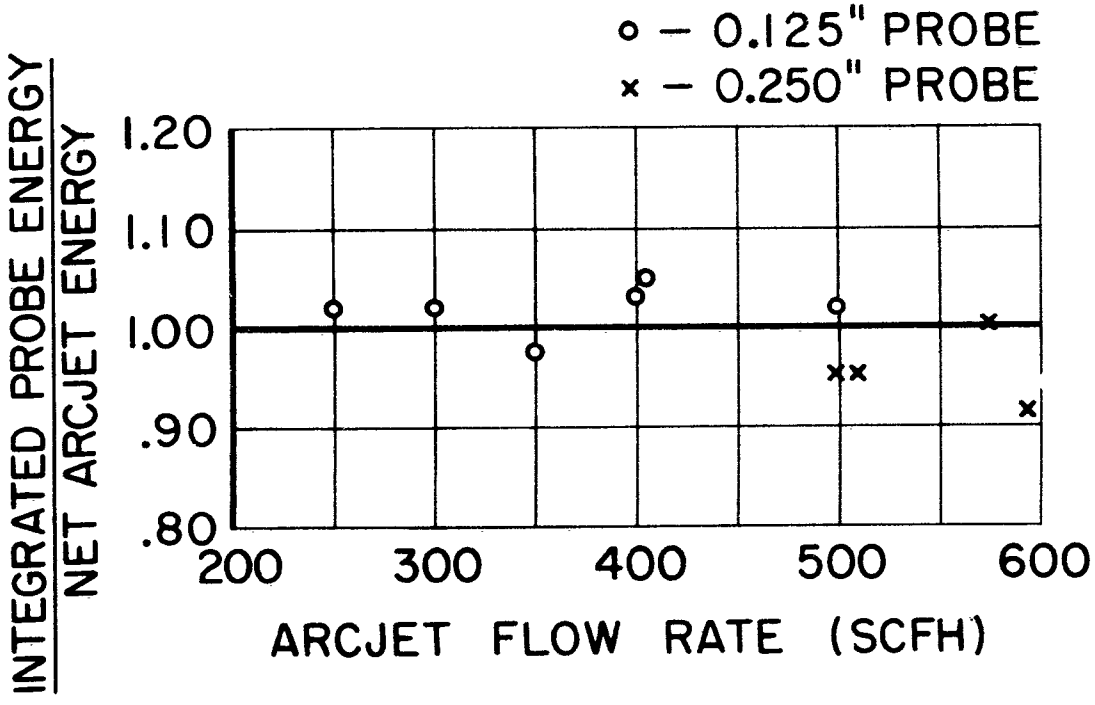

ERROR ANALYSIS :

MEAN VALUE = 0.993
STANDARD DEVIATION* = 0.043
* 0.03 FOR 0.125" PROBE ALONE
0.10 FOR 0.250" PROBE ALONE

FIGURE 9

RESULTS OF ENERGY-BALANCE CALIBRATIONS

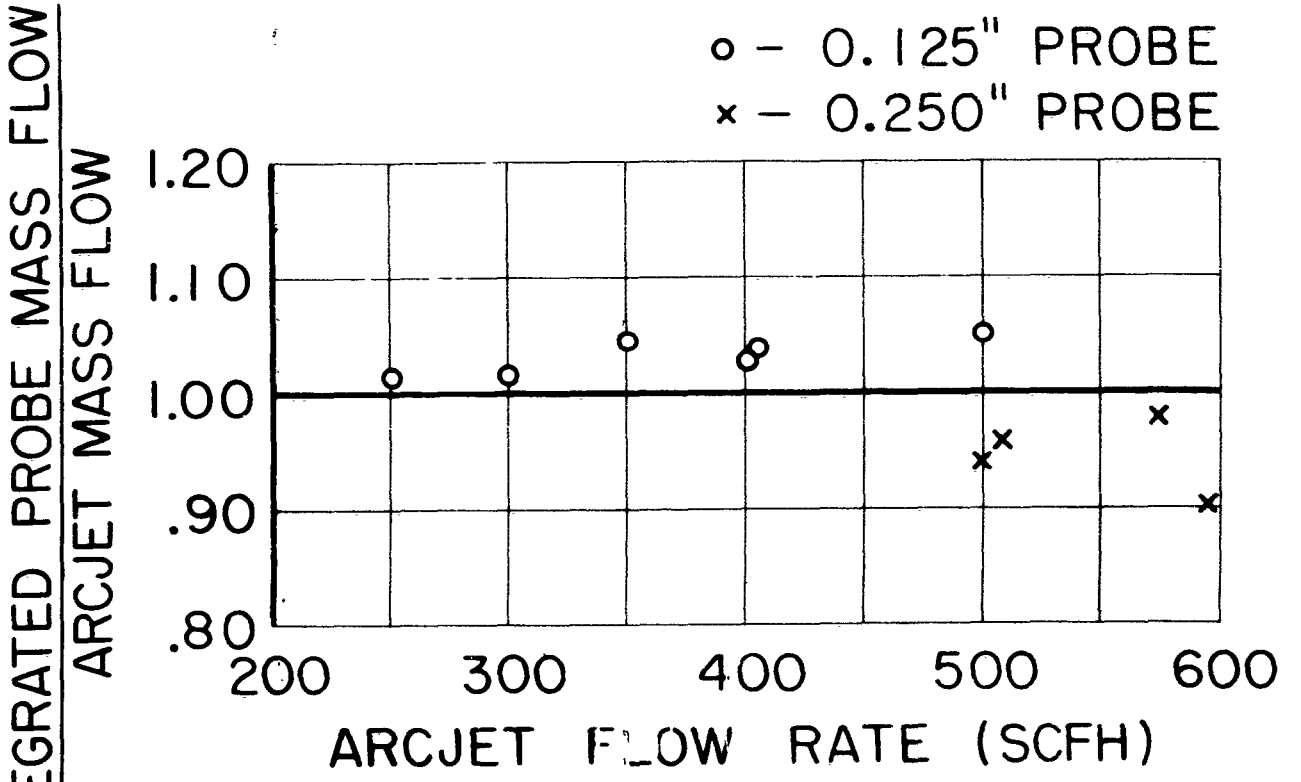

RESULTS OF MASS-BALANCE CALIBRATIONS

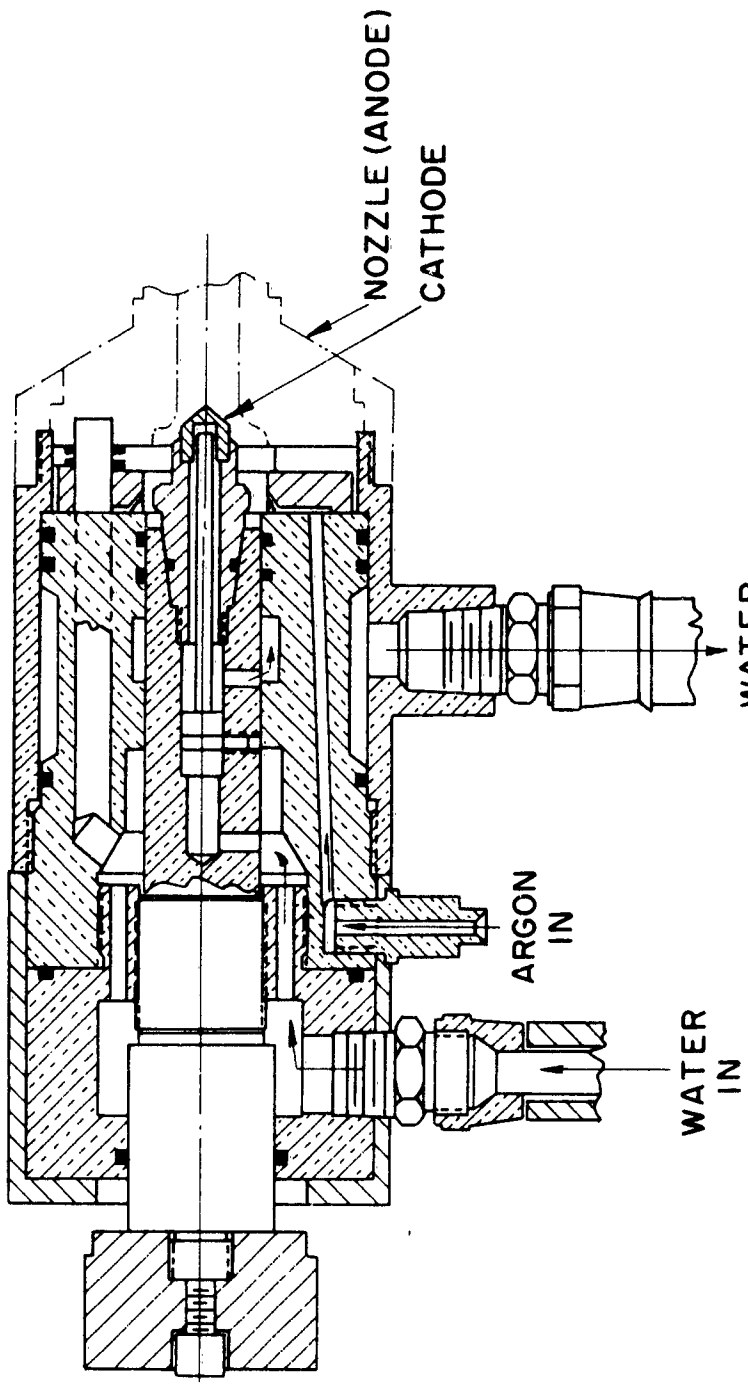

DIAGRAM OF F-80 ARCJET TORCH

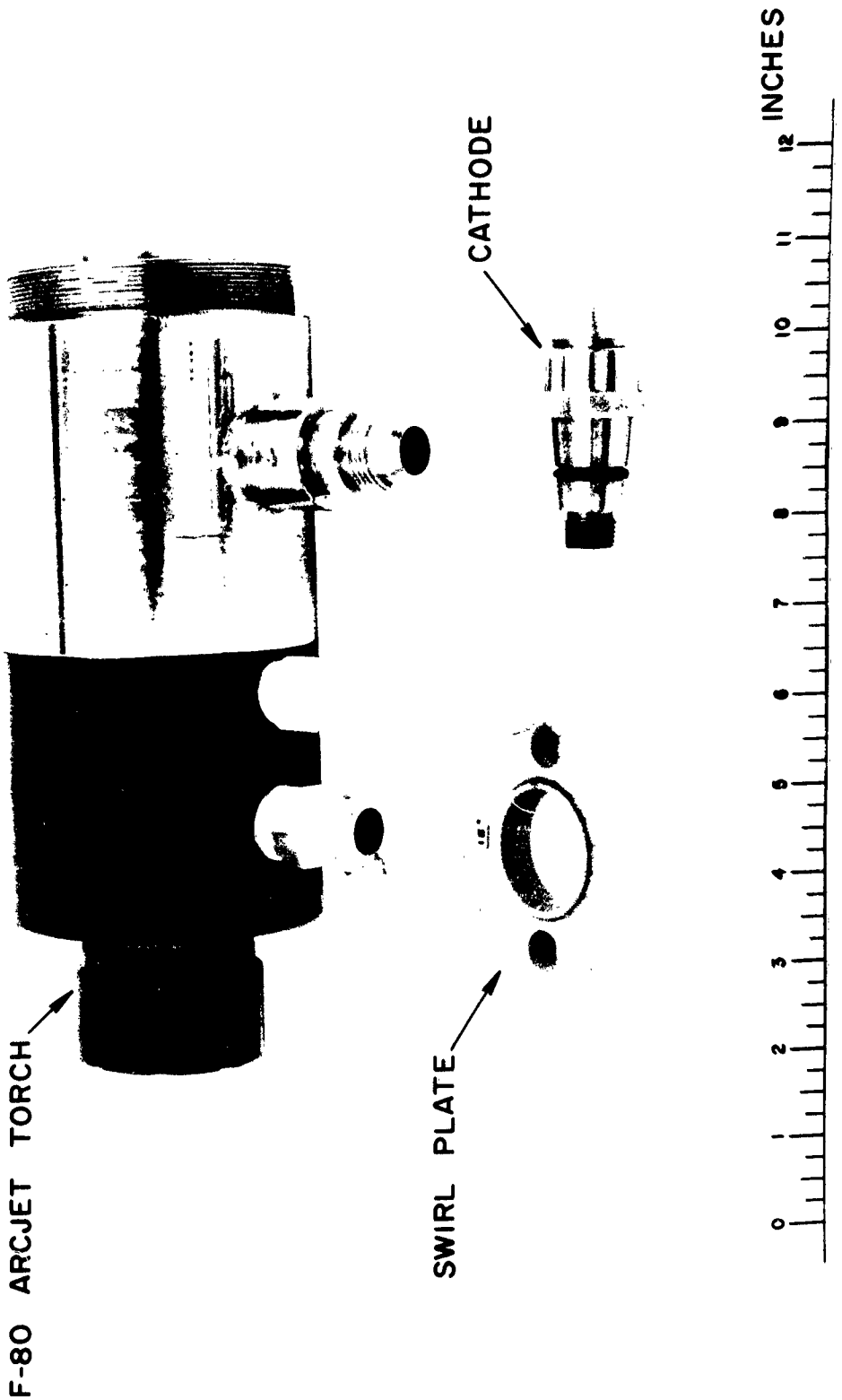

F-80 ARCJET TORCH, SWIRL PLATE, AND CATHODE

FIGURE 12

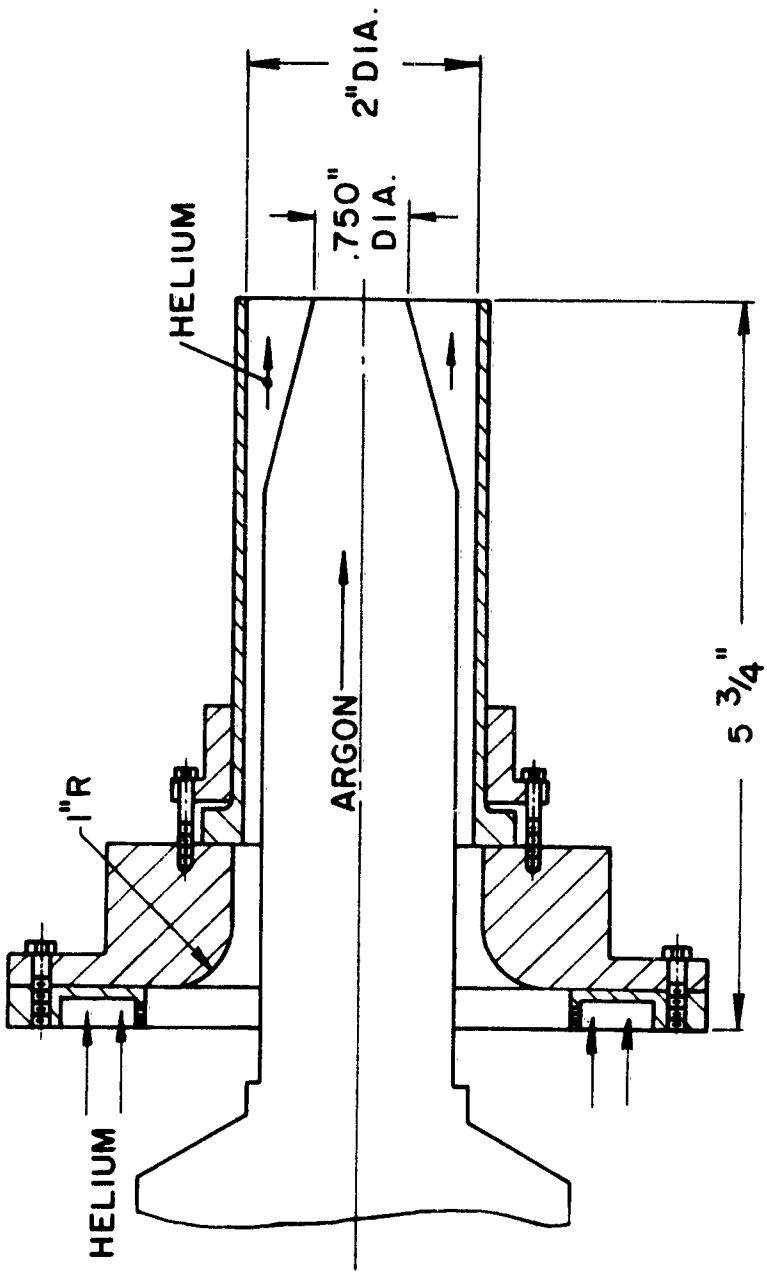

DIAGRAM OF HELIUM NOZZLE ASSEMBLY

JPR 1517

FIGURE 13

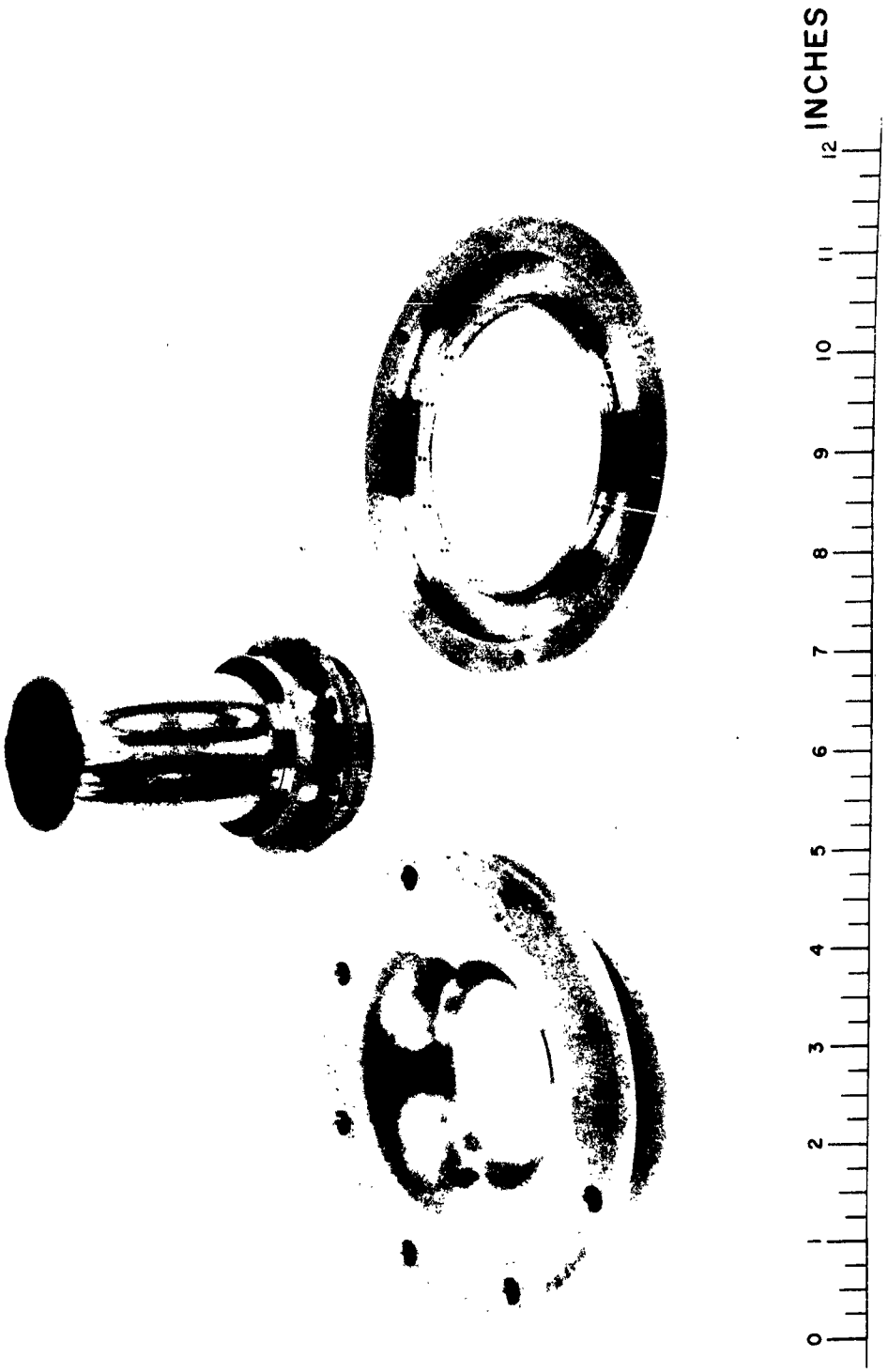

HELIUM NOZZLE ASSEMBLY

FIGURE 14

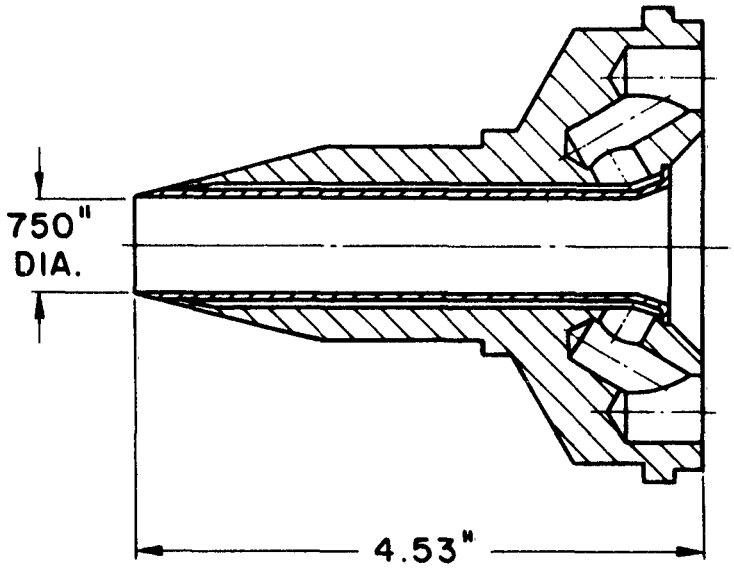

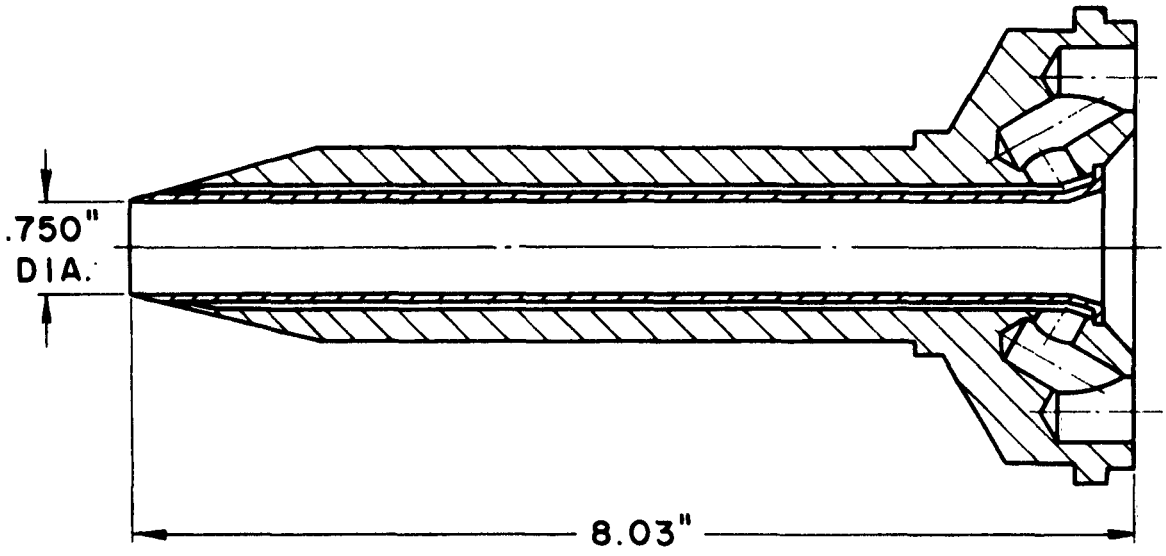

DIAGRAM OF 4" AND 8" ARGON NOZZLES

FIGURE 15

JPR 1518

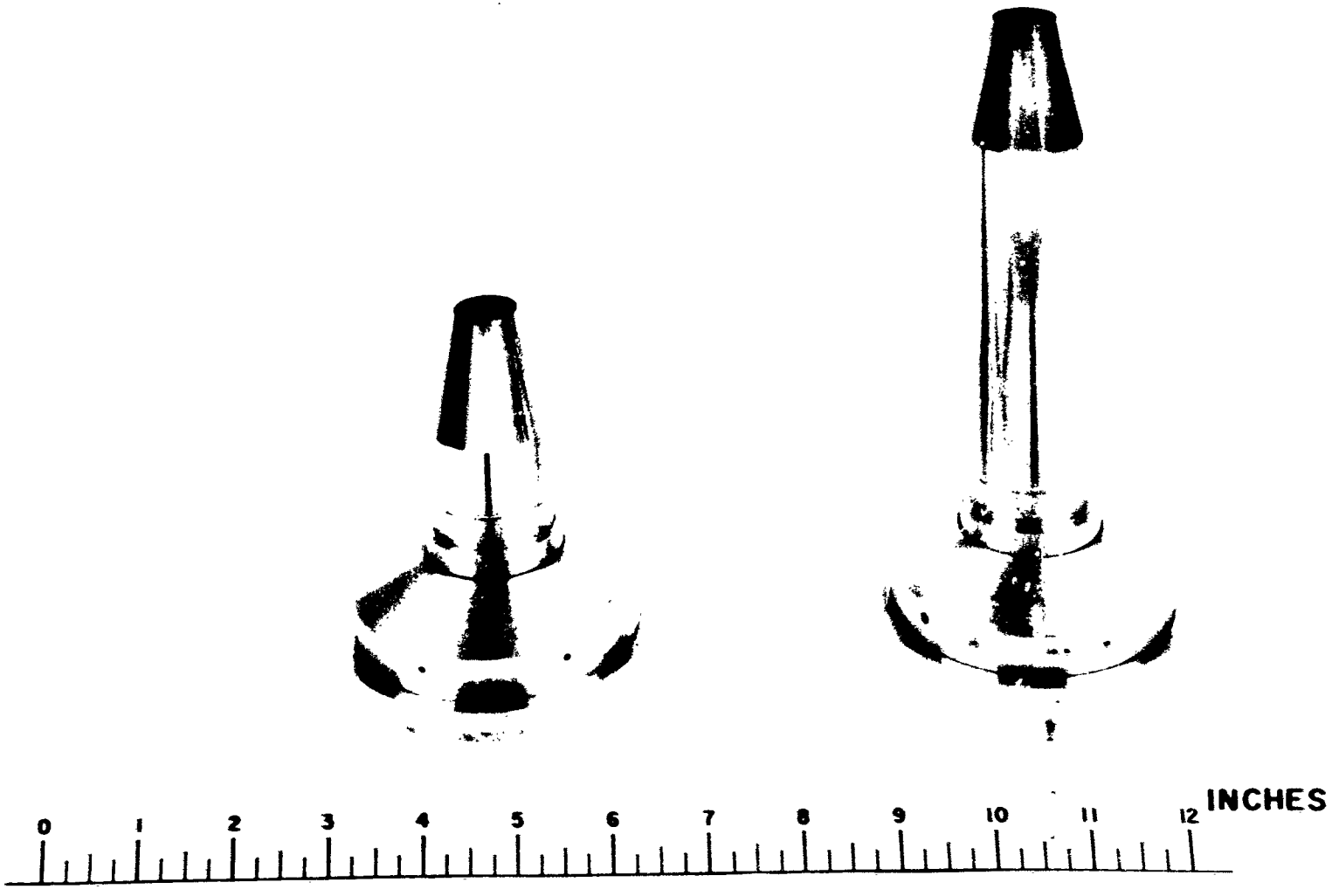

4" AND 8" ARGON NOZZLES

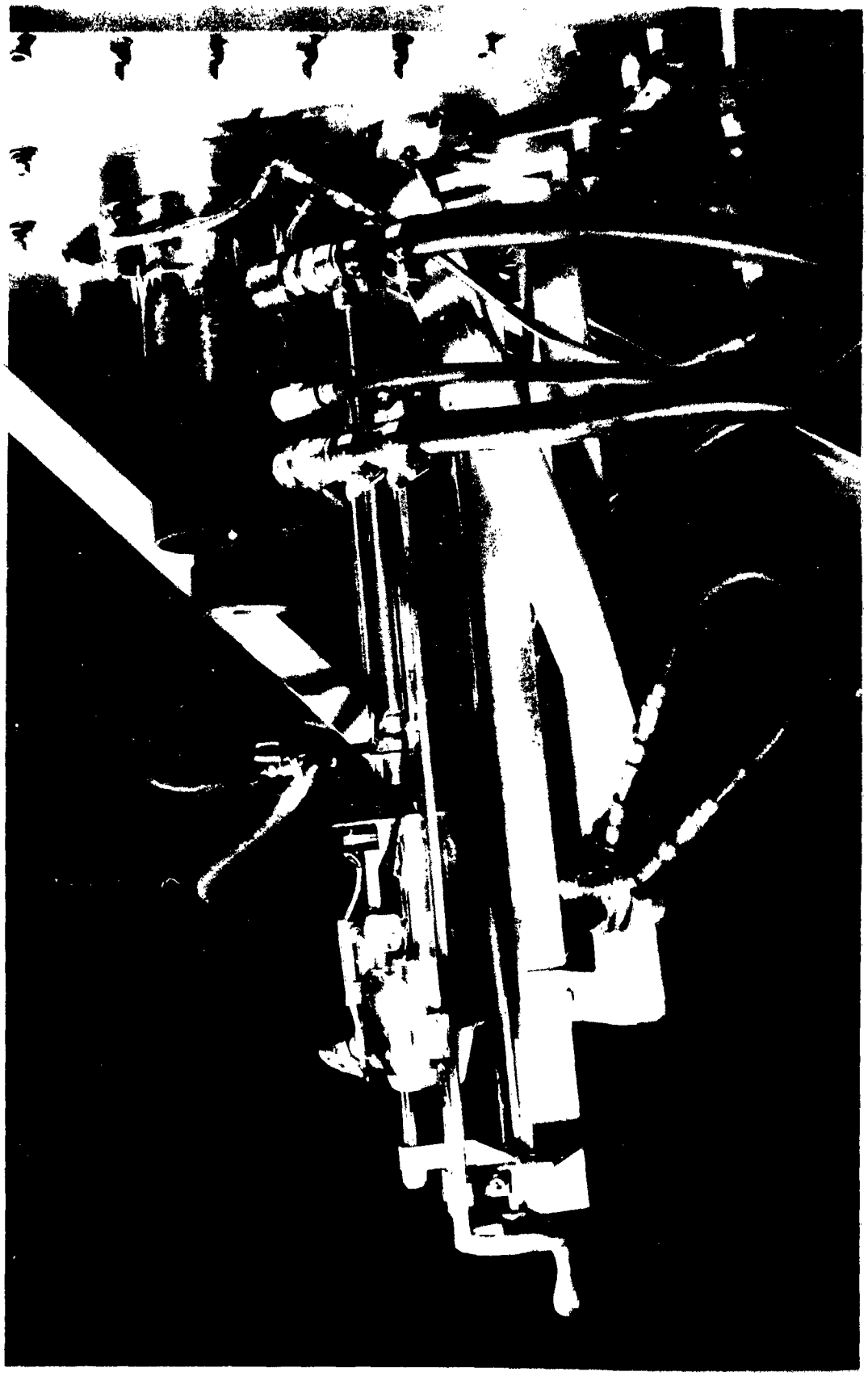

PROBE DRIVE MECHANISM

FIGURE 17

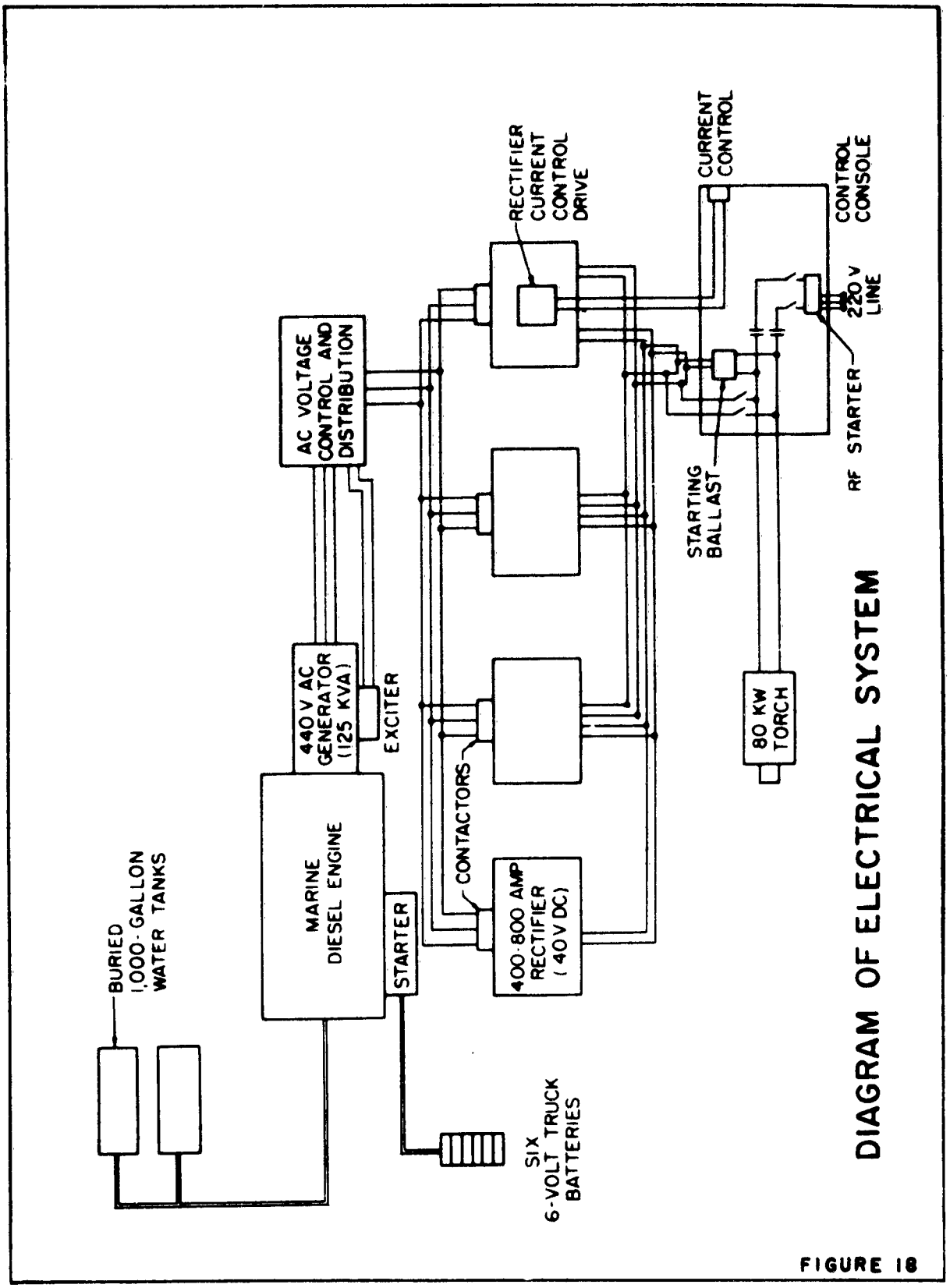
DIAGRAM OF ELECTRICAL SYSTEM
BURIED 1,000-GALLON WATER TANKS
MARINE DIESEL ENGINE
STARTER
SIX 6-VOLT TRUCK BATTERIES
440 V AC GENERATOR (125 KVA)
EXCITER
AC VOLTAGE CONTROL AND DISTRIBUTION
CONTACTORS
400-800 AMP RECTIFIER (40 V DC)
RECTIFIER CURRENT CONTROL DRIVE
CURRENT CONTROL
STARTING BALLAST
80 KW TORCH
RF STARTER
220 V LINE
CONTROL CONSOLE

FIGURE 18

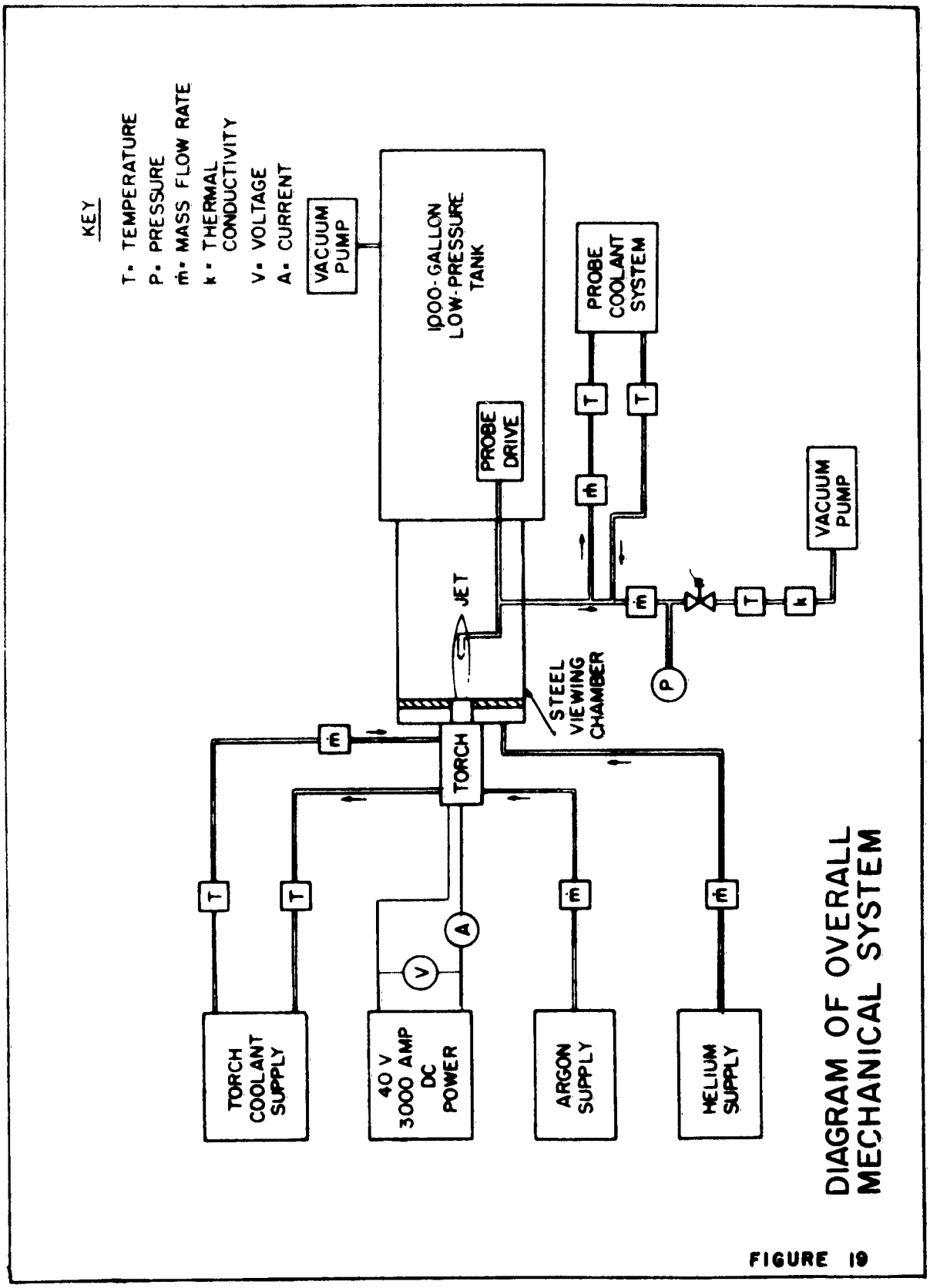
KEY
T• TEMPERATURE
P• PRESSURE
ṁ• MASS FLOW RATE
k • THERMAL CONDUCTIVITY
V• VOLTAGE
A• CURRENT
VACUUM PUMP
1000-GALLON LOW-PRESSURE TANK
PROBE DRIVE
PROBE COOLANT SYSTEM
VACUUM PUMP
JET
STEEL VIEWING CHAMBER
TORCH
TORCH COOLANT SUPPLY
40 V 3000 AMP DC POWER
ARGON SUPPLY
HELIUM SUPPLY
DIAGRAM OF OVERALL MECHANICAL SYSTEM

FIGURE 19

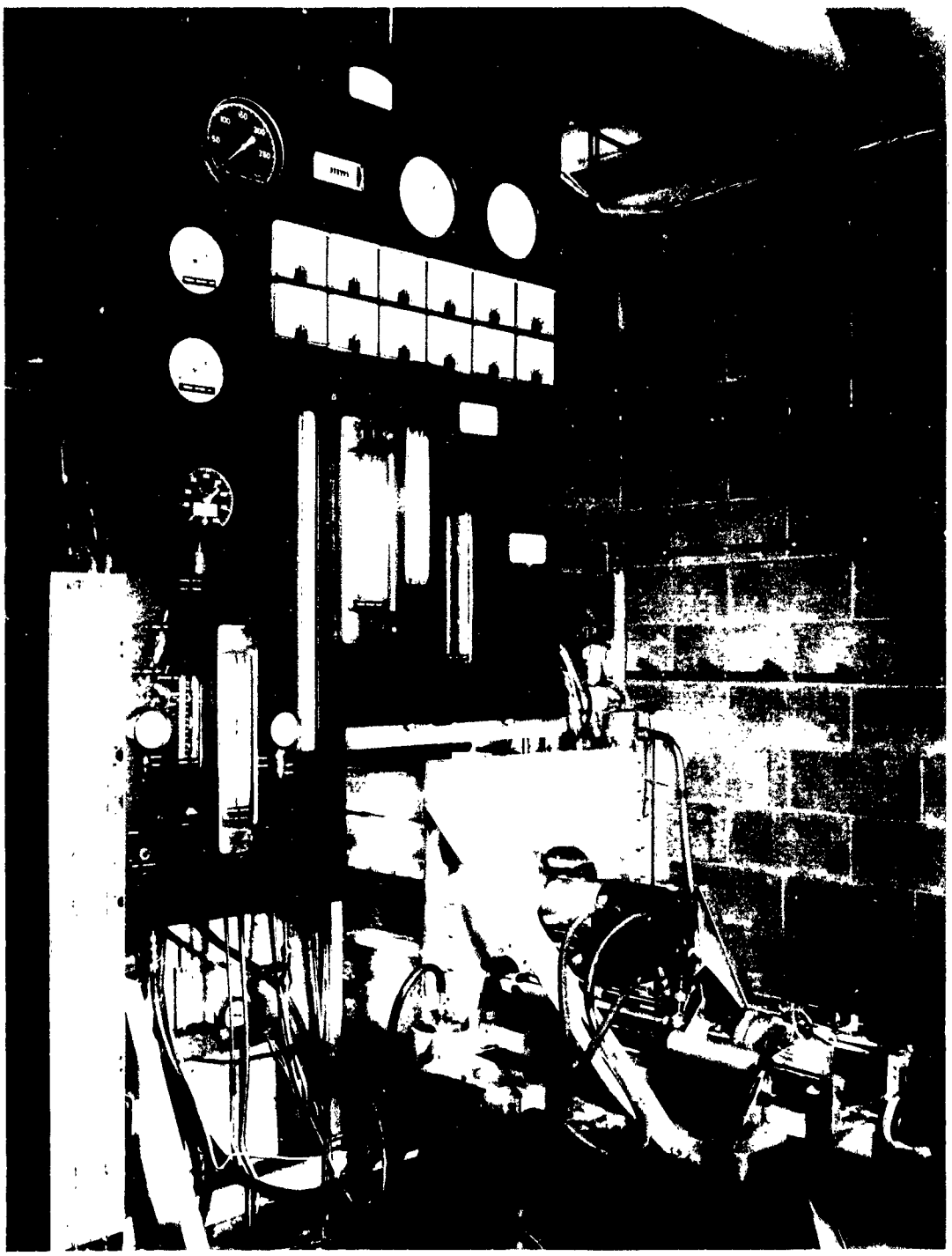

INSTRUMENT PANEL
AND EXPERIMENTAL APPARATUS

FIGURE 20

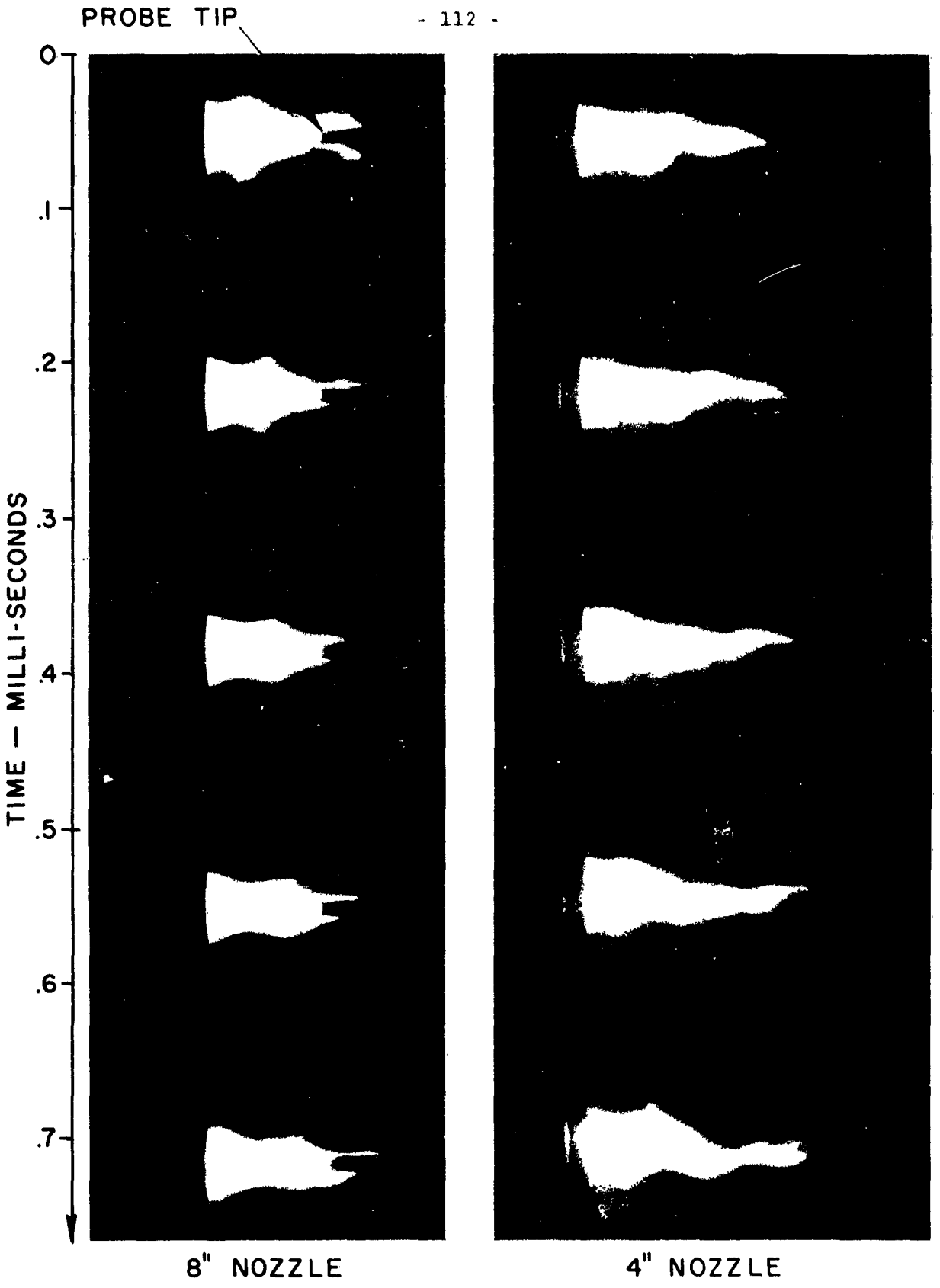

TURBULENCE IN HIGH TEMPERATURE ARGON PLASMA

FIGURE 2

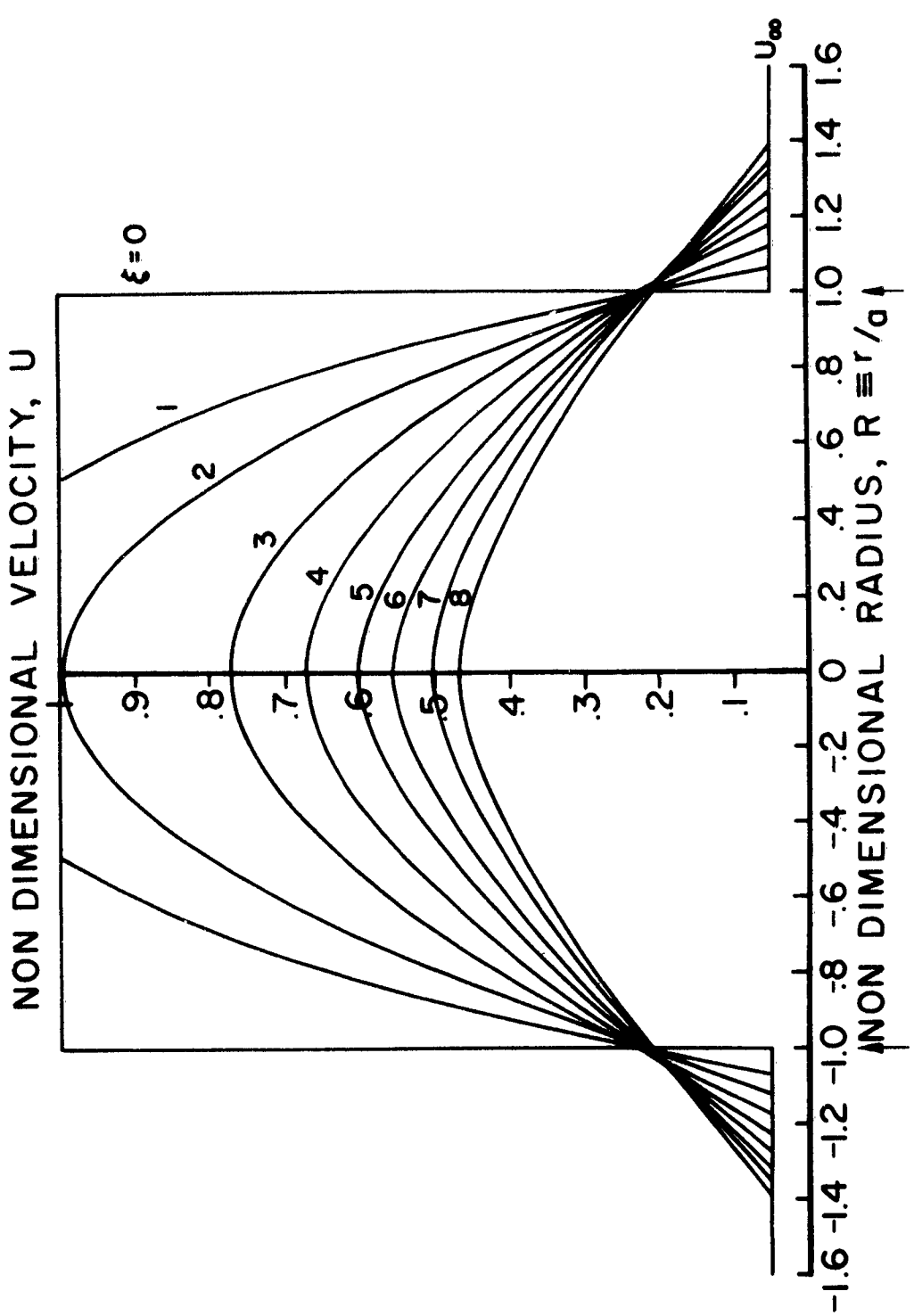

TYPICAL RADIAL VELOCITY PROFILES (ANALYTICAL)

FIGURE 2

JPR 1519

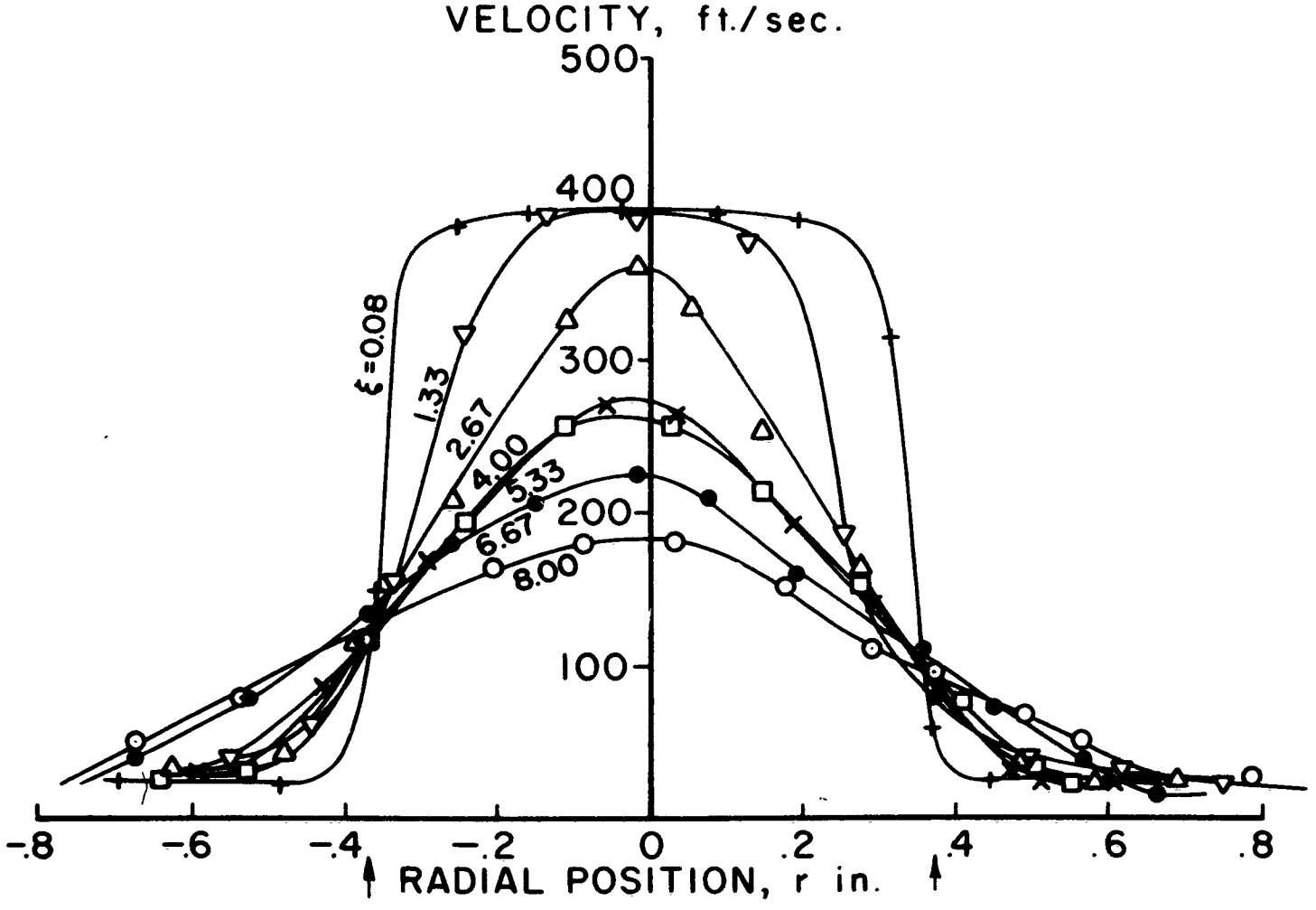

FIGURE 23 TYPICAL RADIAL VELOCITY PROFILES (EXPERIMENTAL)

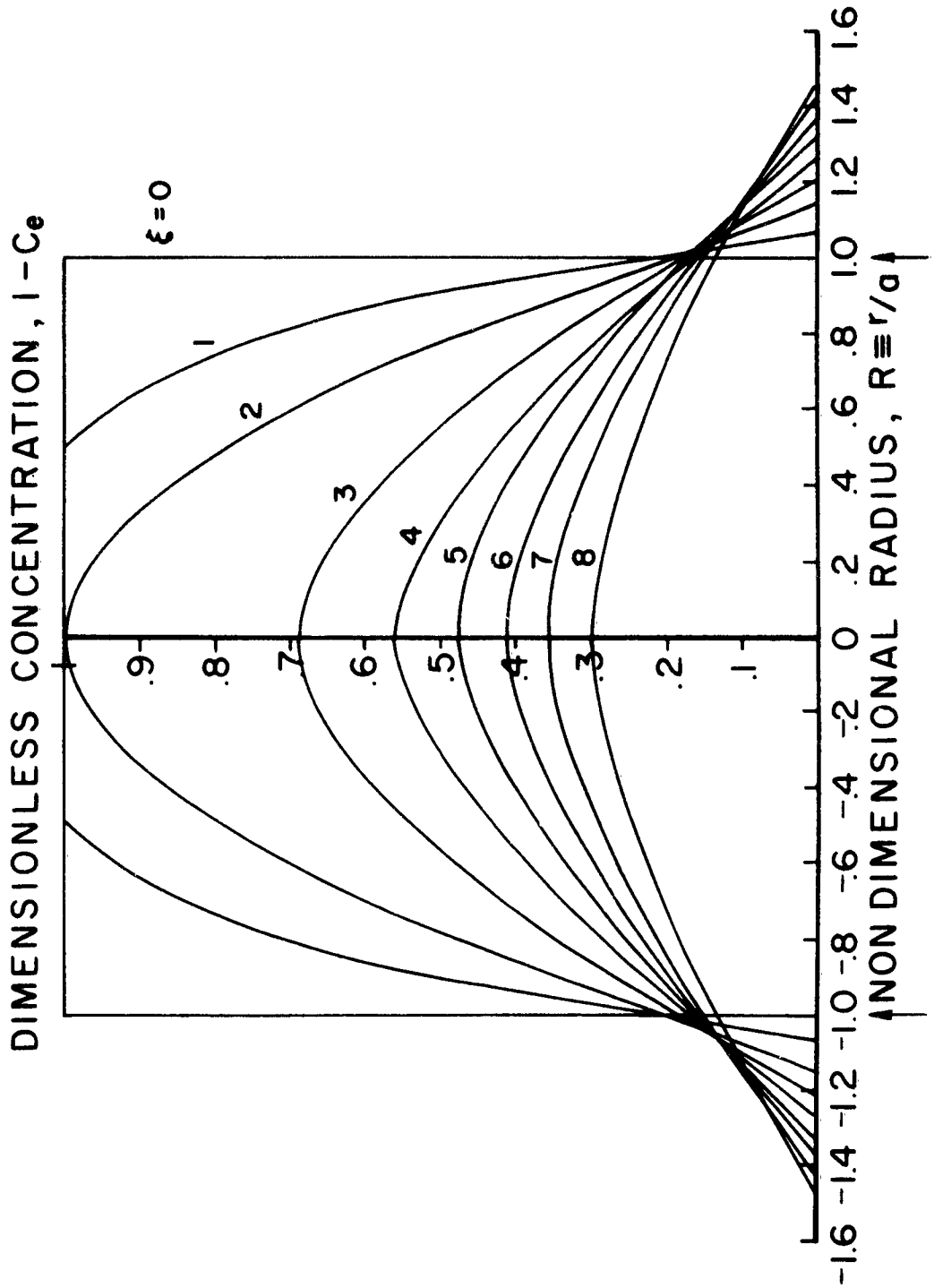

FIGURE 24 TYPICAL RADIAL CONCENTRATION PROFILES (ANALYTICAL)

JPR 1527

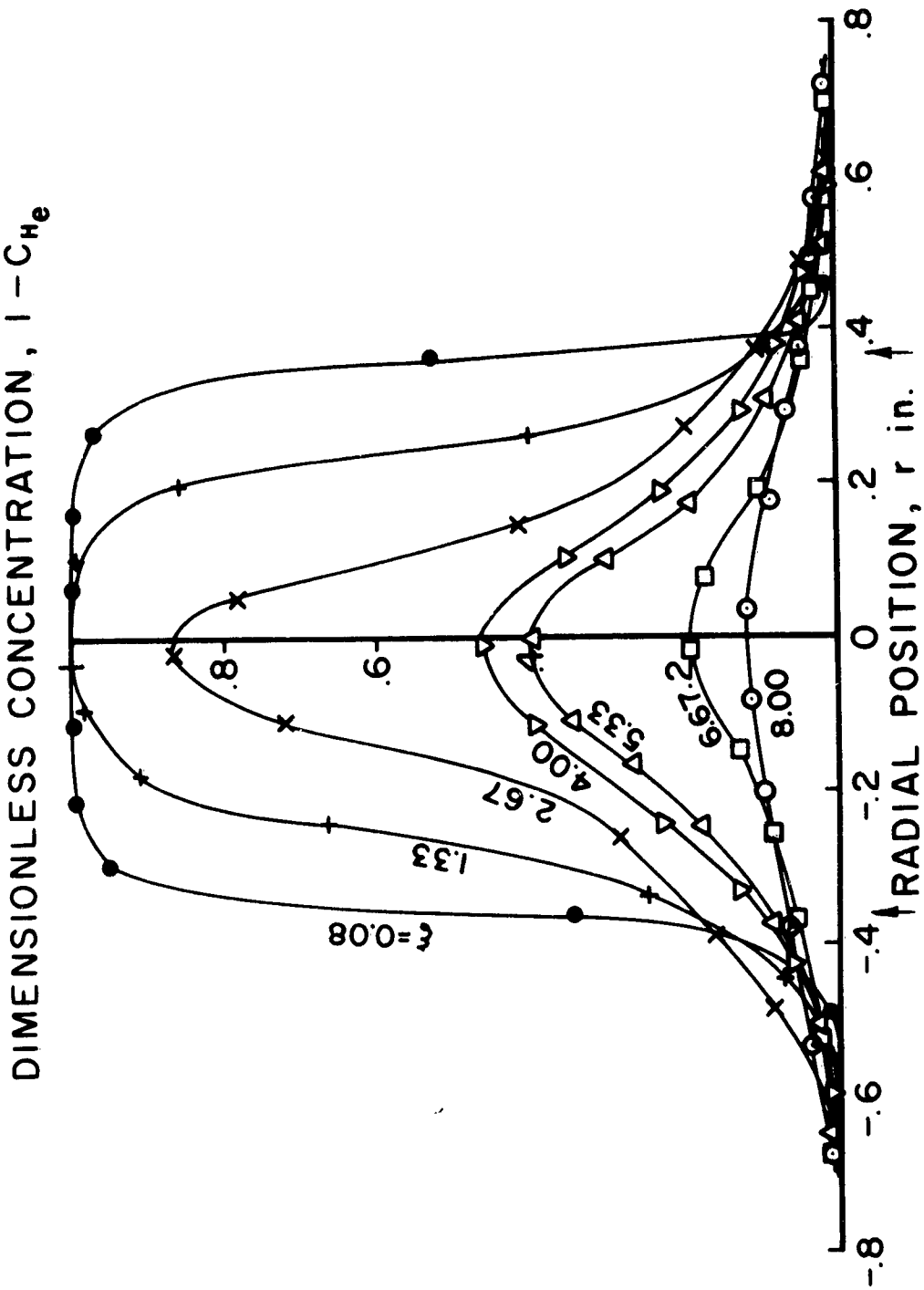

TYPICAL RADIAL CONCENTRATION PROFILES (EXPERIMENTAL)

FIGURE 25

JPR 1522

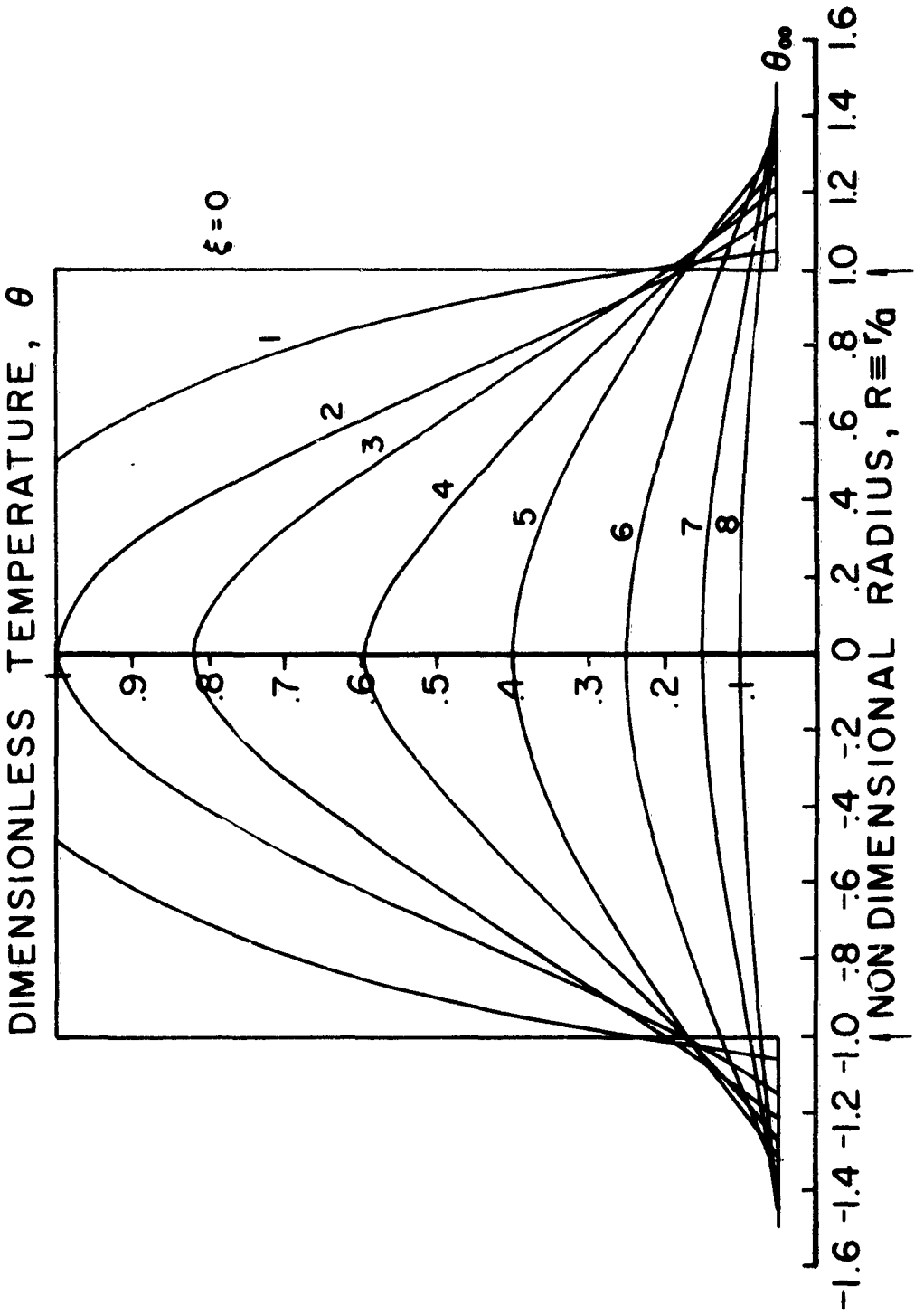

TYPICAL RADIAL TEMPERATURE PROFILES (ANALYTICAL)

FIGURE 26

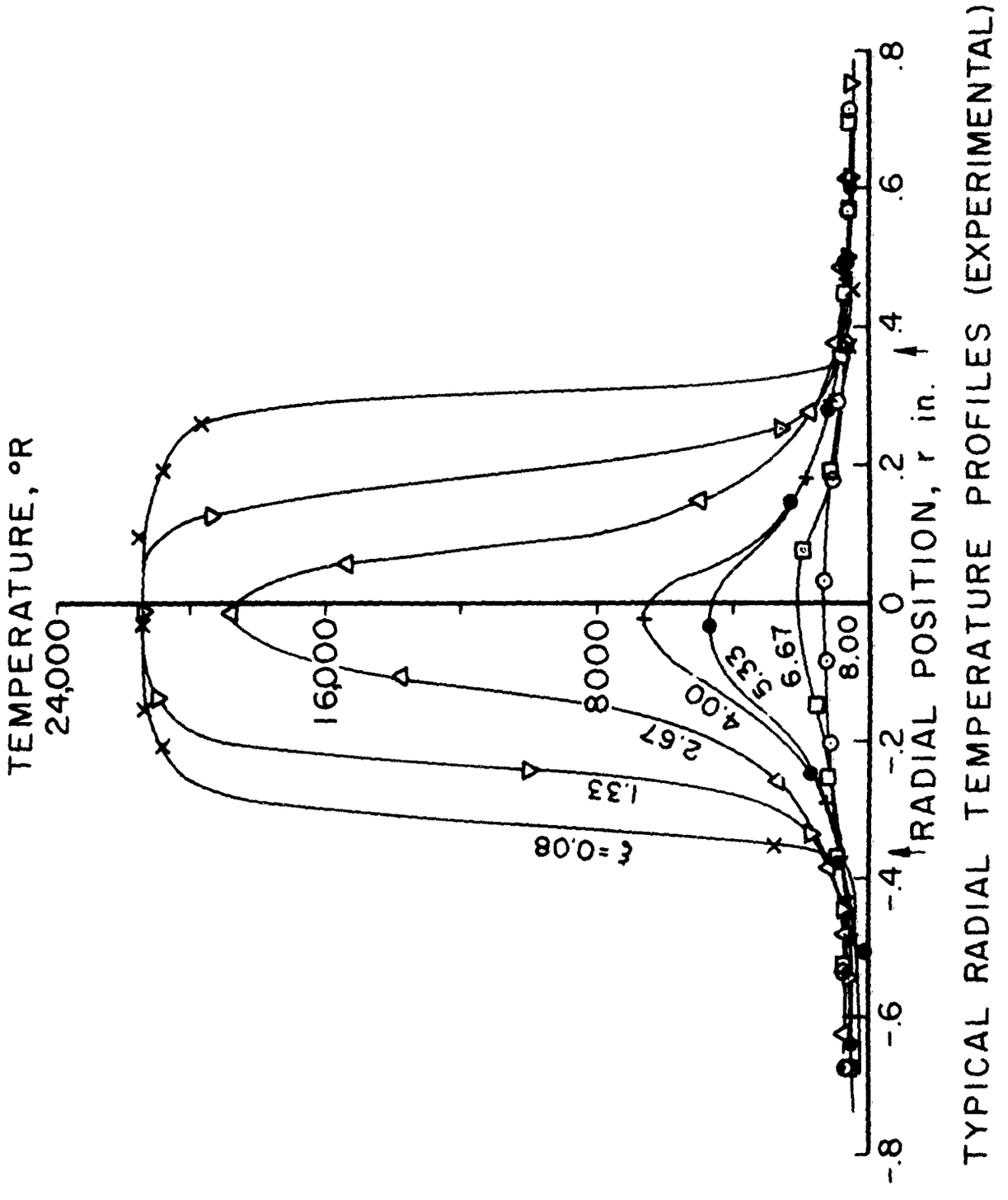

TYPICAL RADIAL TEMPERATURE PROFILES (EXPERIMENTAL)

JPR 1524

FIGURE 27

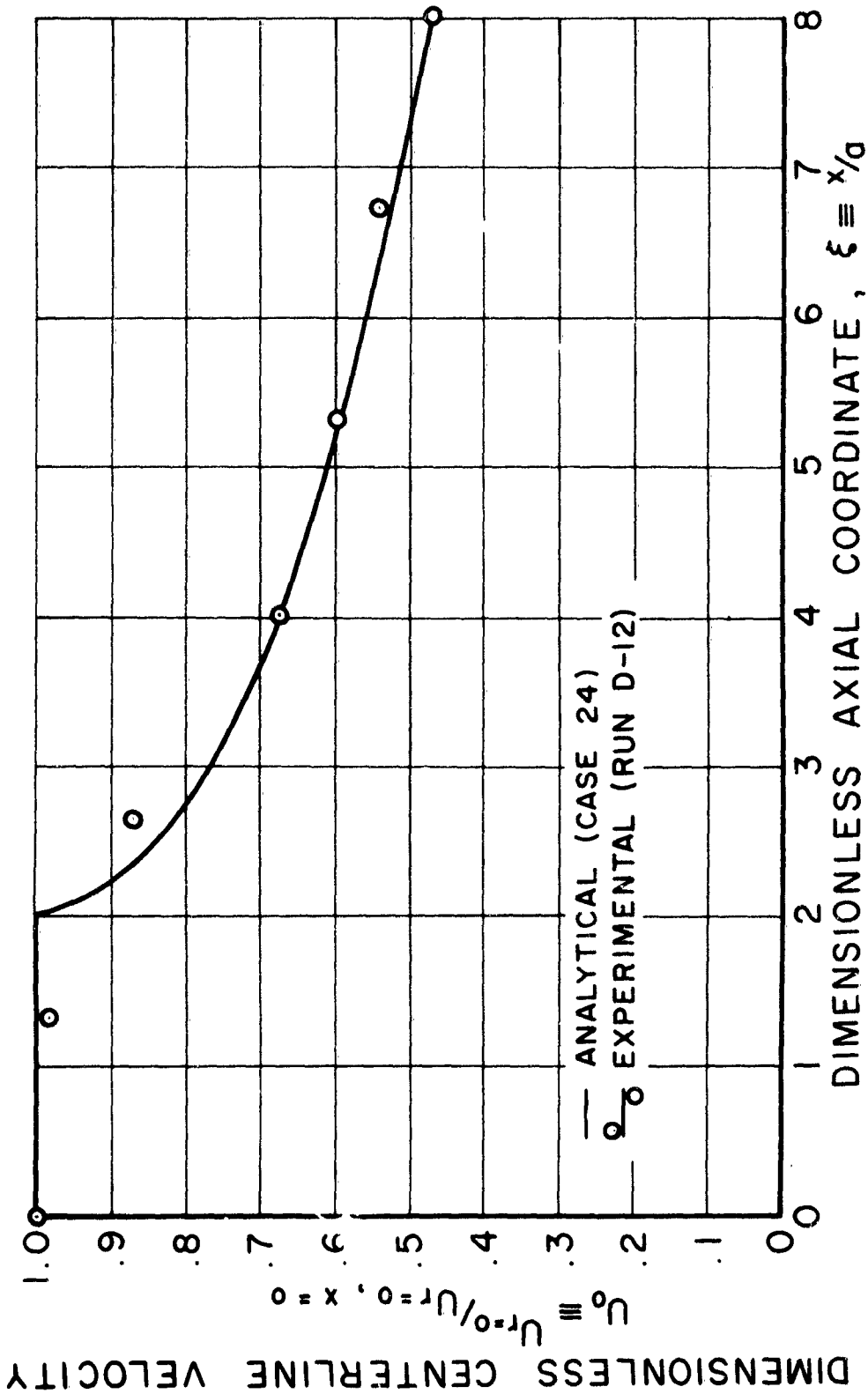

TYPICAL AXIAL DECAY OF VELOCITY

FIGURE 28

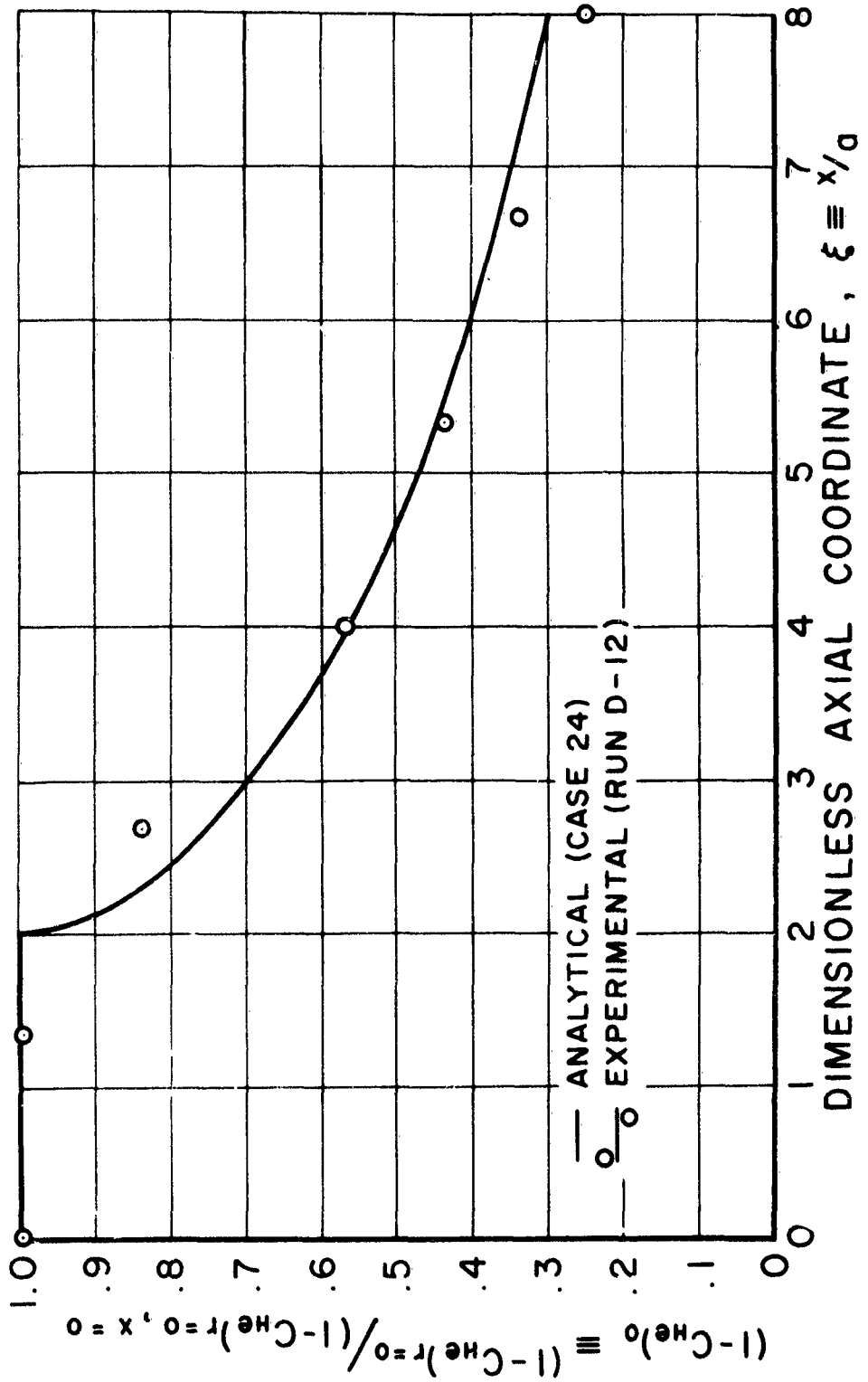

TYPICAL AXIAL DECAY OF CONCENTRATION

JPR 1526

FIGURE 29

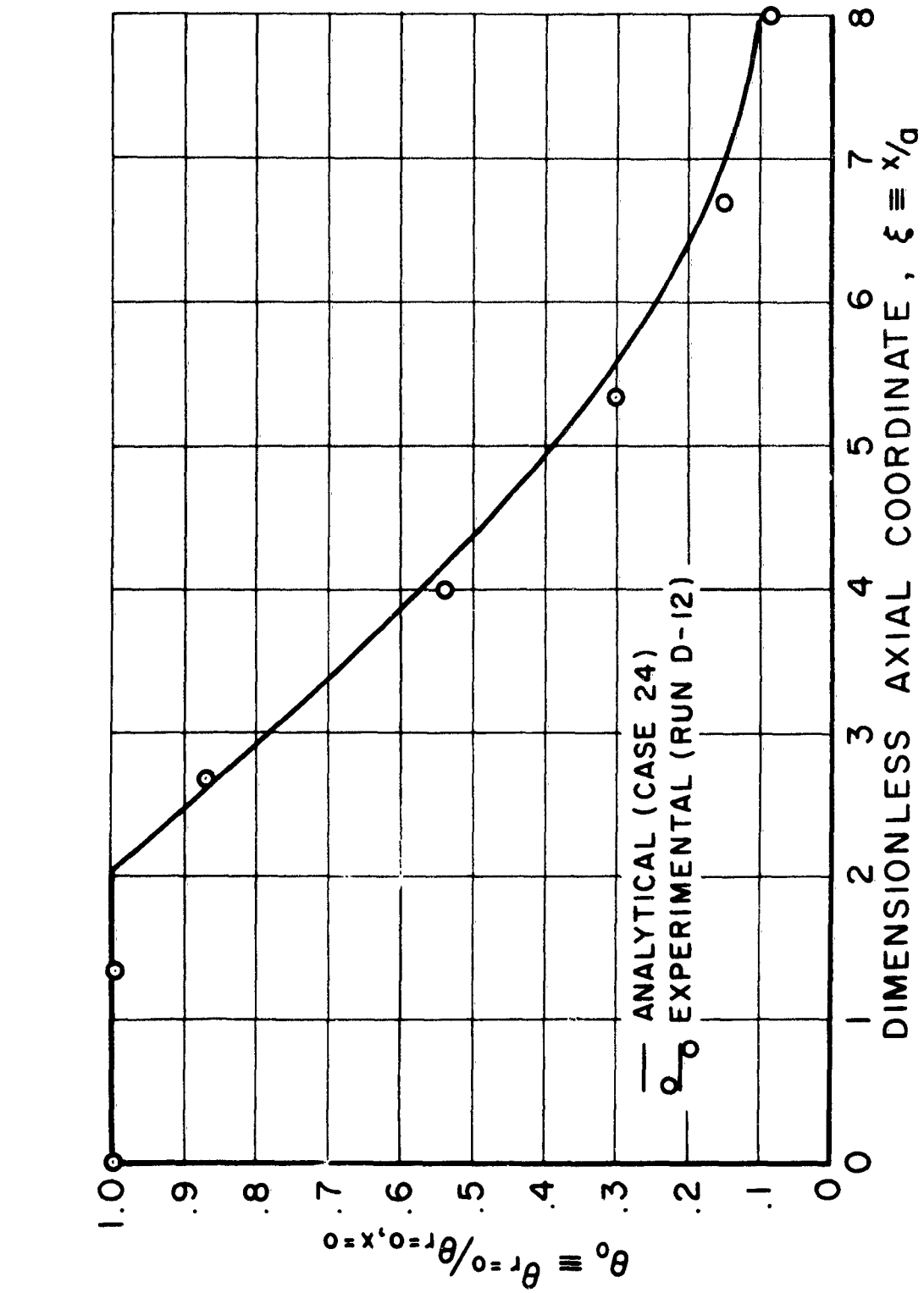

TYPICAL AXIAL DECAY OF TEMPERATURE

FIGURE 30

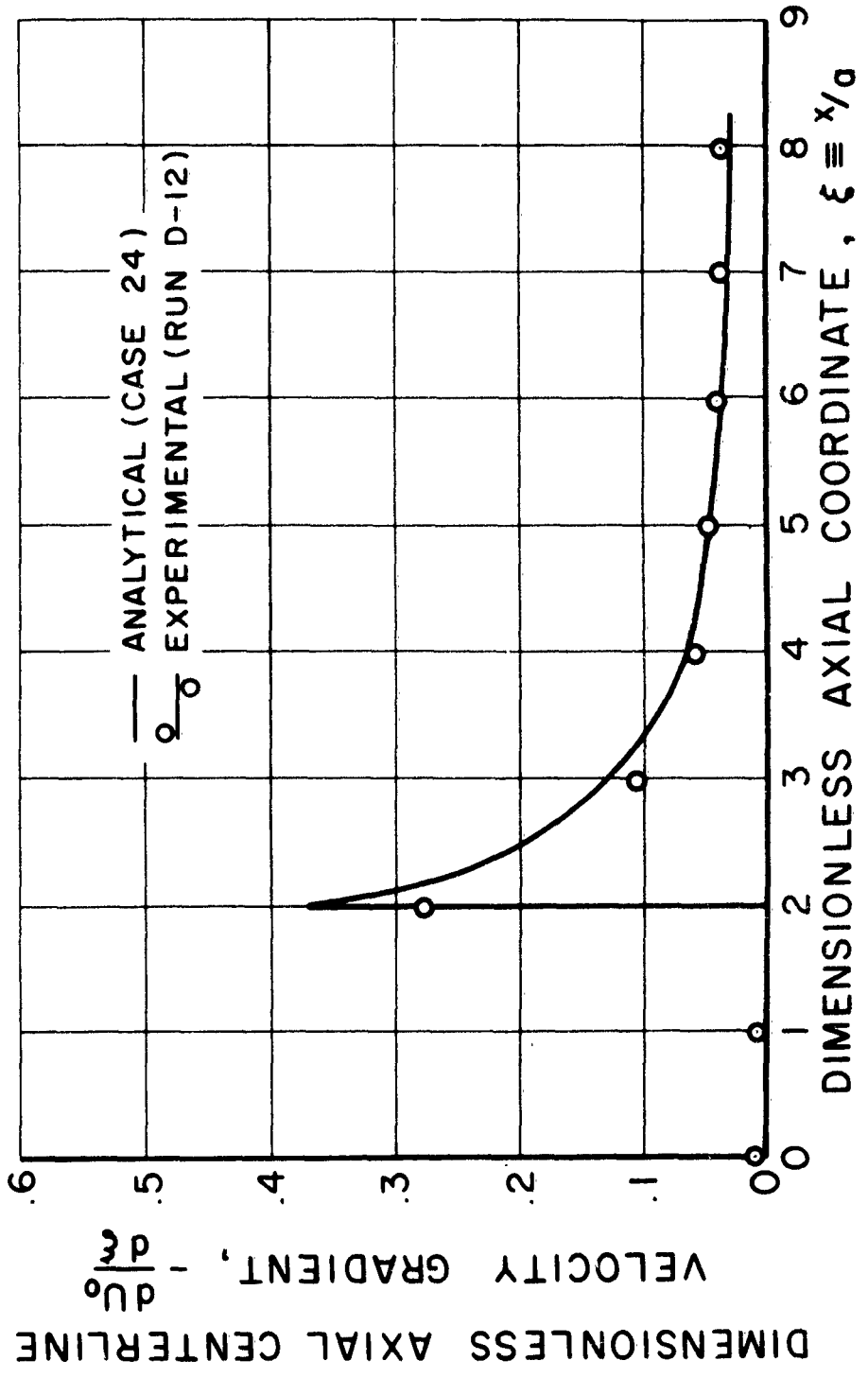

TYPICAL AXIAL GRADIENTS OF VELOCITY

FIGURE 31

JPR 1528

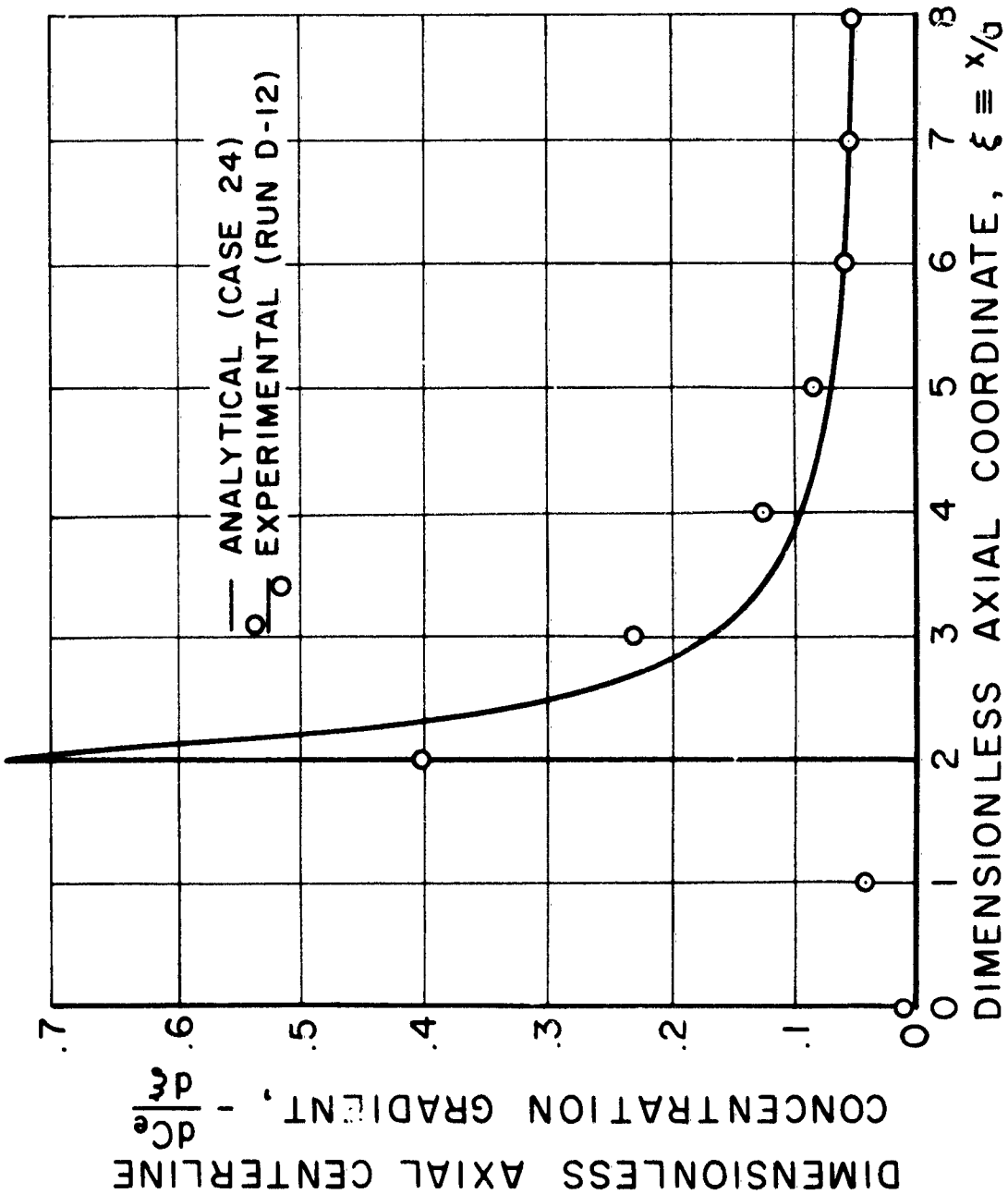

TYPICAL AXIAL GRADIENTS OF CONCENTRATION

FIGURE 32

JPR 1529

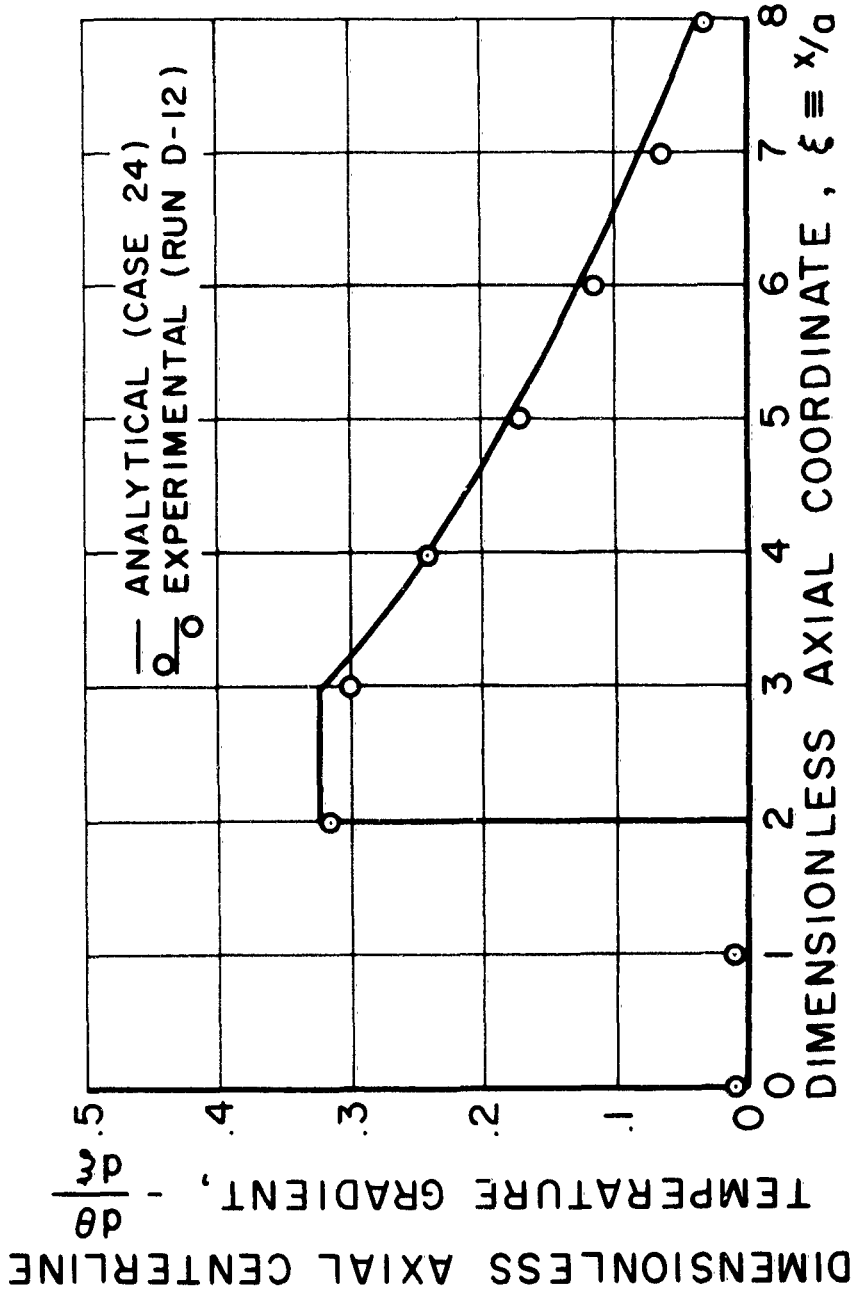

TYPICAL AXIAL GRADIENTS OF TEMPERATURE

JPR 1530

FIGURE 33

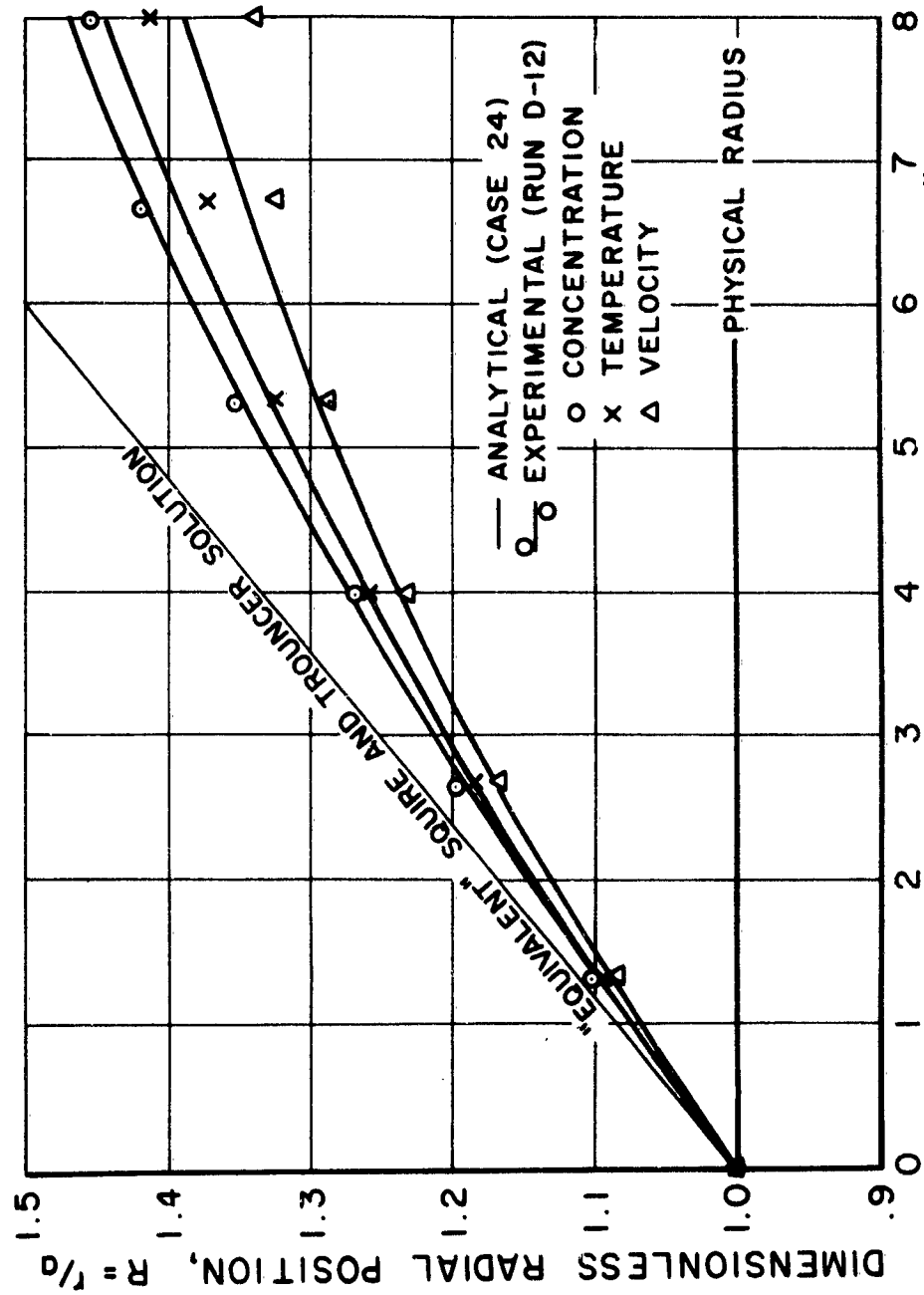

TYPICAL RADIAL SPREADING OF VELOCITY, CONCENTRATION, AND TEMPERATURE WITH RESPECT TO AXIAL POSITION

FIGURE 34

JPR 1531

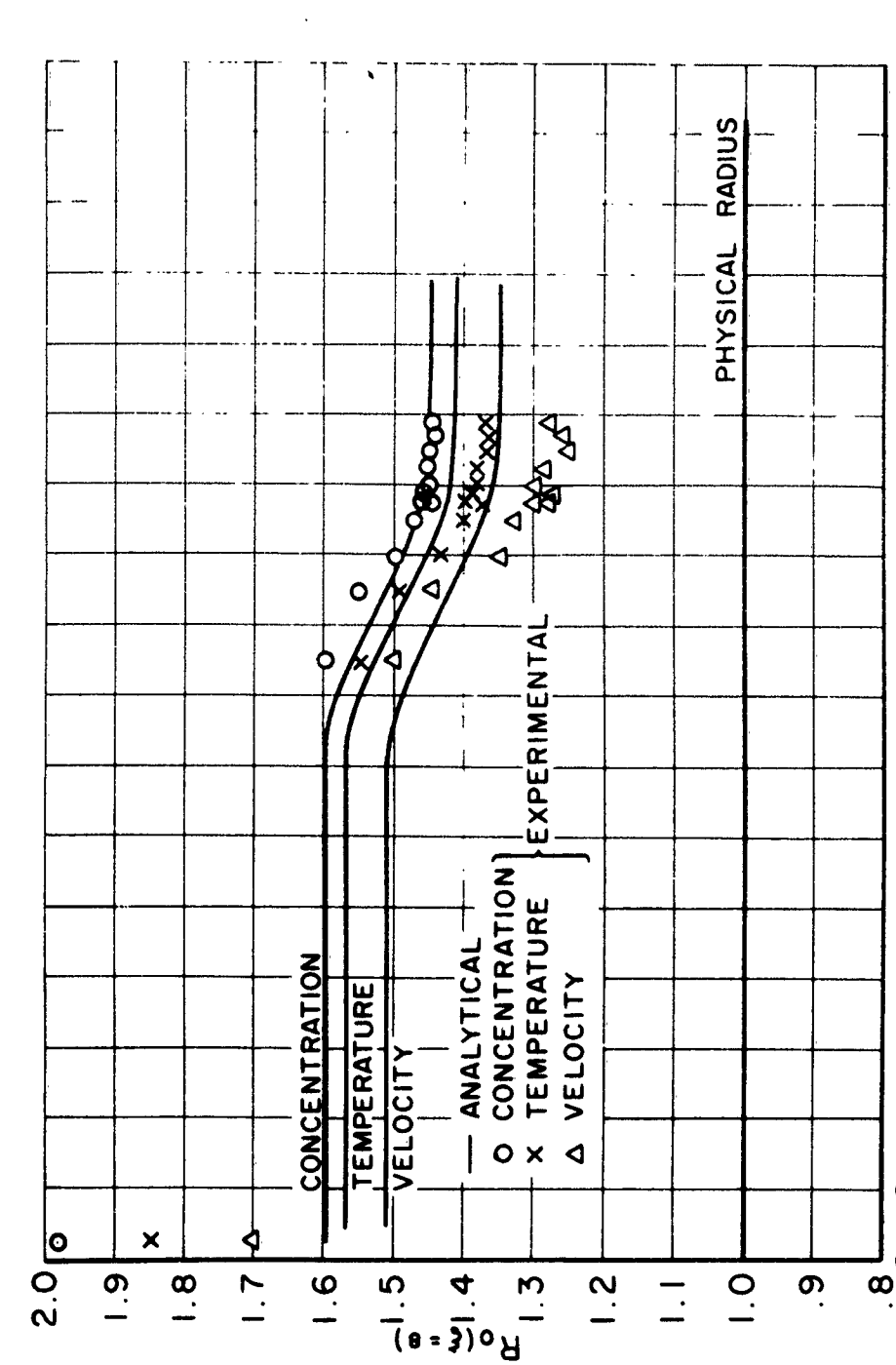

TYPICAL RADIAL SPREADING OF VELOCITY, CONCENTRATION, AND TEMPERATURE WITH RESPECT TO PEAK TEMPERATURE

FIGURE 35

JPR 1532

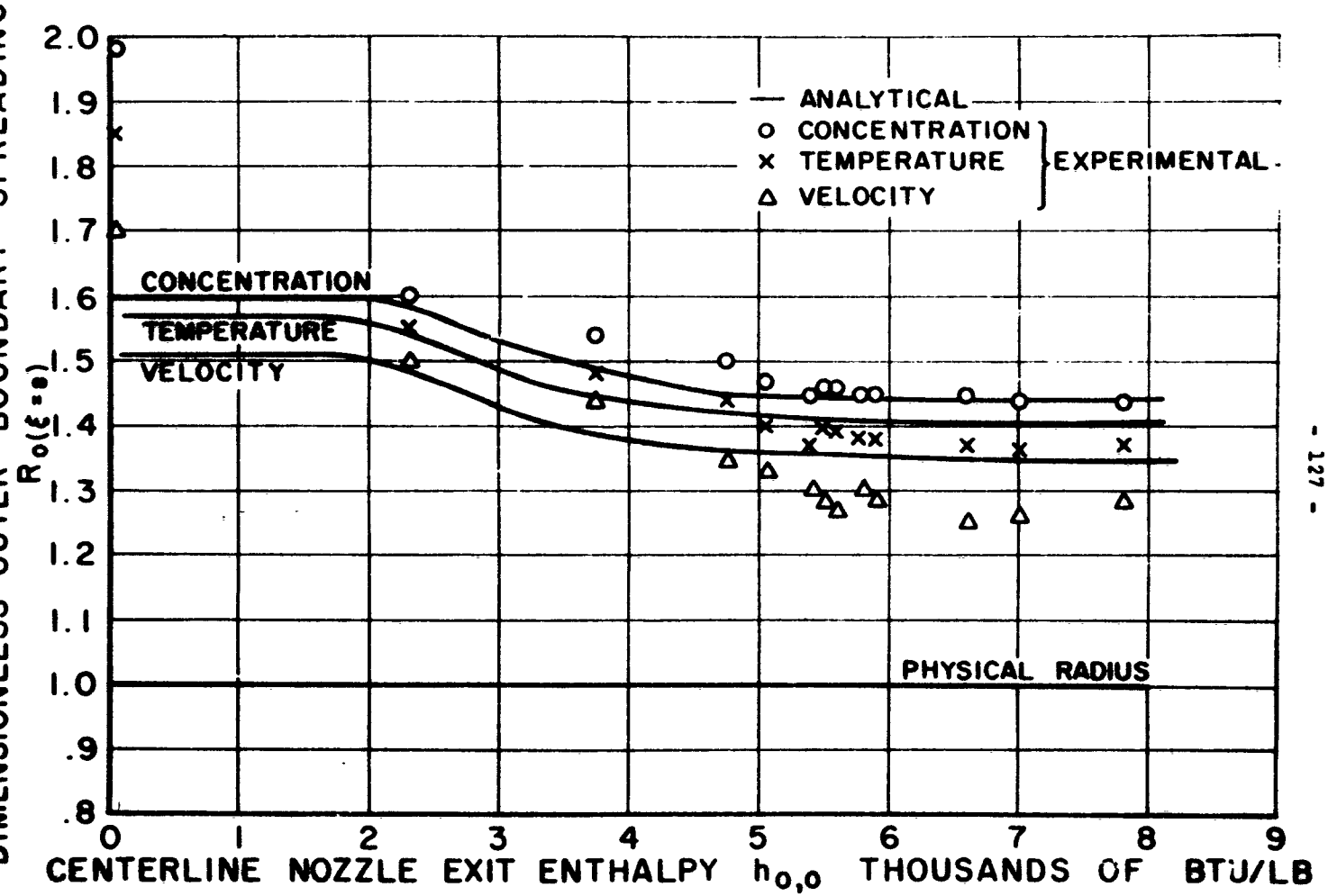

FIGURE 36

TYPICAL RADIAL SPREADING OF VELOCITY, CONCENTRATION, AND TEMPERATURE WITH RESPECT TO PEAK ENTHALPY

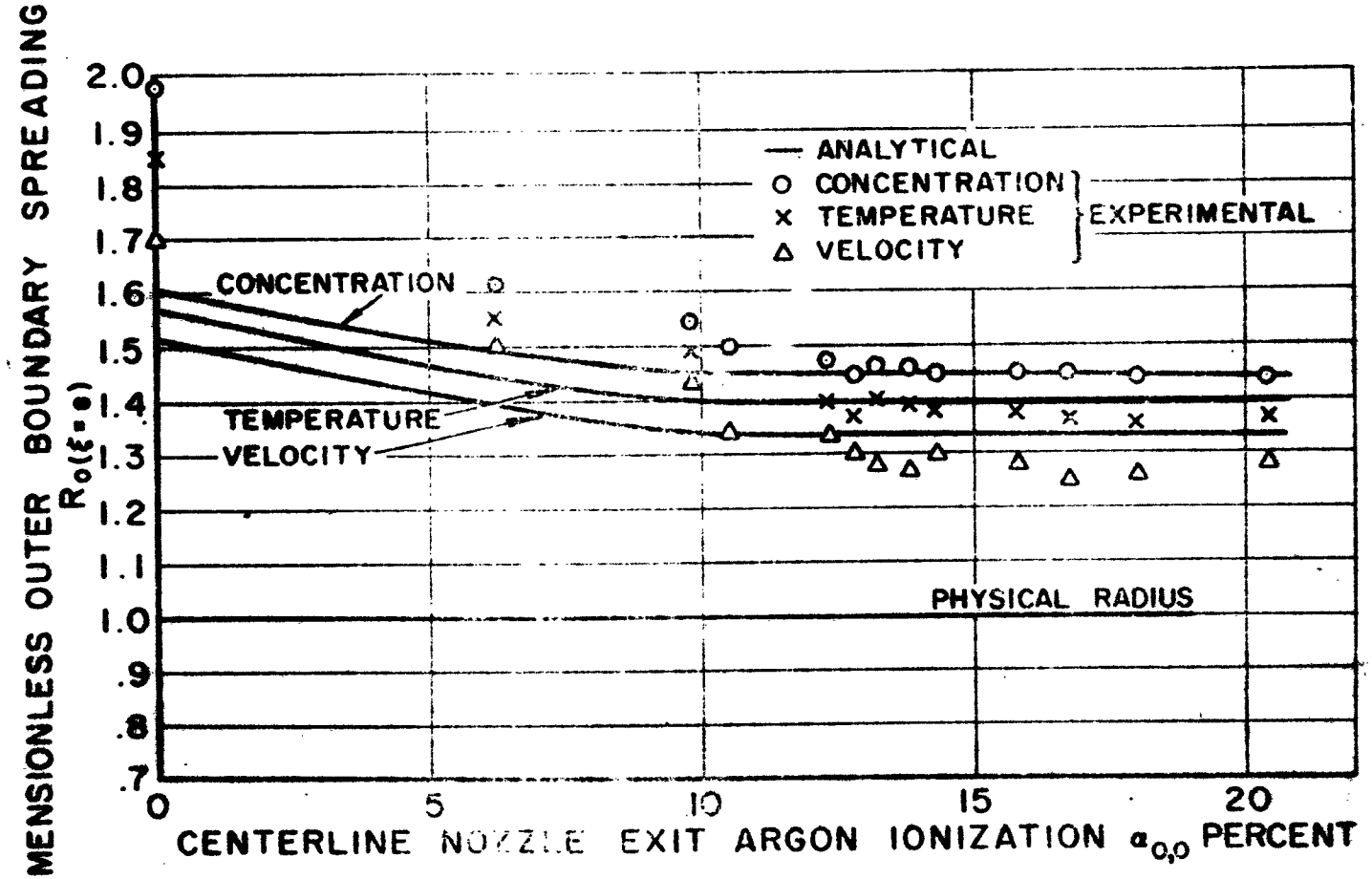

FIGURE 37

TYPICAL RADIAL SPREADING OF VELOCITY, CONCENTRATION, AND TEMPERATURE WITH RESPECT TO PEAK IONIZATION

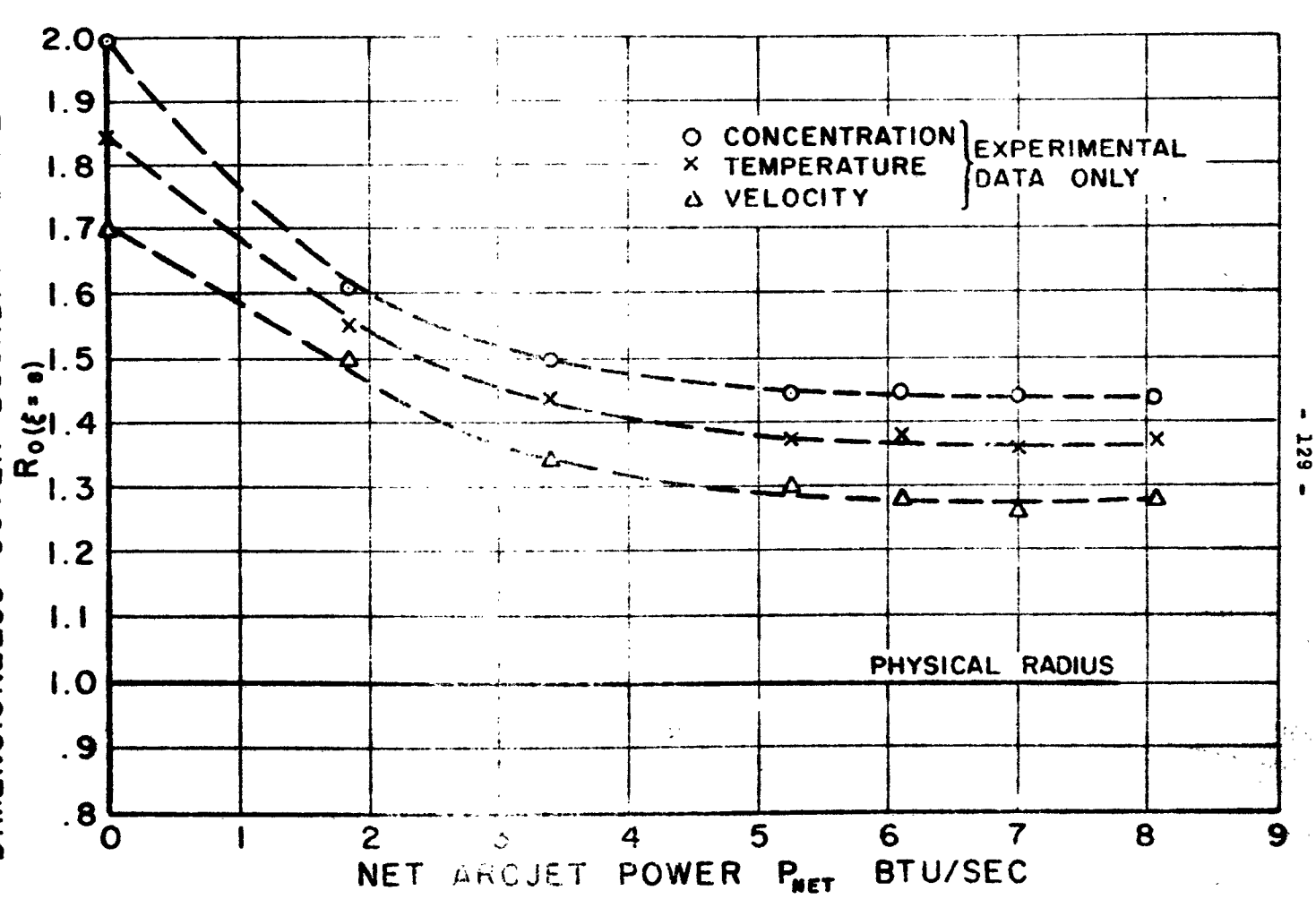

FIGURE 38

TYPICAL RADIAL SPREADING OF VELOCITY, CONCENTRATION, AND TEMPERATURE WITH RESPECT TO NET POWER

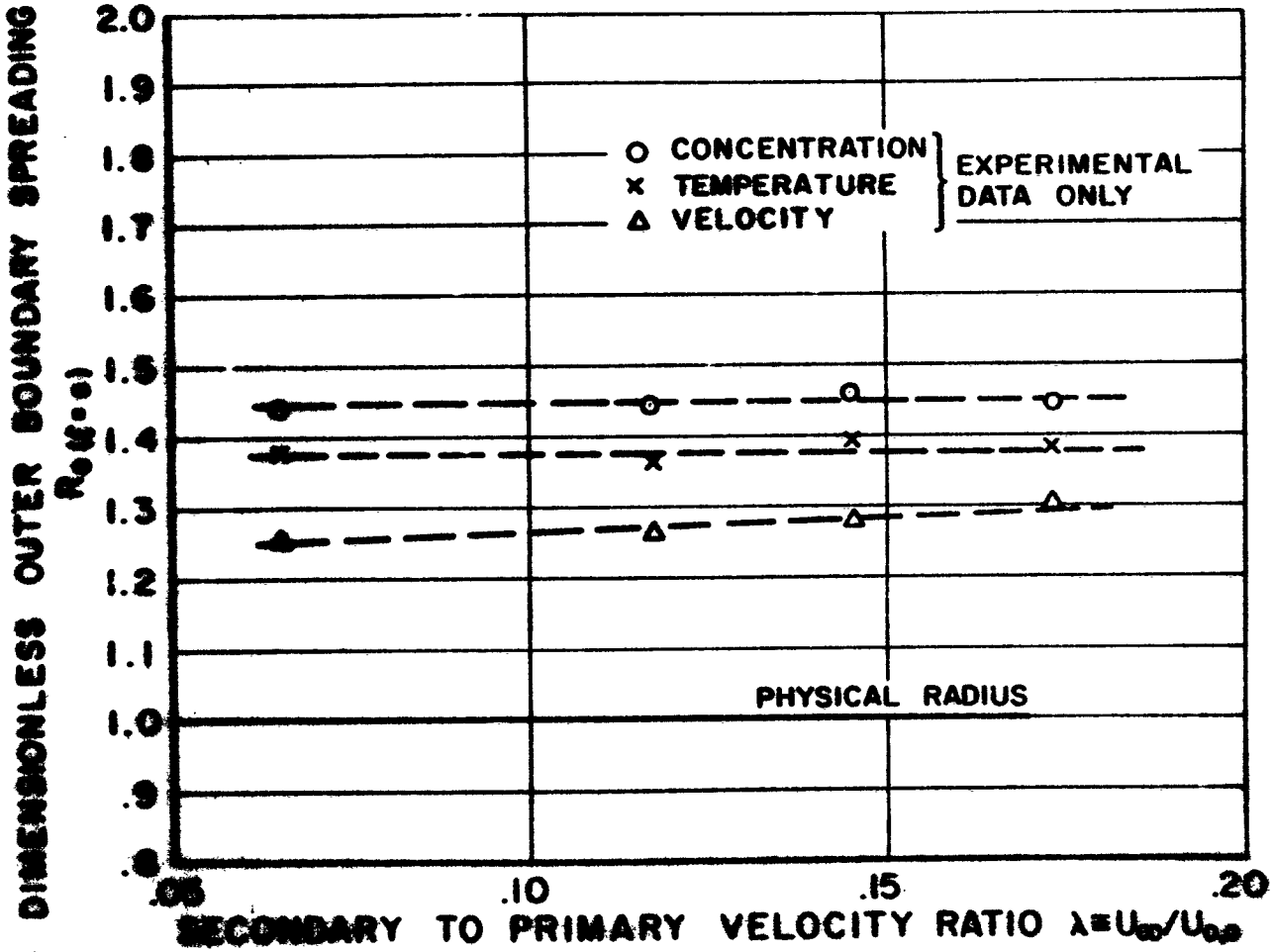

FIGURE 36

TYPICAL RADIAL SPREADING OF VELOCITY, CONCENTRATION, AND TEMPERATURE WITH RESPECT TO THE RATIO OF THE PRIMARY GAS VELOCITY TO THE SECONDARY GAS VELOCITY

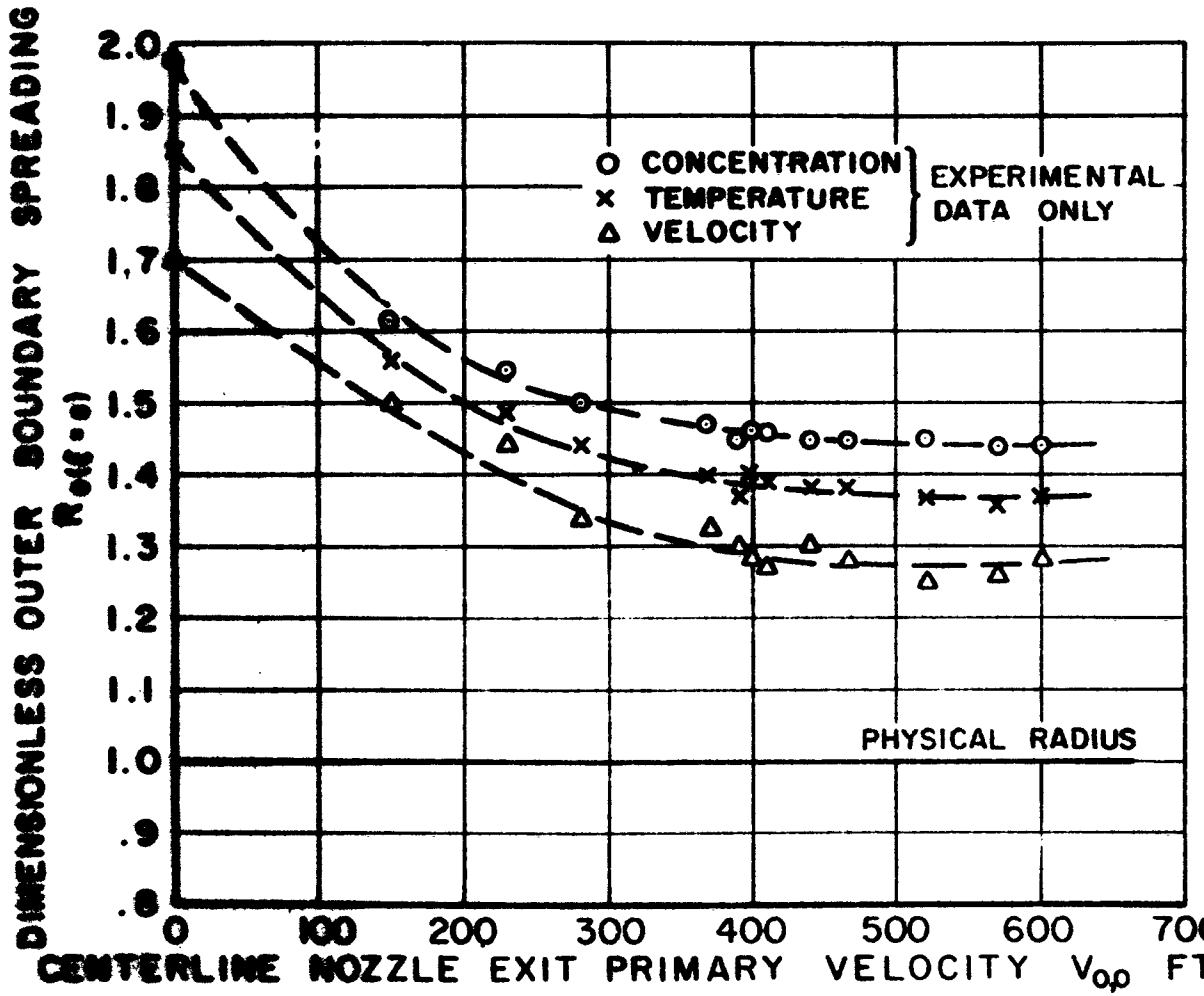

FIGURE 49

TYPICAL RADIAL SPREADING OF VELOCITY, CONCENTRATION, AND TEMPERATURE WITH RESPECT TO PEAK VELOCITY

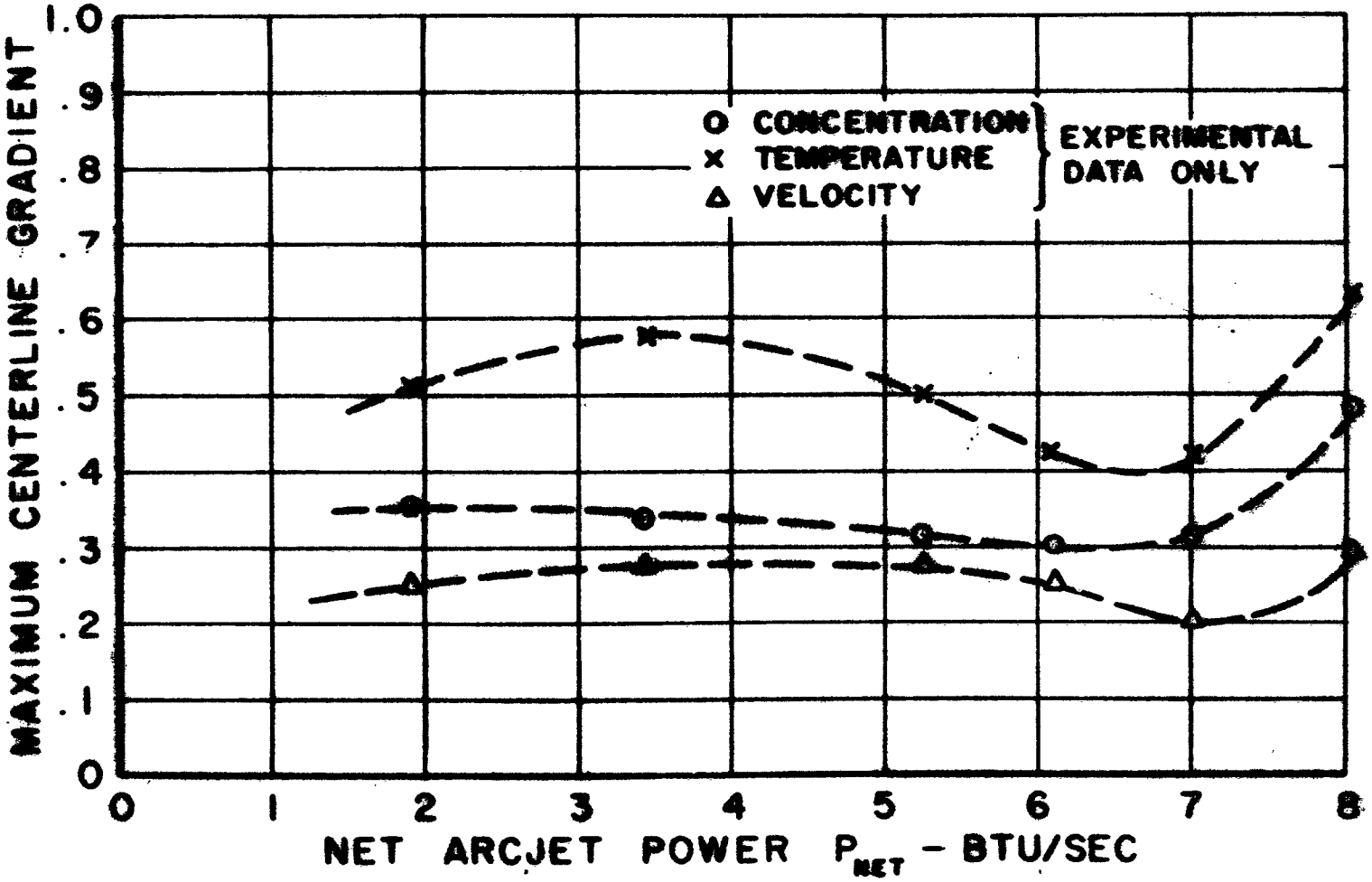

FIGURE 41

TYPICAL MAXIMUM CENTERLINE GRADIENTS OF VELOCITY, CONCENTRATION, AND TEMPERATURE WITH RESPECT TO NET POWER

DISTRIBUTION LIST NONR 1858(31)
TECHNICAL REPORT

AGENCY

Chief of Naval Research
Department of the Navy
Washington 25, D. C.
Attn: Code 429 (5)
Code 438 (1)

Commanding Officer
Office of Naval Research
Branch Officer
1000 Geary Street
San Francisco 9, Calif. (1)

Commanding Officer
Office of Naval Research
Branch Office
1030 E. Green Street
Pasadena 1, Calif. (1)

Commanding Officer
Office of Naval Research
Branch Office
John Crerar Library Building
86 E. Randloph Street
Chicago 1. Illinois (1)

Commanding Officer
Office of Naval Research
Branch Office
Navy #100, Box 39
Fleet Post Office
New York, N. Y. (1)

Commanding Officer
Office of Naval Research
207 West 4th Street
New York 11, New York
via:
Office of Naval Research
Princeton University
Princeton, New Jersey
Attn: Julian Levy
Resident Representative (2)

Director
Advanced Research Projects Agency
The Pentagon
Washington 25, D. C. (2)

AGENCY

Chief, Bureau of Ships
Department of the Navy
Washington 25, D. C.
Attn: Code 335 (1)

Chief, Bureau of Weapons
Department of the Navy
Washington 25, D. C.
Attn: RMMP-1 (1)
RAPP-1 (1)

Director
Naval Research Laboratory
Washington 25, D. C.
Attn: Code 2028 (1)

Naval Engineering Exp. Station
Annapolis, Maryland
Attn: Arthur H. Senner (1)

U. S. Naval Postgraduate School
Monterey, California
Attn: Library (1)

Office of the Asst. Chief of
Staff, G-4
Research and Development Division
Department of the Army
Washington 25, D. C. (1)

Aberdeen Proving Ground
Maryland (1)

Armed Services Technical Info.
Agency
Arlington Hall Station
Arlington 12, Virginia
Attn: DSC (10)

Atomic Energy Commission
Plans and Analysis Branch
Washington 25, D. C.
Attn: Maj. J. B. Radcliff
USAF (1)

Director
Engineering Res. & Dev. Lab.
Fort Belvior, Virginia
Attn: Head, Nuclear Power
Branch (1)

AGENCY

U. S. Coast Guard Hq.
Testing and Development Div.
1300 E. Street
Washington, D. C.
Attn: W. S. Vaughn, Cdr., USCG (1)

Wright Air Development Center
Wright-Patterson AFB, Ohio
Attn: WCREO-2 (1)
WCLOS (1)

National Aeronautics and Space Admn.
Lewis Research Center
21000 Brookpark Road
Cleveland 35, Ohio
Attn: Library (2)

National Aeronautical and Space Admn.
Langley Research Center
Langley Field, Virginia
Attn: Library (3)

Administrator
National Aeronautics and Space Admn.
1520 H. Street, N. W.
Washington 25, D. C. (5)

Oak Ridge National Laboratory
9204 - 1; Y-12
P. O. Box P
Oak Ridge, Tennessee
Attn: Technical Library (1)

Brooklyn Polytechnic Institute
99 Livingston Street
Brooklyn 1, New York
Attn: Engineering Library (1)

California Inst. of Technology
Mechanical Engineering Department
1201 East California Street
Pasadena 4, California
Attn: Mechanical Eng'g Library (1)
Aero. Eng'g Library (1)

National Aeronautics and Space Admn.
Ames Research Center
Attn: Library (1)

University of Pennsylvania
Philadelphia, Pennsylvania
Attn: Dr. Yeh

AGENCY

University of California
College of Engineering
Berkeley 4, California
Attn: Eng'g Library (1)

University of Calif. at
Los Angeles
Engineering Department
Los Angeles 24, California
Attn: Eng'g Library (1)

Cornell University
College of Engineering
Department of Heat Power Eng'g
Ithaca, New York
Attn: Eng'g Library (1)
Aeronautical Eng. Lib. (1)

University of Houston
Mechanical Engineering Department
Attn: Library (1)

Illinois Inst. of Technology
Dept. of Mechanical Eng'g
Technology Center
Chicago 16, Illinois
Attn: Heat Transfer Lab.(1)

Lehigh University
Department of Mech. Eng'g
Bethlehem, Pennsylvania
Attn: Library (1)

Mass. Inst. of Tech.
Department of Mechanical Eng'g
Cambridge 39, Mass.
Attn: Engineering Library (1)

University of Michigan
228 W. Engineering Building
Ann Arbor, Michigan
Attn: Eng'g Library (1)

University of Minnesota
Mechanical Engineering Dept.
Minneapolis, Minnesota
Attn: Library (1)

Union College
Department of Mechanical Eng'g
Schenectady 8, New York
Attn: Dr. G. M. Ketchum

AGENCY

University of New Mexico
Department of Mech. Engineering
Albuquerque, New Mexico
Attn: Library (1)

Prof. Richard E. Balzhiser
University of Michigan
Dept. of Chem & Metallurgical Eng'g
Ann Arbor, Michigan (1)

New York University
College of Engineering
Dept. of Mechanical Engineering
University Heights
New York 53, New York
Attn: Eng'g Library (1)

Northwestern University
Mechanical Engineering Department
Evanston, Illinois
Attn: Library (1)

Project SQUID
University of Virginia
Charlottesville, Virginia
Attn: Dr. J. Scott, Dir. (1)

Purdue University
School of Aero. & Eng'g Sciences
Lafayette, Indiana
Attn: Library (1)

University of Santa Clara
Santa Clara, California
Attn: Library (1)

Stanford University
Stanford, California
Attn: Eng'g Library (1)

Syracuse University
Syracuse, New York
Attn: Eng'g Library (1)

Tufts University
Mechanical Engineering Department
Medford 55, Mass.
Attn: Eng'g Library

University of Washington
College of Engineering
Seattle 5, Washington
Attn: Eng'g Library (1)

AGENCY

University of Wisconsin
Department of Mechanical Eng'g
Madison, Wisconsin
Attn: Eng'g Library (1)

Aerochem Research Laboratories
Inc.
Princeton, New Jersey
Attn: Dr. H. F. Calcote, Pres. (1)

Aerojet-General Corp.
Space Technology Division
Azusa, California
Attn: Library (1)

Aerojet-General Corp.
Liquid Rocket Plant
Sacremento, California
Attn: J. Moise (1)

Aerojet-General Nucleonics
Fostofia Way
San Ramon, California
Attn: Library (1)

Aeronutronic Systems, Inc.
Newport Beach, California
Attn: Dr. T. A. Bergstrall (1)

Aerophysics Development Corp.
P. O. Box 567
Pacific Palisades, California
Attn: Library (1)

Air Reduction Company
Murray Hill, New Jersey
Attn: Library (1)

AiResearch Mfg. Company
9851-9951 Sepulveda Blvd.
Los Angeles 45, California
Attn: Library (1)

Allis-Chalmers Mfg. Company
General Machinery Division
Milwaukee 1, Wisconsin
Attn: Mr. R. C. Allen
Dir. of Mech. Eng'g (1)

Argonne National Laboratories
P. O. 299
Lemont, Illinois
Attn: Technical Library (1)

AGENCY

American-Standard
Atomic Energy Division
369 Whisman Road
Sunnyvale, California
Attn: Mr. Neal F. Lansing (1)

Arnold Equipment Corporation
3080 Main Street
Buffalo 14, New York
Attn: Mr. R. G. Tessmer (1)

Aro, Inc.
Technical Information Branch
Tullahoma, Tennessee
Attn: Mr. G. E. Randall

Atomic Power Dev. Ass. Inc.
1911 First Street
Detroit 26, Michigan
Attn: Library (1)

AVCO Research Laboratory
Wilmington, Massachusetts
Attn: Dr. R. R. John (1)

AVCO-Everett Research Laboratory
2385 Revere Beach Parkway
Everett 49, Massachusetts
Attn: Technical Library (1)
Dr. Arnold Goldburg (1)

The Babcock and Wilcos Company
Research and Development Center
P. O. Box 835
Alliance, Ohio (1)

Bell Aircraft Corporation
Space Flight and Missiles Div.
Buffalo, New York
Attn: Library (1)

California Research Corporation
Richmond, California
Attn: Dr. J. H. Macpherson (1)

Carrier Corporation
300 South Geddes Street
Syracuse 1, New York
Attn: Engineering Library

AGENCY

Cornell Aernautical Lab.
4455 Genesee Street
Buffalo 21, New York (1)

Chrysler Corporation
Automotive Research, Dept. 981
12843 Greenfield Avenue
Detroit 27, Michigan
Attn: Mr. A. Charlamb
Research Eng. (1)

Detroit Edison Company
Nuclear Power Division
Detroit, Michigan (1)

Eitel-McCullough, Inc.
798 San Mateo Avenue
San Bruno, California
Attn: Mr. J. S. McCullough
Mgr. Res. (1)

Electric Boat Company
Groton, Conn.
Attn: Mr. E. S. Dennison (1)

Electro-Optical Systems, Inc.
3016 E. Foothill Blvd.
Pasadena, California
Attn: Library (1)

Fairchild Engine and Airplane
Corporation
Fairchild Astonics Division
Wyandanch, Long Island, N. Y.
Attn: Library (1)

Foster Wheeler Corporation
165 Broadway
New York 6, New York
Attn: Mr. E. L. Daman
Dir. Res. and Eng'g (1)

General Electric Company
Atomic Energy Division
San Jose, California
Attn: Mr. N. E. Tippets (1)

General Electric Company
Cincinnati 15, Ohio
Attn: Aircraft Gas Turbine Div.
Central Library Build. 305
(1)

AGENCY

Ramo Wooldrige Division
8433 Fallbrook Avenue
Canoga Park, California
Attn: Dr. David B. Langmuir (1)

Stanford Research Institute
Menlo Park, California
Attn: Technical Library (1)

Sundstrand Denver
2480 W. 70th Avenue
Denver 21, Colorado (1)

Thermal Dynamics Corporation
Hanover, New Hampshire
Attn: Mr. J. Browning, Pres. (1)

Thiokol Chemical Corporation
Elkton Division
Elkton, Maryland
Attn: Dr. Donald D. Thomas (1)

Thompson Ramo-Wooldridge, Inc.
Research and Development
TAPCO Division
Willoughby, Ohio
Attn: Mr. W. A. Compton, Mgr. (1)
Mr. V. P. Kovacik (1)

Union Carbide Nuclear Company
Oak Ridge Gaseous Diffusion Plant
Plant Records Department
P. O. Box P
Oak Ridge, Tennessee (1)

United Aircraft Corporation
The Library
400 Main Street
East Hartford 8, Conn. (1)

Vitro Laboratories
200 Pleasant Valley Way
West Orange, New Jersey
Attn: Dr. C. Dudley Fitz (1)

Westinghouse Electric Corporation
Atomic Power Division
P. O. Box 1468
Pittsburgh 30, Pa.
Attn: Tech. Library (1)

Westinghouse Electric Corp
Research Laboratory
East Pittsburgh, Pa.
Attn: Dr. Stewart Way (1)

AGENCY

Stewart-Warner Corporation
1514 Drover Street
Indianapolis 7, Indiana
Attn: Mr. R. D. Randell
Mgr. Research (1)

Nucor Research, Inc.
2421 Wolcott Avenue
Ferndale 20, Michigan
Attn: Mr. A. R. Bobrowski
V. Pres. (1)

Heat Division
Mech. Eng. Res. Lab.
D.S.I.R., East Kilbride
near Glasgow, Scotland
Attn: Mr. A. J. Ede
SEND TO
Office of the Asst. Naval
Attache for Research
Naval Attache, American Embassy
Navy No. 100, Fleet P. O.
New York, New York (1)

Dept. of Mechanical Engineering
Queen Mary College
London E. 1., England
Attn: Mr. E. J. LeFevre (1)

Minneapolis-Honeywell Regulator
Company
Research Center
500 Washington Avenue South
Hopking, Minnesota
Attn: Mr. A. J. Oberg (1)

Ingersoll-Rand Company
Painted Post, New York
Attn: John B. Garet,
Librarian (1)

Dr. Clark A. Dunn
Director, Eng'g Research
Oklahoma State University
Stillwater, Oklahoma (1)

ASTRO
A Div. of the Marquardt Corp.
16555 Saticoy Street
Van Nuys, California
Attn: Edward T. Pitkin, Mgr.
Space Propulsion Dept.

Dr. Julio Cordero, AVCO RAD
Wilmington Massachusetts (1)

AGENCY

General Electric Company
General Engineering Laboratory
Schenectady 5, New York
Attn: Mrs. Florence F. Buckland (1)
Dr. H. T. Nagamatsu, Dir.,
Hypersonic Lab. (1)

General Metals Corporation
Enterprise Division
18th and Florida Streets
San Francisco, California

General Motors Corporation
Allison Division
Indianapolis 6, Indiana
Attn: Mr. R. M. Hazen
Dir. of Eng. (1)

General Motors Corporation
Research Labs, Division
Detroit 2, Michigan
Attn: Library (1)

Hughes Aircraft Company
Florence and Teake Streets
Culver City, California
Attn: Tech. Library (1)

Lawrence Radiation Laboratory
Box 808
Livermore, California
Attn: Dr. T. Merkle (1)

Linde Company
Div. of Union Carbide Corp.
Speedway Laboratories
1500 Polco Street
Indianapolis 25, Indiana
Attn: Librarian (1)

Lockheed Aircraft Corporation
Missile Systems Division
Aerodynamics Department
Sunnyvale, California
Attn: Mr. G. A. Eteme (1)

Glenn L. Martin Company
Baltimore 3, Maryland
Attn: Mr. W. Corliss,
Nuclear Division (1)

AGENCY

MHD Research
1571 Placentia Avenue
Newport Beach, California
Attn: Dr. V. Blackman (1)

North American Aviation, Inc.
International Airport
Los Angeles 45, California
Attn: Mr. M. S. Sulkin (1)

Plasmadyne Corporation
3839 South Main Street
Santa Ana, California
Attn: Library (1)

Radio-Corporation of America
Astro-Electronic Products Div.
Route 1
Princeton, New Jersey
Attn: Mr. S. Sternberg
Chief Engineer (1)

Reaction Motors Division
Thiokol Chemical Corporation
Denville, New Jersey
Attn: Dr. E. Seymour
Dir. Research (1)

Plasma Propulsion Laboratory
Republic Aviation Corporation
Farmingdale, Long Island, N. Y.
Attn: Mr. A. E. Kunen, Mgr. (1)

Rocketdyne Division
6633 Canoga Avenue
Canoga Park, California
Attn: Librarian (1)
Dr. R. Dillaway,
Nucllonics Div. (1)

Shell Development Company
4560 Horton Street
Emeryville, California
Attn: Dr. C. R. Garbett (1)

Solar Aircraft Company
San Diego 12, California
Attn: Mr. P. A. Pitt,
Chief Engineer (1)

AGENCY

U. S. Atomic Energy Commission
Tech. Info Service Extension
P. O. Box 62
Oak Ridge, Tennessee (1)
via:
Commanding Officer
Office of Naval Research
Branch Office
Navy No. 100, Fleet P. O.
New York, New York

Arthur D. Little, Inc.
15 Acorn Park
Cambridge 40, Mass.
Attn: Miss Dorothy E. Hart
Librarian (1)

Convair
A Div. of General Dynamics Corp.
Fort Worth 1, Texas
Attn: Div. Research Library (1)

Aerojet-General Corporation
P. O. Box 296
Azusa, California
Attn: Robert D. Waldo
Corporate Research
Operation Department (1)

Chance Vought Aircraft, Inc.
Research Division
Box 5907
Dallas, Texas (1)

Cross Malaker Laboratories, Inc.
191 Mill Lane
Mountainside, New Jersey
Attn: Mr. Richard A. Rossi (1)

Commanding Officer
U. S. Army Signal Res. & Dev. Lab.
Fort Monmouth, New Jersey
Attn: SIGFM/EL-PRG (1)

Dartmouth College
Thayer School of Engineering
Hanover, New Hampshire
Attn: Prof. R. C. Dean, Jr. (1)

B. F. Goodrich Company
Research Center
Bucksville, Ohio
Attn: Mgr. of Res. Operation (1)

AGENCY

Goodrich-High Voltage Astronautics
Inc.
Burlington, Massachusetts
Attn: Dr. C. H. Stockman
Vice President

VIDYA Associates
2626 Hanover Street
Palo Alto, California
Attn: Mr. D. T. Flood (1)

Warner and Swasey Company
Control Instrument Division
32-16 Downing Street
Flushing, Queens, New York
Attn: Mr. G. J. Penzias (1)
Dr. R. Tourin (1)

Prengle, Dukler and Crump
5417 Crawford Street
Houston 4, Texas
Attn: Mr. H. Wm. Prengle, Jr.
Vice President (1)

Aeronautical Research Laboratory
USAF Office of Aerospace Research
Wright-Patterson A.F. Base, Ohio
Attn: Mr. Erich Soehngen (2)

Allied Research Associates, Inc.
43 Leon Street
Boston, Massachusetts
Attn: Alan Mironer
Physics Department (1)

Dr. M. P. Freeman
American Cyanamid Company
1937 W. Main Street
Stamford, Conn. (1)

Engineering Projects Laboratory
School of Engineering
MIT
Cambridge 39, Mass.
Attn: Gail E. Portridge (1)

Mr. F. C. Gray
Space Technology Laboratories, Inc.
1 Space Park
Redondo Beach, California (1)